THE ROLES OF GLUK4 IN AMYGDALA AND ASSOCIATED BEHAVIOURS

Doctoral Thesis presented by

Vineet Arora

- Year 2019 -

Thesis Director:

Juan Lerma*, PhD*

Doctoral Program in Neuroscience

Neuroscience Institute – UMH-CSIC

UNIVERSITAS
Miguel
Hernández

DOCTORAL THESIS BY COMPENDIUM OF PUBLICATIONS

Sant Joan d'Alacant, 2019

To whom it may concern,

The doctoral thesis introduced hereafter under the title "The roles of GluK4 in amygdala and associated behaviours" has been developed by myself, Vineet Arora. This thesis includes the following publication, of which I am the first author:

Arora V., Pecoraro V., Aller MI., Roman C., Paternain AV., Lerma J (2018). "Increased Grik4 Gene Dosage Causes Imbalanced Circuit Output and Human Disease-Related Behaviours". **Cell Rep**. 2018 Jun 26;23(13):3827-3838. doi: 10.1016/j.celrep.2018.05.086

I declare that the publication has not been used and will not be used in any other thesis in agreement with my thesis director Juan Lerma:

Yours sincerely,

Vineet Arora

UNIVERSITAS
Miguel
Hernández

INSTITUTO DE NEUROCIENCIAS

EXCELENCIA SEVERO OCHOA

Centro de Excelencia «Severo Ochoa» 2014-2018

UNIVERSITAS Miguel Hernández

DOCTORAL THESIS BY COMPENDIUM OF PUBLICATIONS

Sant Joan d'Alacant, 2019

To whom it may concern,

The doctoral thesis developed by Vineet Arora, with title: "The roles of GluK4 in amygdala and associated behaviours¨ includes a publication in Cell Reports (doi: 10.1016/j.celrep.2018.05.086), corresponding to the main topic of the dissertation.

As the director of this PhD. Thesis and the corresponding author of the article, I declare that Mr. Vineet Arora is a first author of the article and is a major contributor of the work presented in this publication. I declare that this publication has not been used and will not be used in any other thesis.

This article was published in a journal that belongs to the first quartile (Q1) for the corresponding discipline according to the last Journal Citation Reports (JCR).

Cell Reports: Impact factor 8.032 (2017 Q1 Multidisciplinary Sciences)

Yours sincerely,

Vineet Arora Prof. Juan Lerma

UNIVERSITAS
Miguel
Hernández

Consejo Superior de Investigaciones Científicas
Universidad Miguel Hernández
Instituto de Neurociencias

Dr. Miguel Valdeolmillos
Coordinator of the Neuroscience PhD Program

INFORME DE LA COMISION ACADEMICA DEL PROGRAMA DE DOCTORADO EN NEUROCIENCIAS

Por la presente, la Comisión Académica del Programa de Doctorado en Neurociencias:

Informa FAVORABLEMENTE el depósito de la Tesis presentada por D. Vineet Arora

Realizada bajo la dirección de la Prof. Juan Lerma

Titulada: ***The Roles of GluK4 in amygdala and associated behaviours***

Presentada por compendio de publicaciones.

San Juan de Alicante de de 2019

Dr. Miguel Valdeolmillos

Coordinador del programa de Doctorado en Neurociencias

E-mail : miguel.valdeolmillos@umh.es
www.ina.umh.es

Tel: +34 965 91 9540
Fax: +34 965 91 9549

Av Ramón y Cajal s/n
Campus de San Juan
03550 SAN JUAN DE ALICANTE– ESPAÑA

UNIVERSITAS
Miguel
Hernández

INSTITUTO DE NEUROCIENCIAS

Consejo Superior de Investigaciones Científicas
Universidad Miguel Hernández
Instituto de Neurociencias

Juan Lerma, PhD
Científico titular del CSIC

Sant Joan d'Alacant, de de 2019

D. Juan Lerma, Científico titular del Consejo Superior de Investigaciones Científicas (CSIC),

AUTORIZO la presentación de la Tesis Doctoral titulada "The roles of GluK4 in amygdala and associated behaviours" y realizada por D. Vineet Arora, bajo mi inmediata dirección y supervisión como director y tutor de su Tesis Doctoral en el Instituto de Neurociencias (CSIC-UMH) y que presenta para la obtención del grado de Doctor por la Universidad Miguel Hernández.

Y para que conste, a los efectos oportunos, firmo el presente certificado.

Prof. Juan Lerma

j.lerma@umh.es
www.ina.umh.es

Tel: +34 965 91 9238 / 9239
Fax: +34 965 91 9238

Av Ramón y Cajal s/n
Campus de San Juan
03550 SAN JUAN DE ALICANTE– ESPAÑA

UNIVERSITAS
Miguel
Hernández

ACKNOWLEDGEMENTS

This thesis work has been made possible by the support of innumerable wonderful people inside and outside of the Instituto of Neuroscience, Alicante (INA). After 3.5 years of efforts, learnings, sacrifice, good and less good times, I want to thank all the people who have made this work fulfilling and productive in all respects. First of all, my deepest gratitude goes to my PhD supervisor, Prof. Juan Lerma, who chose me as PhD student for his lab. He has been extremely kind and encouraging throughout my PhD work. Due to the intellectual freedom and unprecedented support that he provided me in his supervision, I never lost passion and motivation for research.

The research work I performed for my PhD greatly benefited from all members of the lab namely Valeria Pecoraro, Mª Isabel Aller Alvarez, Sergio Valbuena, Celia Román de la Calle, Laura Navío Marín, Amr Fawzy Kamel Eed, Mónica Llinares Domínguez, Marija Gjorgoska and Alvaro García Avilés. They all were amazing in providing me with a cooperative and friendly atmosphere to work, and even contributed to my work with their helpful suggestions, constructive criticism and insightful feedback.

I am very grateful to all the great scientists and great people who have surrounded me during these years and from whom I have had the opportunity to learn; Prof. Ramon Reig, Prof. Santiago Canals, Javier Alegre Cortés, Roberto Montanari, María Sáez García, Adam Matic, Saurabh Gupta and Kaviya Chinnapa.

I thank all the veterans who were in the lab when I arrived and who made the beginning of the Journey easier Valeria, Sergio and, above all, Mª Isabel Aller, who guided my first steps and taught me the basics. I am also indebted to Mónica Llinares for patient technical help she provided which was indispensable for my successful research work.

In particular, a heartfelt thanks to all my colleagues and friends who have been a part of this journey, because no matter how bad the day goes, they always had time for a fruitful discussion over a coffee. Thank you very much for filling in great moments, conversations and laughter all these years; Aitor, Sheila, Sandra, Javier, Luisa, Miguel and Rita.

I would also like to thank my friends and professors back in India for their constant guidance and the many blessings they always bestowed upon me, Prof. Baljinder Singh, Prof. Mohan Garg, Dinesh Rawat, Shashank Awasthi and Nivedita Rana. Without their support pursuing a PhD and successfully completing it while living abroad would have been an impossible task.

Last but not the least my sincerest and warmest thanks to my brothers and my father back home who kept pushing me hard to achieve the goals and they have a fundamental role to play in making me what I am today. And this research work is dedicated to one of the most incredible and beautiful person i have ever known, my mother. You never left me, you have always been besides me, smiling while holding my hand. Your hand on my hand and your blessings made it through! Love you so much mom!

Thank you a lot, everyone!!!!

In Memory of My Beloved Mom…

UNIVERSITAS
Miguel
Hernández

TABLE OF CONTENTS

UNIVERSITAS
Miguel
Hernández

UNIVERSITAS
Miguel
Hernández

LIST of ABBREVIATIONS

A

AC	Auditory Cortex
AdBNST	Antero-dorsal bed nucleus of stria terminalis
AHPs	After-hyperpolarization currents
AMPA	α-amino-3-hydroxy-5-methyl-4-isoxazolepropionic acid
AMPARs	α-amino-3-hydroxy-5-methyl-4-isoxazolepropionic acid receptors
ASDs	Autism Spectral Disorders
4-AP	4-amino pyridine
AP	Action Potential
APs	Action Potentials
ATD	Amino-terminal domain
ATP	Adenosine Triphosphate
ATPA	2-amino-3-(3-hydroxy-5-tert-butylisoxazol-4-yl) propanoic acid

B

BA	Basal amygdala
BLA	Basolateral amygdala
BMA	Basomedial amygdala
BNST	Bed nucleus of stria terminalis

C

Ca^{2+}	Calcium ion
CaMKII	Calcium/Calmodulin-dependent protein kinase II
CB, CALB	Calbindin
CB^{+} INs	Calbindin interneurons
CB1R	Cannabinoid 1 receptor

CCK	Cholecystokinin
CeA	Central amygdala
CeLA/CLA	Centrolateral amygdala
CeMA/CMA	Centromedial amygdala
ChR2	Channelorhodopsin-2
CNS	Central Nervous System
CNVs	Copy Number Variations
CNQX	6-cyano-7-nitroquinoxaline
CR	Calretinin
CRF	Corticotropin-releasing factor
CS	Conditioned stimulus
CTD	Carboxy terminal domain

D

D-APV	(2R)-amino-5-phosphovalerric acid; (2R)-amino-5-phosphopentanoate
D1R	Dopamine 1 receptor
DIC	Differential interference contrast
DG	Dentate Gyrus
DNA	Deoxyribonucleic Acid
DNQX	Dinitroquinoxaline-2,3-dione
dPAG	Dorsal periaqueductal gray
DRN	Dorsal raphe nuclei
DVN	Dorsal vagal nucleus

E

EC	External Capsule
eEPSC	Evoked excitatory postsynaptic current
EGTA	Ethylene glycol-bis(β-aminoethyl ether)-N,N,N′,N′-tetraacetic acid

EPM	Elevated plus maze
EPSC	Excitatory postsynaptic current
EPSP	Excitatory postsynaptic potential

G

GAD67	Glutamate decarboxylase isoform 67 (Molecular weight: 67 kDa)
GFP	Green fluorescent protein
GluK4	Glutamatergic ionotropic kainite receptor subunit 4
GluK4-KARs	GluK4 containing KARs
GPCR	G protein coupled receptor
GTP	Guanosine Tri-phosphate

H

HFS	High Frequency stimulation
HTR 2A	Serotonin receptor 2A
HPC	Hippocampus
Hyp	Hypothalamus

I

IC	Internal capsule
ICMs	Intercalated cell masses
ID	Intellectual disability
iGluRs	Ionotropic Glutamate Receptors
ISI	Inter-stimulus interval
IL	Infralimbic Cortex
IN	Interneuron
IPSC	Inhibitory postsynaptic current
ISI	Inter-stimulus interval

IITC	Lateral intercalated cell clusters
ITCd	Dorsal intercalated cell clusters
ITCm	Medial intercalated cell clusters
ITCv	Ventral intercalated cell clusters

K

K^+	Potassium ion
KA	Kainate
KAR	Kainate receptor
KO	Knock out mice

L

LA	Lateral amygdala
LAd	Lateral amygdala – dorsal division
LAdl	Lateral amygdala – dorsolateral division
LAv	Lateral amygdala – ventral division
LAvl	Lateral amygdala – ventrolateral division
LBD	Ligand binding domain
LC	Locus coeruleus
L-CCK^+	Large- cholecystokinin positive cell type
LTD	Long-term depression
LTP	Long-term potentiation

M

MAPK	Mitogen-activated protein kinase
MePD	Posterodorsal medial amygdala
mGluR	Metabotropic glutamate receptor
Mg^+	Magnesium ion

MGN	Medial geniculate nucleus
mEPSC	Miniature excitatory postsynaptic current
mIPSC	Miniature inhibitory postsynaptic current
mITC	Medial interstitial cell cluster of the amygdala
mPFC	Medial prefrontal cortex
mRNA	Messenger Ribonucleic acid

N

NAc	Nucleus accumbens
NK1	Neurokinin-1 receptor
NMDA	N-methyl-D-aspartate
NMDAR	N-methyl-D-aspartate receptors
nNOS	Neuronal nitric oxide synthase
NPY	Neuropeptide Y

O

OT	Oxytocin
OTR	Oxytocin receptor
OFT	Open field test

P

PAG	Periaqueductal gray
PKC	Protein Kinase C
PLC	Phospholipase C
PN	Principal neurons/Pyramidal cells
PPR	Paired pulse ratio
PSD 95	Post Synaptic Density Protein 95

PSP	Postsynaptic potential
PTSD	Post-traumatic stress disorder
PVT	Periventricular thalamus
PV	Parvalbumin

R

RI	Rectification Index
Rin	Input resistance
RNA	Ribonucleic acid
RT	Room temperature

S

S-CCK	Small- Cholecystokinin positive cell type
SEM	Standard error of the mean
sEPSC	Spontaneous excitatory postsynaptic current
sIPSC	Spontaneous inhibitory postsynaptic current
SNPs	Single- Nucleotide Polymorphism
SOM	Somatostatin
SO	Stratum oriens
SR	Stratum radiatum
SSRI	Selective serotonin reuptake inhibitor
STDP	Spike-timing-dependent plasticity

T

Tac2	Tachykinin 2
TeA	Temporal association cortex
TEA	Trastornos del espectro autista
TLE	Temporal-Lobe Epilepsy

TM	Transmembrane domain
TTx	Tetrodotoxin

U

UBP310	S)- 1- (2- Amino-2-carboxyethyl)-3-(2-carboxy-thiophene-3-yl-methyl)-5-methylpyrimidine-2, 4-dione
US	Unconditioned stimulus

V

VGAT	Vesicular γ-aminobutyric acid transporter
V/I	Voltage-Current relationship curve
VPR	Vasopressin receptor
vHPC	Ventral hippocampus
VIP	Vasoactive intestinal peptide
Vm	Membrane potential
VPL	Ventroposterolateral nuclei of the thalamus
VPM	Ventroposteromedial nuclei of the thalamus

W

WT	Wild-type

UNIVERSITAS
Miguel
Hernández

ABSTRACT

Kainate receptors (KARs) are a class of ionotropic glutamate receptors ubiquitously present throughout the central nervous system. Mounting evidence indicates the presence of these receptors at both pre- and post-synaptic sides of the synapses. Presynaptically KARs are involved in controlling both inhibitory and excitatory synaptic transmission via the modulation of the release of neurotransmitters like GABA and Glutamate. Postsynaptically, KARs cause membrane depolarisation and mediate postsynaptic responses. KARs have a small contribution to the postsynaptic currents, but they do impart synapses with certain integrative properties and have capabilities to regulate synaptic transmission beyond their role as ion channel forming receptor. GluK1 subunit containing KARs have been found in presynaptic terminals of interneurons and postsynaptically in interneurons and pyramidal cells of the basolateral amygdala (BLA). In this structure, they mediate a fraction of the postsynaptic depolarization, while presynaptically, GluK1 containing KARs in interneurons controls GABA release.

Altered glutamatergic neurotransmission is considered to be one of the primary factors contributing to mental diseases such as autism spectral disorders (ASD). The amygdala is involved in emotional behaviours and its relation with some psychiatric illnesses is subject of active research. Alterations in copy number of genes coding for KAR subunits have been linked to neuropsychiatric syndromes such as ASD and bipolar disorders. This is the case of *Grik4*, a gene coding for a high affinity subunit, GluK4, as de novo duplications of this gene have been described in cases of ASD and schizophrenia.

To start delineating the role played by GluK4 containing KARs in brain circuits underlying emotionally relevant behaviours, we followed a gain of function strategy and generated the transgenic mouse C57BL/6J-Tg(Camk2a-grik4), which over-expresses *Grik4* in the forebrain under the control of the CaMKII promoter and that was nicknamed GluK4^{Over}. These mice displayed anhedonia, enhanced anxiety and depressive states and impaired social interaction, common endophenotypes

associated to ASD. To start looking for functional neural correlates of these abnormal behaviours in amygdala circuits, we studied the effect of *Grik4* overexpression on the presynaptic and postsynaptic excitatory activity in identified cells of BLA and Centrolateral amygdala (CeLA). Overexpression of *Grik4* led to enhanced spontaneous and external capsule-evoked glutamate excitatory activity in the BLA and consequently increased excitatory inputs to the regular firing cells (RFCs) of CeLA. Overexpressed GluK4 subunits were present both presynaptically and postsynaptically leading to higher release probability of glutamate in cortico-amygdala synapses. In addition to the enhanced probability of release, amplitude was also enhanced in evoked responses mediated by AMPARs in BLA pyramidal cells. Decreased rectification index in these evoked responses mediated by AMPARs in BLA neurons indicated a change in subunit composition of AMPARs, which imposed an increased conductance of postsynaptic AMPARs in BLA pyramidal cells, leading to increased postsynaptic response.

In synaptic connections between BLA pyramidal cells and RFCs of CeLA, the probability of release was also enhanced. On the other hand, the probability of release of glutamate and thus excitatory input in synaptic connections between BLA pyramidal cells and late firing cells (LFCs) of CeLA was decreased in GluK4^{Over} mice. A large population of cells in CeLA consists of these LFCs and their activation is known to take part of an anxiolytic circuit. Accordingly, depression of excitatory input to LFCs in GluK4^{Over} mice led to an anxiogenic phenotype in GluK4^{Over} mice. Moreover, *in-vivo* c-Fos expression studies indicated enhanced resting activity in the BLA and Centromedial amygdala (CeMA) in the GluK4^{Over} mice. Thus overall, depression of activity of late firing cells in the CeLA forming part of the anxiolytic circuit leads to dis-inhibition of CeMA neurons, which further inhibit neurons of downstream targets like Bed Nucleus of the Stria Terminalis (BNST) and Periaqueductal Gray (PAG) and this increased inhibition is known to increase anxiety and fear related behaviour.

Finally, we showed that restoring levels of GluK4 protein in GluK4^{Over} mice to normal levels rescue synaptic and behaviour alterations thus indicating excess of GluK4 as the major cause behind increased synaptic gain in anxiogenic circuits provoking

aberrant behaviours that are evident in neuropsychiatric diseases like autism and schizophrenia.

Taken together, these observations suggest that GluK4 subunit containing high affinity KARs have a significant role in regulating excitatory transmission in the BLA and from BLA to CeLA networks and modest increases in GluK4 protein are associated with increased synaptic gain at selected synapses in the amygdala producing an unbalanced circuit output, which may account for the behavioural abnormalities that concur with diseases such as autism and schizophrenia. *Grik4* duplication may be relevant to such disease behaviours in humans given that amygdala is structurally and functionally conserved across species.

RESUMEN

Los receptores de kainato (KAR) son una clase de receptores ionotrópicos de glutamato que están presentes de manera ubicua en todo el sistema nervioso central. Las evidencias apuntan a que estos receptores se encuentran tanto en la región presináptica como en la región postsináptica de las neuronas. Presinápticamente, los KAR participan en la modulación de la transmisión sináptica tanto inhibitoria como excitadora a través de la modulación de la liberación de neurotransmisores como GABA y glutamato, e influyen en la maduración de los circuitos neuronales. Postsinápticamente, los KAR causan la despolarización de la membrana y las respuestas postsinápticas. Los KAR tienen una pequeña contribución a las corrientes postsinápticas, pero otorgan ciertas propiedades integradoras a la sinapsis y tienen la capacidad de regular la transmisión sináptica más allá de su función como receptor ionotrópico. Se han encontrado KARs que contienen la subunidad GluK1 en terminales presinápticos de interneuronas y postsinápticamente en interneuronas y células piramidales de la amígdala basolateral (BLA). En esta estructura, estos receptores median una fracción de la despolarización postsináptica, mientras que de manera presináptica, los KARs que contienen GluK1 controlan la excitabilidad a través de la modulación de la liberación de GABA.

La alteración de la neurotransmisión glutamatérgica ha sido considerada como uno de los factores principales que contribuyen a enfermedades mentales, como por ejemplo los trastornos del espectro autista (TEA). La amígdala participa en conductas emocionales y su relación con algunas enfermedades psiquiátricas está sujeta a investigación activa. Alteraciones en el número de copias de los genes que codifican las subunidades KARs han sido relacionadas con síndromes neuropsiquiátricos como puede ser el TEA y la depresión. Este es el caso del gen *Grik4*, un gen que codifica una subunidad de alta afinidad de los KARs, GluK4, cuya duplicación de *novo* se ha encontrado en casos de TEA.

Para comenzar a entender el papel de los KARs que incluyen la subunidad GluK4, en el laboratorio se ha seguido una estrategia de ganancia de función. Generamos una línea transgénica de ratón C57BL / 6J-Tg (Camk2a-grik4), que sobreexpresa *Grik4* en el telencéfalo bajo el control del promotor CaMKII y que denominamos GluK4^{Over}. Estos ratones mostraron síntomas de anhedonia y un aumento de la ansiedad lo que conlleva un estado depresivo y un déficit de interacción social, endofenotipos comunes asociados a TEA. Para comenzar a buscar correlaciones funcionales de estos comportamientos anormales con la actividad de los circuitos de la amígdala, estudiamos el efecto de la sobreexpresión de *Grik4* sobre la actividad excitadora presináptica y postsináptica en las células características de BLA y de la amígdala centrolateral (CeLA). La sobreexpresión de *Grik4* condujo a una mayor actividad excitatoria glutamatérgica tanto espontánea como evocada por la estimulación de la cápsula externa en el BLA y, en consecuencia conllevó un aumento de la entrada excitatoria a las células de disparo regular (RFCs) de CeLA. Las subunidades GluK4 sobreexpresadas están presentes tanto presinápticamente como postsinápticamente, lo que llevó a una mayor probabilidad de liberación de glutamato en las sinapsis cortico-amígdala. Además de la mayor probabilidad de liberación, la amplitud también se incrementó en las respuestas mediadas por AMPARs en las células piramidales de BLA, indicando una mayor conductancia de AMPARs. El índice de rectificación disminuyó en estas respuestas evocadas, lo que indicó un cabio en la composición

subunitaria de los AMPARs postsinápticos, que conlleva un incremento en la conductancia unitaria.

En las conexiones sinápticas entre las células piramidales BLA y los RFCs de CeLA, la probabilidad de liberación también se incrementó. Por otro parte, la probabilidad de liberación de glutamato y, por lo tanto, la entrada excitadora en las conexiones sinápticas entre las células piramidales BLA y las células de disparo tardío (LFCs) de CeLA se encontraba disminuida en los ratones GluK4^{Over}. Una gran población de células en CeLA consiste en estas LFCs y es conocido que participan en un circuito ansiolítico. En consecuencia, la depresión de la entrada de excitación a las LFCs en ratones GluK4^{Over} condujo a un fenotipo ansiogénico en estos ratones. Además, los estudios de expresión de c-Fos *in vivo* indicaron en los ratones GluK4^{Over} un aumento en la actividad de reposo en la BLA y en la amígdala centromedial (CeMA), el origen del circuito ansiogénico. Por lo tanto, la depresión de la actividad de las LFCs en el CeLA conduce a la desinhibición de las neuronas CeMA, lo que inhibe aún más las neuronas de conexiones posteriores como puede ser los núcleos de la estría terminal del tálamo (BNST) y la sustancia gris periacueductal (PAG) y esta inhibición aumentada puede ser el origen de la ansiedad y el comportamiento relacionado con el miedo.

Finalmente, demostramos que la restauración de los niveles de proteína GluK4 en ratones GluK4^{Over} a niveles normales conduce al rescate de las alteraciones sinápticas y comportamentales, lo que indica el exceso de GluK4 como la causa principal detrás del aumento sináptico en los circuitos ansiogénicos que provocan comportamientos aberrantes que son evidentes en enfermedades neuropsiquiátricas como el autismo y la esquizofrenia.

Estas observaciones, tomadas en conjunto, sugieren que los KARs que contienen la subunidad GluK4 de alta afinidad tienen un papel importante en la regulación de la transmisión excitadora en las redes BLA y de BLA a CeLA. La salida desequilibrada del circuito puede explicar las anomalías de comportamiento que coinciden con enfermedades como el autismo y esquizofrenia. La duplicación de *Grik4* puede ser

relevante para estos comportamientos observados en las enfermedades humanas, dado que la amígdala se conserva estructural y funcionalmente en todas las especies.

UNIVERSITAS
Miguel
Hernández

UNIVERSITAS
Miguel
Hernández

CHAPTER 1. GENERAL INTRODUCTION

1.1 SYNAPTIC TRANSMISSION

Synapses are excitatory or inhibitory depending on the chemical neurotransmitter used. In a chemical synapse, an action potential (AP) arrives at the presynaptic terminal activating voltage dependent calcium channels allowing calcium to enter into the cell at the presynaptic site. Entry of calcium promotes fusion of vesicles with the presynaptic site releasing the neurotransmitters. Neurotransmitters released in the synaptic cleft further activates the receptors on the postsynaptic membrane. As a consequence, the channels associated to these receptors open and ions flow down their electrochemical gradient exciting or inhibiting the cell depending on the ion channel selectivity. Any alteration in synaptic transmission resulting in over-efficient or less efficient information transfer between synapses can lead to neuropsychiatric abnormalities such as anxiety and depression.

Synapses are either electrical or chemical in nature. Contrary to electrical synapses, chemical synapses are slow, active and unidirectional in nature requiring ligand activated receptors, which could form or not an ion channel.

There are two types of neurotransmission in the brain depending on the type of chemical synapses, excitatory neurotransmission controlled by principal neurons (PNs) releasing excitatory neurotransmitter such as Glutamate and inhibitory neurotransmission controlled by interneurons (INs) releasing inhibitory neurotransmitter such as GABA.

GABA is the main inhibitory neurotransmitter in the CNS, synthesised by either GAD65, that is more frequently localised in presynaptic terminals, and GAD67, that is expressed throughout the cytoplasm (Soghomonian and Martin, 1998). Packing GABA into vesicles is carried out by vesicular GABA transporter (VGAT; McIntire et al., 1997). Once the INs synaptic terminals are depolarized, N-type (Cav2.2) Ca^{2+} and Voltage-gated P/Q-type (Cav2.1) open leading to calcium entry provoking the fusion of vesicles with the plasma membrane. This releases GABA from axon terminals. The neurotransmitter release may be independent of an AP (Fatt and Katz, 1952), being considered these events as miniature synaptic currents (mIPSCs or mEPSCs in the case of glutamate).

After being released, GABA binds to postsynaptic GABA receptors namely ionotropic (GABA-A) and metabotropic (GABA-B or GABA-C) receptors.

Glutamate on the other hand is the most abundant neurotransmitter controlling excitatory synaptic transmission across the vertebrate brain and spinal cord (Zhou and Danbolt, 2014). It controls neuron excitability with the assistance of more than thirty membrane bound receptor proteins located at the pre- and post-synaptic membrane of neurons and astrocytes. Glutamate concentration outside the neurons is regulated by a number of different factors. Changes in these factors, such as the increased release or disruption in re-uptake mechanisms, may induce disorders related to neuropsychiatric diseases. The glutamate receptors can be divided into two major categories: metabotropic glutamate receptors (mGluRs) which interact with G proteins and activate or inhibit second messenger signalling cascades and ionotropic receptors (iGluRs), which are ligand gated ion channels that permeates cations to cause postsynaptic depolarization.

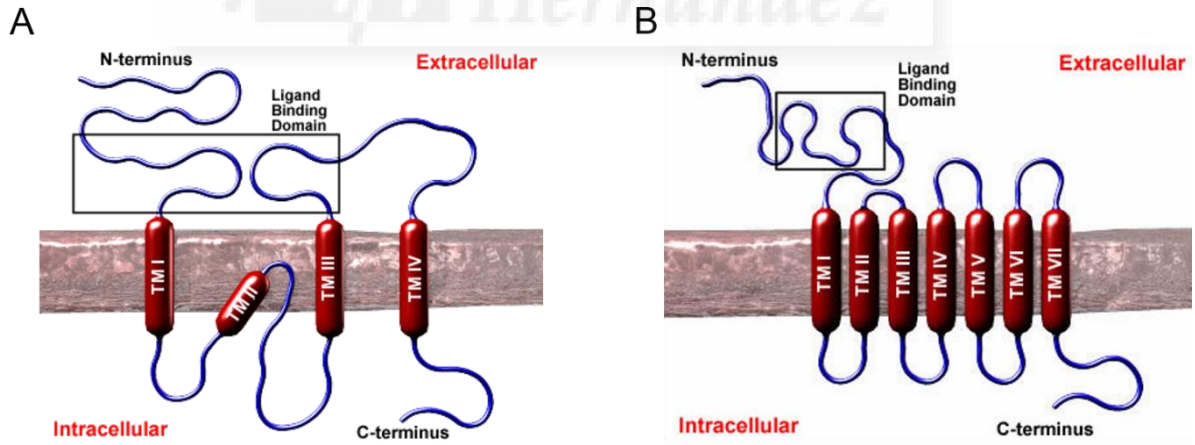

Figure 1: Structure of ionotropic and metabotropic glutamate receptors. A) All ionotropic glutamate receptors are heteromultimers formed by four iGluR subunit proteins, the extracellular ligand binding domains, S1 and S2 formed by half of N terminus and long loop between TMIII and TMIV respectively, the 4 hydrophobic domains, TM1-TM3 and the pore region. Pore region is constituted by TMII via re-entrant loop extending into extracellular N terminus and intracellular C terminus. B) Metabotropic glutamate receptors on the other hand are constituted by seven mGluR subunit proteins, extracellular N terminus consisting of a ligand binding domain and an intracellular C terminal domain. They do not possess inter-helical loops. Source: Reiner and Levitz, (2010)

1.2 METABOTROPIC GLUTAMATE RECEPTORS

mGluRs signal through G proteins activating a series of protein kinases and signal messenger pathways. Unlike iGluRs, mGluRs have seven transmembrane domains separated by loops. The extracellular N terminus consisting of a ligand binding domain and an intracellular C terminal domain.

They have many critical functions in glutamatergic neurotransmission such as to enhance excitability of PNs, to cause changes in presynaptic release and mGluRs are also involved in postsynaptic effects such as long-term potentiation (LTP) and depression (LTD) (Lesage and Steckler, 2010). Glutamate binding at the postsynaptic site activates a G protein coupled to the mGluR receptor and a signaling cascade is activated that subsequently opens a membrane channel for signal transmission. mGluRs have been divided into three groups based on differences in pharmacology and signal transduction properties. A total of 8 mGluRs coding genes have been cloned so far.

- Group I mGluRs include mGluR1 and mGluR5. Their location is predominantly postsynaptic and they are present abundantly in cerebellum, thalamus and hippocampus (HPC). In the HPC, Group I mGluRs are abundant on interneurons, cells of CA1 and the dendritic fields of the dentate gyrus (DG) and CA3. Group 1 mGluRs are coupled to Phospholipase C (PLC) and intracellular calcium signalling and their dysfunction has been implicated in many neural diseases, including those related to learning and memory, such as Fragile X syndrome (Niswender and Conn, 2010)

- Group II mGluRs includes mGluR2 and mGluR3 and these are present on both postsynaptic and presynaptic membranes. This group of receptors have abundant presence throughout the cerebral cortex, and in particular in the cerebellum. The mGlu2 receptor is found in the deeper layers of the cortex. While Golgi cells in the cerebellum has mGlu3 receptors. Presynaptically, group 2 mGluRs regulate the release of neurotransmitters

like glutamate, so can modulate glutamatergic transmission. These have been implicated in mood disorders.

- Group III receptors (mGlu4, mGlu6, mGlu7 and mGlu8) like group II mGluRs are negatively coupled to adenylyl cyclase. These are predominantly present on the presynaptic membrane except in retina where they exist postsynaptically in ON-bipolar retinal cells. They are mainly involved in modulation of glutamate release. These receptors are widespread in neurons of granule cells of the cerebellum, in the CA1-CA3 regions of the HPC, olfactory bulb, striatum and entorhinal cortex. Their dysfunction may be associated, amongst others, to Parkinson's disease (Swanson et al., 2005).

1.3 IONOTROPIC GLUTAMATE RECEPTORS

The ionotropic glutamate receptors are quick acting, ligand gated ion channels. They undergo a conformational change when glutamate binds thus facilitating the ion channel opening. The ion channel opening leads to influx of cations like Na^+ Ca^{2+} and the efflux of K^+. Even a small voltage difference across the postsynaptic membrane leads to enormous current flow leading to depolarization.

1.3.1 Structure of ionotropic glutamate receptors

All glutamate receptors are constituted by 4 subunits arranged in either homotetrameric or heterotetrametric form. Each subunit has an approximate molecular weight of 120 kDa comprising of 800-900 amino acid residues. iGluRs have an extracellular amino domain, which encompasses the amino terminal domain (ATD), the ligand binding domain (LBD), the transmembrane domains (TM1, TM3 and TM4), and a membrane spanning segment, TM2, which forms a membrane re-entrant loop that is integrated within the membrane and contributes to the channel pore domain (Roche et al., 1994; Wo and Oswald, 1994).

Lastly the carboxy terminal domain (CTD) extends intracellularly interacting with a number of intracellular proteins (Roche et al., 1994, Taverna et al., 1994). ATD carries out the organizational assembling the iGluR subunits while CTD is involved in trafficking of subunits to the cell membrane and protein interaction at the synapses (Taverna et al., 1994). Glutamate binding pocket is formed by the extracellular segments S1 and S2 (Stern Bach et al., 1994; Wo and Oswald, 1994). The S1 segment is an extension of TM1 connecting with the ATD, while the S2 connects TM3 and TM4 (Stern-Bach et al., 1994). The “dimer of dimers” arrangement (Stern-Bach et al., 1994) of iGluRs is achieved through interactions of ATDs which assembles the dimers, while incorporation of iGluRs into a tetramer is carried out by the S2 domain and TM4 segments of each dimer structure (Madden et al., 2002).

1.3.2 Types of Ionotropic Glutamate receptors

The iGluRs are classified into three categories according to the ligand that activates them.

NMDA RECEPTORS (NMDARS)

NMDARs are glutamate gated ion channels presenting a slow activation and deactivation kinetics (Lester et al., 1990) and are permeable to Na^+ K^+ and in particular to Ca^{2+} (Ascher and Nowak ., 1998). The Ca^{2+} entry through NMDARs are essential for synaptogenesis, experience-dependent synaptic remodelling, and long-lasting changes in synaptic efficacy such as LTP and LTD (Collingridge et al., 2004).

NMDARs are constituted by three different subunits GluN1-3. GluN1 mRNA has 8 splice variants, so give rise to 8 different GluN1 subunits that are glycine binding subunits (Nakanishi et al., 1992). While GluN2 has four isoforms called GluN2(A-D) (Dingledine at al., 1999), GluN3 has two different isoforms, GluN3A and GluN3B (Cull Candy et al., 2001). Like other glutamate receptors, NMDARs are

heterotetramers constituted by two essential GluN1 subunits in combination with two GluN2 and/or GluN3 subunits (Monyer et al., 1992).

Whereas NMDARs consisting of GluN1/GluN2 receptors needs two molecules of glutamate and two of glycine for activation, GluN3-containing NMDARs are either glutamate/glycine-activated triheteromeric receptors composed of GluN1, GluN2, and GluN3 subunits or glycine-activated diheteromeric receptors composed of GluN1 and GluN3 subunits (Furukawa and Gouaux, 2003; Furukawa et al., 2005). Both assemblies containing GluN3 subunits form cationic channels with strongly reduced Ca^{2+} permeability and Mg^{2+}-block compared to GluN1/GluN2 receptors. The modular design of NMDARs is the same of AMPA receptors, the subunits having regions with an extracellular ATD and ligand binding domain. However, at the resting membrane potential (ca -65mV) they do not permeate ions owing to Mg^{2+} channel block (Nowak et al., 1984). Hence binding of co-agonists glycine and glutamate should coincide with membrane depolarization to trigger permeation through NMDARs (Lerma et al., 1990). The latter remove Mg^{2+} blockage and allows entry of Ca^{2+}.

In the amygdala, NMDARs are present both in the BLA and Centrolateral amygdala (CeLA) neurons though the composition of subunits are different depending on the amygdala region. They consist of GluN1 and GluN2A/2B subunits. NMDARs in Central amygdala (CeA) neurons with slower kinetics have been shown to consist of GluN1/GluN2B subunits hence permeating more Ca^{2+} ions. The NMDARs in the BLA appear critical to the association of CS US in fear conditioning and also involved in dissociation of CS and US subsequently during fear extinction (Davis 1997; Killcross et al. 1997). Indeed, the local infusion of NMDA antagonists into the amygdala blocks the acquisition (Fanselow et al., 1994) and extinction (Zimmerman, 2010) of fear conditioning.

AMPA RECEPTORS (AMPARs)

AMPARs are activated by α-amino-3-hydroxy-5-methyl-4-isoxazolepropionic acid (AMPA) and hence they are named after this ligand. They have four subunits GluA1-4 with a 68% to 75% homology, and forms homotetramers or heterotetramers (Boulter et al., 1990). Each subunit has an identical membrane topology and core structure with 900 amino acids with a molecular weight of 105 kDa. Extracellular ATD is joined by four hydrophobic transmembrane segments TM1-TM4 connecting extracellular ATD and intracellular CTD, with TM2 forming an intramembrane loop. Variability is determined by intracellular CTD affecting protein interaction of AMPARs and post translational modifications that regulate subunit trafficking. GluA1 is critical for activity dependent recruitment of AMPARs to synapses during induction of LTP. This is mainly mediated by CamKII dependent phosphorylation of GluA1 which facilitates interaction with PDZ domain (80-90 amino acids) that further interacts with synaptic proteins leading to trafficking and insertion of GluA1 and GluA2 containing receptors in the post synaptic membrane. Different composition leads to difference in properties like ion selectivity, receptor trafficking to the membrane and conduction properties. AMPARs mediate the largest component of fast synaptic excitatory transmission. A smaller component is mediated by NMDA and Kainate receptors (KARs) (Li and Rogawski, 1998). AMPARs are permeable to Na^+, K^+ and some types to Ca^{2+} ions.

Immunohistochemical studies indicate that AMPARs in BLA PNs carry edited GluA2 forms, hence they present V/I curves which are outwardly rectifying or linear and hence these AMPARs are Ca^{2+} impermeable. Whereas INs express AMPARs which lack GluA2, making them inwardly rectifying and Ca^{2+} permeable (Keller et al., 1991; Jonas and Sakmann, 1992; Mahanty and Sah ,1999). But later on, specific immunohistochemistry studies using antibodies against GluA2 recognising a unique sequence in the carboxy terminus of rat GluA2, suggested that edited GluA2 is restricted to cell soma and proximal dendrites and is absent in the synapses over BLA PNs (Gryder et al., 2005).

Therefore, since targeting of GluA2 to synapses is restricted, AMPARs in synapses of BLA PNs may be more calcium permeable and could play critical role in synaptic plasticity (Gryder et al., 2005). In addition, whole cell recordings from BLA PNs in rat slices indicated that about 70% of the cells show rectification indexes in the intermediate range (from 0.25 to1 of rectification index). These data indicate the co-existence of both Ca^{2+} permeable and impermeable receptors in BLA (Gryder et al., 2005) and hippocampal (Lerma et al., 1994) principal cells. The existence of Ca^{2+} permeable AMPARs (CP-AMPARs) in the BLA may be involved in several NMDA independent synaptic plasticity in interneurons.

Trafficking of AMPARs that lack GluA2 (i.e CP-AMPARs) in the postsynaptic sites of BLA PNs may lead to hyperexcitability in different regions (e.g. the BLA), causing neuropsychiatric disorders like autism spectral disorders (ASDs) and schizophrenia.

KAINATE RECEPTORS (KARs)

KARs are a class of ionotropic receptors distributed throughout the central nervous system (CNS) and localized at both presynaptic and postsynaptic sites (Lerma et al., 2001; Lerma, 2003; Pinheiro and Mulle, 2006).

KAR subunits are encoded by five separate genes (*GRIK1-5*). These have been divided into two separate categories based on their primary sequence homology and whether they assemble as functional homomeric receptors or heteromeric receptor channels. The subunits, GluK1, GluK2 and GluK3 (previously known as GluR5-7) have low affinity for kainic acid and they form homomers or heteromers (along with GluK4 or GluK5) while giving rise to functional receptors. GluK4 and GluK5 subunits are high affinity subunits, displaying low nanomolar affinity for kainic acid and they cannot independently form functional receptors channels but need to co-assemble with low affinity subunits to traffic to the membrane surface and form functional receptors channels (Herb et al., 1992; Werner et al., 1991).

Unlike other iGluRs, KARs function through two modes of signaling, ionotropic as well as metabotropic (Rodríguez-Moreno and Lerma, 1998; Rozas et al., 2003). Ionotropically they gate ion channels permeable to Na^+ and K^+ to cause postsynaptic membrane depolarization. Presynaptically, KARs modulate the release of neurotransmitters like GABA and glutamate and hence modulates inhibitory and excitatory neurotransmission (Rodriguez-Moreno et al., 1997; Contractor et al., 2001; Rodrigues and Lerma, 2012). A little fraction of postsynaptic current is mediated by KARs in some synapses, but they impart synapses with new integrative properties of transmission through a tonic depolarization of the neurons and charge transfer over a longer time window (Frerking et al., 2002).

Metabotropically, they activate G proteins and signal through protein kinase C (PKC) and PLC to cause several effects. For instance KARs cause G protein and PKC dependent reduction of after-hyperpolarization currents (AHPs) to cause increase in neuronal firing in CA1 pyramidal cells of rodents (Melyan et al., 2002). Subsequent evidence from dorsal root ganglion cells strengthened the notion of this non-canonical signaling of KARs (Rozas et., 2003; Rutkowska-Wlodarczyk et al, 2015). In the cultured neurons from dorsal root ganglia, GluK1 containing KARs interacts with G protein, increasing intracellular Ca^{2+} by releasing them from intracellular reservoirs, following inhibition of voltage gated Ca^{2+} channels (Rozas et al., 2003). Later, the non-canonical metabotropic signaling by KARs has been described in many regions of CNS. This metabotropic signaling mediated by KARs is also involved in neuronal and circuit maturation (Marques et al., 2013) and in the formation of synapses in the HPC (Lauri et al., 2005).

Alternative splicing as in AMPARs and NMDARs, leads to diversity in KARs. Different carboxy terminal and amino terminal sequences exist for GluK1-3 subunits but not for high affinity GluK4-5 subunits. A splice site gives rise to two GluK1 isoforms that differs in 15 amino acids segment in the ATD. GluK1-1 variant contains 15 extra amino acids in N-domain lacking in variant GluK1-2 (Bettler et al., 1992). In addition, GluK1-2 subsequently consists of four different isoforms (GluK1-2a- GluK1-2d) based on splice sites in carboxy terminal domain

(Bettler et al., 1990; Sommer et al., 1992; Gregor et al., 1993). Splicing sites in DNA coding for C terminal domain leads to 4 different subunits, two each for GluK2 and GluK3. GluK2 subunit have two isoforms, GluK2a and GluK2b that differs in the last 29 amino acids present in carboxy terminal domain (Egebjerg et al., 1991). GluK3 subunit also has two different isoforms, GluK3a and GluK3b, which are different due to the presence of 13 amino acids in variant GluK3b which are absent in GluK3a. The presence of these 13 amino acids introduces a premature stop codon in GluK3b and makes the carboxy terminal tail end 9 amino acids shorter than variant GluK3a (Schiffer et al., 1997). GluK4-5 doesn't have any isoforms.

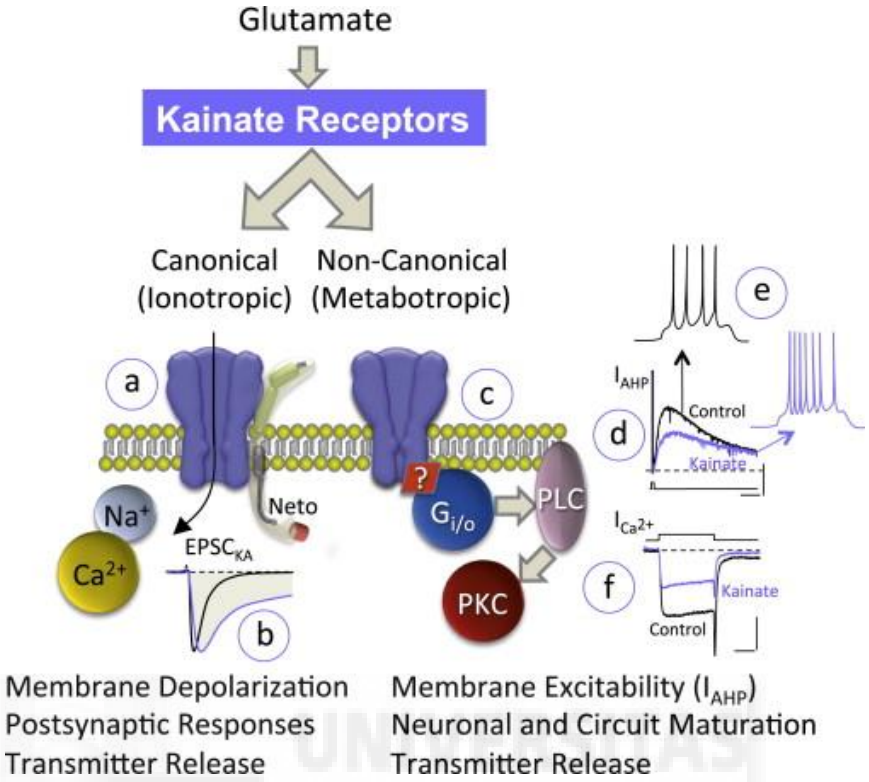

Figure 2: Kainate receptors signal through two modes of signalling: Ionotropically (a) they gate ion channels to cause membrane depolarization and postsynaptic response (b) and facilitation of neurotransmitter release at some synapses. Ionotropic receptors exert their action via some ancillary proteins like Neto. Metabotropically they activate G proteins (c) coupled to several downstream targets such as PKC and PLC. This leads to a several effects such as depression of after hyperpolarization currents (AHPs) d) to cause increased neuronal firing in CA1 hippocampal neurons (e), or modulation of calcium currents (f) to cause facilitation or inhibition of transmitter release leading to neuronal and circuit maturation in hippocampal circuits. Source: Lerma and Marques (2013)

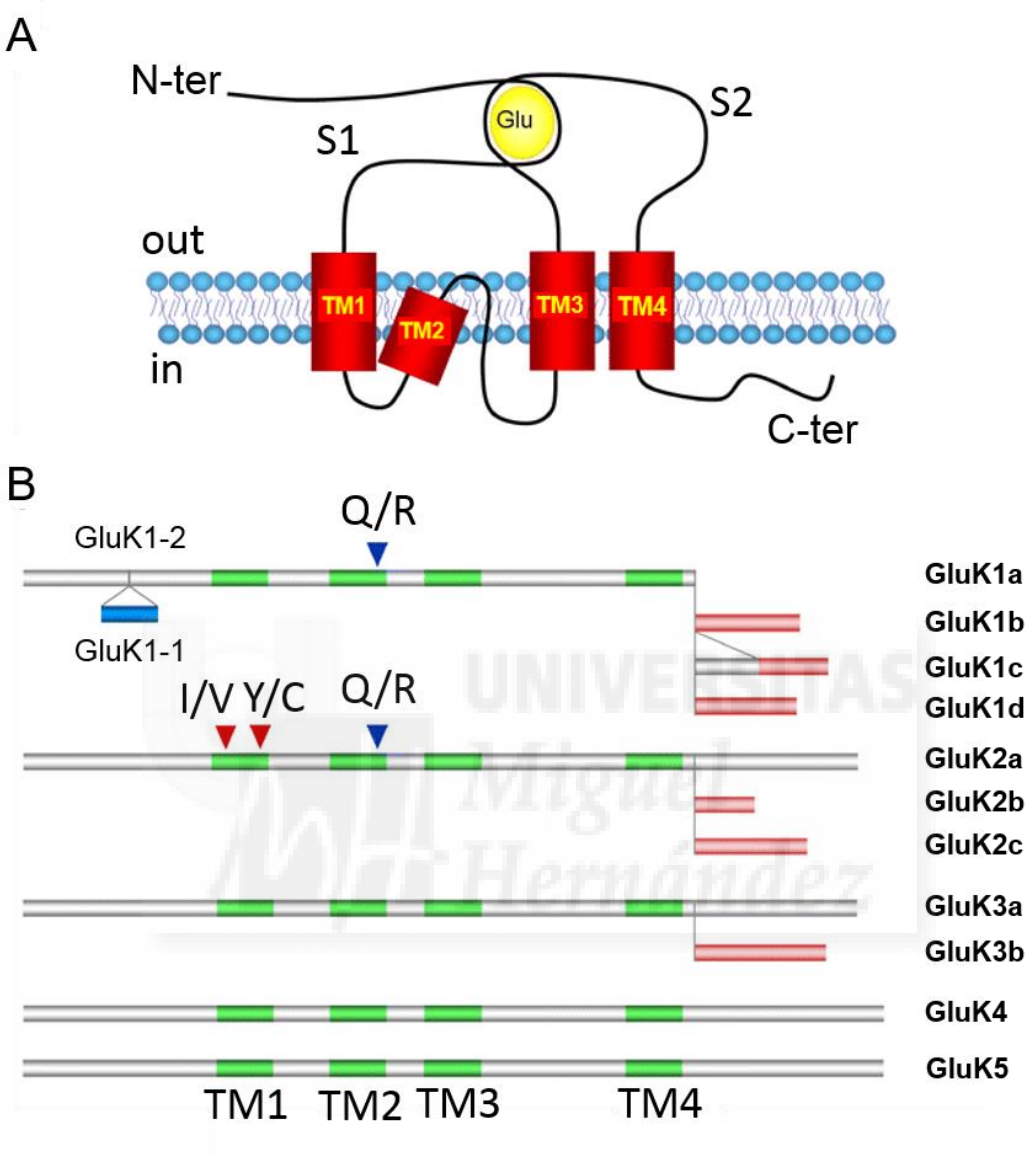

Figure 3: Structure and diversity of KAR subunits (A) Membrane topology of KAR subunits. KAR subunits have extracellular N terminal domain followed by transmembrane domains (TM1, TM3 AND TM4) Like AMPARs, TM2 forms a re-entrant loop in KAR subunits that dips in the lipid bilayer forming the pore. Extracellular glutamate binding domain is formed by S1 (region arising from TM1) and S2 (region between TM3 and TM4). N terminal domain maintains the assembly of tetrameric KARs. TM4 leads to an intracellular C terminal domain that regulates trafficking of KARs (B) Different splice variants of GluK1, GluK2 and GluK3 subunits. mRNA editing sites have also been illustrated for GluK1 and GluK2. Adapted from Pinheiro and Mulle (2006)

1.3.3 Ca^{2+} permeability of AMPARs and KARs

Both AMPARs and KARs undergoes post-transcriptional modification, better known as Q/R editing, which occurs at the mRNA level at TM2 in GluK1 and GluK2 of KARs and GluA2 of AMPARs. This modifications determine conductance of the channels, rectification properties and calcium permeability. Replacement of glutamine (Q) by an arginine (R) at TM2 in GluK1 and GluK2 of KARs and in GluA2 of AMPARs makes the channels calcium impermeable (Burnashev et al., 1996), thus also modifying their rectification properties. This Q/R editing makes the AMPAR and KAR ion channels less conductive to cations and slightly outwardly rectifying (Sommer et 1991). The mechanism by which Q/R editing in AMPAR and KAR channels decreases Ca^{2+} conductance is based on the presence of an arginine positively charged residue that prevents cations to pass through the channel pore. Also, in the Q/R edited channels, arginine presence inhibits the entry of polyamines through the pore formed by TM2 segment making the channel non rectifying or slightly outward rectifying (Bowie and Mayer et al., 1995). The Q/R edited AMPAR and KAR receptor channels thus show linear or outward rectification in voltage to current (V/I) relationships. On the other hand, the presence of a glutamine instead of arginine at TM2 domain of unedited GluA2 of AMPARs and unedited GluK2 of KARs leads to CP-AMPARs and KARs respectively. The latter type is inwardly rectifying in V/I relationships and permits Ca^{2+} entry through its ion channel (Burnashev et al., 1992). In addition to Q/R editing, KAR subunit GluK2 can also undergo I/V editing (isoleucine replaced by valine) and Y/C editing (tyrosine replaced by valine) in the M1 domain. These editing sites in GluK2 also play a role in reducing Ca^{2+} conductance (Kohler at al., 1993).

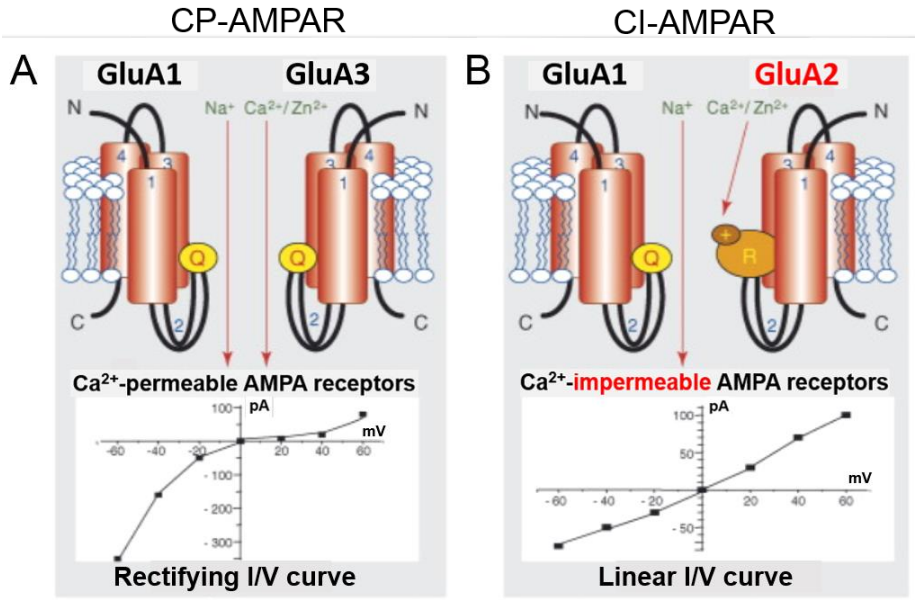

Figure 4: Subunit composition control calcium permeability of AMPARs. AMPARs containing edited GluA2 are Ca^{2+} impermeable with linear current voltage relationships. Q/R editing or replacement of glutamine by arginine at TM2 abolishes calcium permeability of AMPARs decreasing single channel conductance and leading to outward rectification properties. On the contrary Heteromeric AMPARs lacking GluA2 or containing unedited GluA2 are Ca^{2+} permeable and display inward rectification properties. Source: Liu and Zukin (2007)

1.4 DISTRIBUTION AND PHARMACOLOGY OF KAINATE RECEPTORS

1.4.1 DISTRIBUTION OF KAR SUBUNITS

The distribution of KAR subunits in the CNS have been studied mainly by *in situ* hybridization at the mRNA level. At the protein level, lack of availabilities of antibodies to detect KAR subunits has been a major limitation to investigate KARs protein distribution in the CNS. Nevertheless, some antibodies for determining the distribution of GluK2 subunit containing KARs in the CNS are now available. Analysis by *in situ* hybridization has revealed widespread and heterogenous distribution of KAR subunits throughout the nervous system (Bahn et al., 1994; Wisden and Seeburg et al., 1993).

GluK1 transcripts has been detected in layer 2 and layer 6 of neocortex, cingulate and pyriform cortex, hippocampal formation, cerebellar Purkinje cells, striatum and Hyp. *Grik1* expression is also abundant in temporal lobe structures like amygdala circuits. Also, INs of CA1 and CA3 express GluK1 subunits in stratum oriens and stratum pyramidale (Paternain et al., 2000). Levels were quite abundant in the pyriform cortex and bed nucleus of stria terminalis (BNST). GluK2 subunits have been detected in the PNs of the cortex and hippocampus (Paternain et al., 2000). GluK2 is most abundant in CA1 and CA3 regions of hippocampal and cerebellar granule cells. GluK2 containing receptors mediates post synaptic response at the mossy fiber-CA3 synapse where GluK2/5 is the most commonly detected configuration. mRNA levels of GluK2 are also high in most regions of the amygdala. GluK3 has the lowest mRNA expression amongst all the subunits, being localized in the cortex, especially cingulate cortex and the layer 4. Also, GluK3 has been detected in granule cells of DG in the HPC and the stellate basket cells of the cerebellum.

GluK4 mRNA is seen mostly in the HPC, most abundantly in CA3 and DG granule cells. Also, weak expression of GluK4 was noted in cortex, striatum, and hypothalamus (Hyp) (Wisden and Seeburg.,1993). Purkinje cell layer of the cerebellum also showed GluK4 mRNA and protein (Darstein et al., 2003; Werner et al., 1991). A recent study in our lab using more specific non-radioactive in situ hybridization indicated GluK4 to be more widely distributed and contrary to previously believe, the expression was not just restricted to hippocampal CA3, DG and Purkinje cells of the cerebellum. Abundant mRNA transcripts were also detected in CA1 and putative INs of stratum lucidum and stratum oriens in HPC (Arora et al., 2018). All layers of neocortex showed a significant expression of GluK4 mRNA along with temporal lobe structure such as the amygdala complex (Arora et al., 2018).

Lastly, GluK5 transcripts are widely distributed throughout the brain including neocortex, HPC, striatum, thalamus, Hyp, granule cells of cerebellum and pineal gland. There is a mild expression observed also in amygdala circuits.

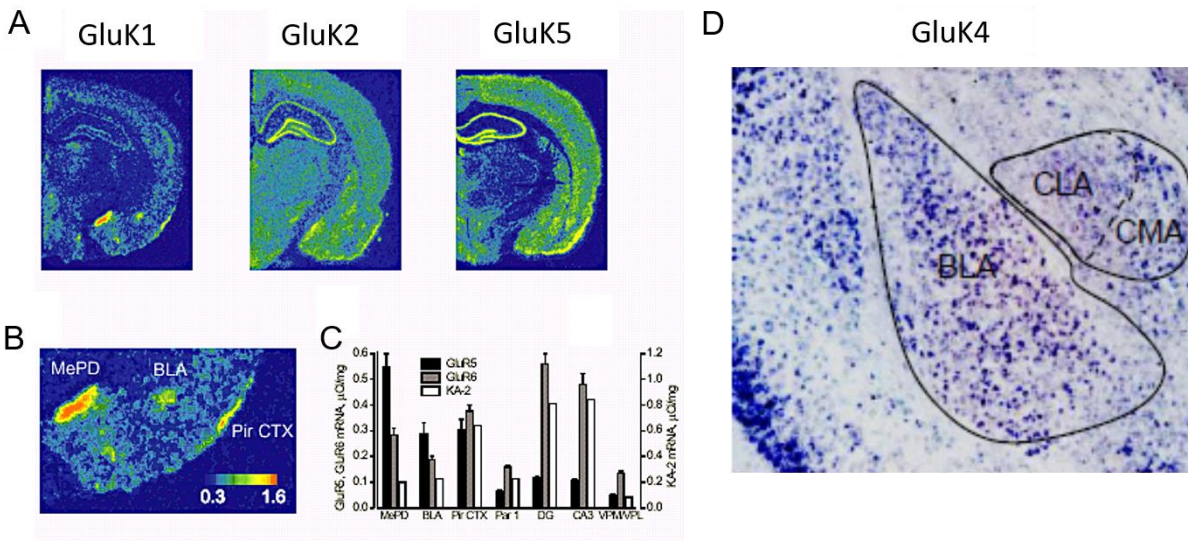

Figure 5: Expression of different KAR subunits in the amygdala. (A) Pseudocolor images of GluK1, GluK2 and GluK5 mRNA expression as revealed by radioactive in situ hybridisation at the level of the amygdala. (B) Enlarged view of temporal lobe region showing dense expression of GluK1 mRNA in limbic lobe structures such as MePD, BLA amygdala nuclei and Pir CTX. (C) Quantification of kainate receptor subunit mRNA expression in five brain regions. GluK1 mRNA expression is highest in temporal lobe structures, including the BLA while GluK2 and GluK5 mRNA levels are strongest in the HPC. (D) Recent study in our lab using more specific non-radioactive in-situ hybridisation found GluK4 mRNA as abundantly expressed in BLA and all central amygdala nuclei including CLA and CMA. MePD, posterodorsal medial amygdala; BLA, basolateral amygdala; Pir CTX, piriform cortex; Par 1, parietal cortex; DG, dentate gyrus; CA3, hippocampal CA3 subfield; VPM/VPL, ventroposteromedial and ventroposterolateral nuclei of the thalamus; CLA centrolateral amygdala; CMA, centromedial amygdala. Adapted from Li et al., 2001 and Arora et al., 2018

1.4.2 PHARMACOLOGY OF KARS

The major limitation in the study of function of KARs has been lack of availability of specific agonists and antagonists (Lerma, 2003). Most of the agonists and antagonists developed against KARs have been through studies using the cloned KAR subunits in heterologous expression systems. Since GluK4 and GluK5 cannot form functional KARs without assembling with low affinity subunits GluK1-3, success in the studies using cloned KAR subunits in heterologous expression systems have been limited. Radioligand binding assays involving Kainate (KA) binding to KARs paved the way for identification of low affinity subunits of KARs (GluK1-3) having dissociation constant (K_d) of 50-100 nM and high affinity KAR subunits (GluK4-5) with dissociation constant (K_d) of 4-15 nM. Glutamate as an

agonist of KARs has similar properties. Other subunit selective KARs agonists are available including ATPA that has 500-fold more affinity for GluK1 containing KARs than for AMPARs.

Amongst iGluRs, pharmacological isolation of KARs over AMPARs mediated currents was unsuccessful until the identification of GYKI53655 (Paternain et al, 1995). Until then, the only available compounds were specific non-NMDARs antagonists, like 6 cyano-7nitroquinoxaline-2, 3-dione (CNQX), 6,7-dinitroquinoxaline-2,3-dione (DNQX), which were antagonists of both AMPARs and KARs.

Available agonists were not of a help either. For instance, AMPA, which is the prototypic agonist of AMPARs does activate KARs too, especially those heteromeric receptors including GluK5 and GluK4 having also an effect on GluK1 containing KARs (EC_{50} of 3 mM). This was true for both cloned subunits in heterologous systems (Egebjerg et al., 1993) and native KARs in cultured hippocampal neurons (Lerma et al., 1993). On the contrary, Kainate, an agonist of KARs, also activates both KARs and AMPARs. KA is able to behave as an agonist on AMPARs at very low doses, with EC_{50} being just 5 to 30-fold lower for KARs than AMPARs (Paternain et al., 1996)

Major breakthrough in KAR pharmacology was the discovery of the compound GYKI 53655, a noncompetitive antagonist of the AMPARs which allowed direct measurement of KAR mediated currents (Paternain et al., 1995; Wilding and Huettner, 1995). Many other antagonists were subsequently discovered and made available. For instance, LY382884 is a GluK1 specific antagonist with a similar effect on GluK1 homomers and GluK1 containing heteromers (Christensen et al., 2004). LY382884 is quite specific and has a weak action at NMDARs and no effect whatsoever on GluA1-4 containing AMPARs and GluK2-3 containing KARs. UBP310, a willardine derivative is another KAR antagonist originally developed against GluK1 containing KARs (Dolman et al., 2007) but later it was found that UBP310 antagonize diverse KARs including GluK1 containing KARs, GluK2/5 heteromeric and GluK3 containing homomeric KARs (Perrais et al., 2009).

1.5 THE AMYGDALA: CYTOARCHITECTURE, CIRCUITARY AND PHYSIOLOGICAL ROLE

Amygdala, located in the anterior region of the temporal lobes is a critical brain structure of the limbic system that regulates a myriad of emotional behaviours especially fear and anxiety responses. In the first half of nineteenth century, the German physician Karl Burdach coined the term amygdala (Greek for ´Almond´) for a group of cell bodies in the anterior temporal lobe. This later came to be known as BLA. Further, with the advancement of histological techniques, Johnston (Johnston, 1923) found that regions dorsal and medial to this group of cell bodies have anatomical connections with BLA. Hence in the 20th century, the whole structure was referred to as amygdaloid complex, consisting of 13 nuclei divided into four major physiologically and morphologically distinct regions.

Emotionally relevant experiences are exceptionally stored in memory irrespective of whether they are gratifying or disturbing, as they carry information indispensable for survival and reproductive success. For instance, we can always effectively recall events that are emotionally relevant, e.g. watching great artwork gradually establishes feelings towards a person, we tend to connect the art with. These emotional instances get stored in the memory forever. Or even walking in a forest and encountering wildlife can arouse feelings of anxiety and fear essential to survival of the person and hence these instances also becomes imprinted vividly in person's memory. Decades of research have focussed on mechanisms of strengthening of emotionally relevant memories. The well-known emotional tagging theory (Bergado et al., 2011) proposes that amygdala gets activated in response to environmental stimuli of emotional significance. Consequently, amygdala strengthen the connections to vHPC via synaptic plasticity thus encoding those memories that are associated to facts or events or in other words explicit memories (Vouimba et al., 2007). It is essential to understand the process of formation and storage of memories of pleasant (feelings of love towards something) and traumatic experiences like fear and

anxiety because recall of such memories can become dysfunctional or maladaptive. For instance, post-traumatic stress disorders (PTSD) or exposure to acute and intense fearful situations and anxiety related disorders can lead to excessive anguish or anxiety even if there is no real situation involving threat.

The amygdala is a promising target for therapeutic interventions which are in progress for the treatment of pathological fear and anxiety related disorders. As it is clear that amygdala is critical in controlling declarative or explicit memories via connections to the HPC and it also acquires and stores fear or anxiety related and several other emotional memories. Accordingly, lesions of amygdala leads to disruption of perception of associative fear learning (Bechara et al., 1995; LaBar et al., 1995). Mounting evidence from a number of behavioural, electrophysiological and optogenetic studies have led to the notion that synaptic plasticity between amygdala neurons in the BLA and CeLA is the driving force behind formation of memories related to association of aversive (or appetitive) stimuli in response to an auditory, olfactory or visual cue (Duvarci and Paré, 2014).

The amygdala is extensively wired to other brain regions like HPC, BNST, and the Hyp, the nucleus accumbens (NAc), the medial prefrontal cortex (mPFC), the periaqueductal gray (PAG) to name a few, and dynamic plastic interactions between these connections are involved in orchestrating acute and chronic behavioural responses to emotionally relevant stimuli (Janak and Tye, 2015; Tovote et al., 2015). Decades of neuropharmacological investigations aimed at drug discovery were unsuccessful in yielding major breakthroughs providing therapy for pathological fear and anxiety related disorders, like PTSD. Hence cell specific circuit manipulations via optogenetics to explore interaction of amygdala neurons with other brain areas are starting to unravel mechanisms behind amygdala powered encoding of aversive, appetitive or other emotional information. Further reprogramming these functionally aberrant circuits in case of fear and anxiety related neural diseases is a step forward in leading us to therapeutic discoveries (Janak and Tye, 2015).

The amygdaloid complex comprises a number of nuclei. The BLA is often subdivided into lateral (LA) and basal nuclei (BA). Other nuclei include the basomedial amygdala (BMA) and CeA.

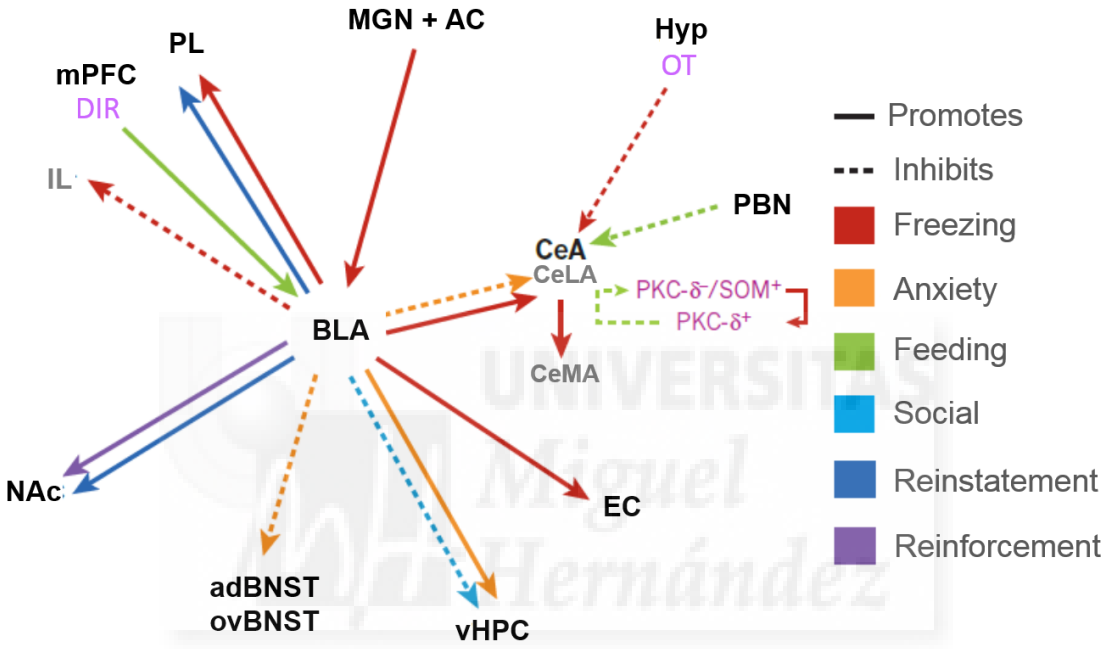

Figure 6: Defined neural innervations to the amygdala and outputs from the amygdala that control emotionally relevant behaviours. Anatomically or electrophysiologically defined afferent and efferent pathways of the amygdala that facilitate or suppress specific emotional behaviours. AC, auditory cortex; adBNST, anterodorsal bed nucleus of the stria terminalis; CeA, central nucleus of the amygdala; IL, infralimbic; NAc, nucleus accumbens; OT, oxytocin; mPFC, medial prefrontal cortex; EC, entorhinal cortex; Hyp, hypothalamus; MGN, medial geniculate nucleus; ovBNST, oval nucleus of the BNST;; PKC, protein kinase C; PL, prelimbic; SOM, somatostatin; vHPC, ventral hippocampus; CeLA, lateral CeA; CeMA, medial CeA; D1R, dopamine 1 receptor; PBN, parabrachial nucleus; Source: Janak and Tye, (2015).

CeA is subdivided into CeLA and centromedial amygdala (CeMA) and lastly intercalated cell masses (ICMs) also forms part of the amygdala surrounding the BLA and at the interface between BLA and CeA (Pitkänen, 2000; Sah et al., 2003). The BLA, CeA and ICMs have received particular attention, mainly due to

their unambiguous involvement in fear conditioning and anxiety circuits (Duvarci and Paré, 2014; Janak and Tye, 2015).

The lateral amygdala (LA) is the most dorsal part of the BLA and receives the majority of the sensory inputs, while CeMA functions as the major output of the amygdala transmitting decisive information to brainstem effector regions through inhibitory projections. BLA resembles more the cerebral neocortex in cytoarchitecture and has a predominant population of PNs that use glutamate as neurotransmitter with a minority of cells being GABAergic INs (McDonald, 1984). On the contrary, CeA is like the ventrocaudal extension of striatum, so neurons in CeA are entirely GABAergic neurons (McDonald, 1982). The amygdala anatomical organization is well conserved across the species (Pabba., 2013; Janak and Tye., 2015).

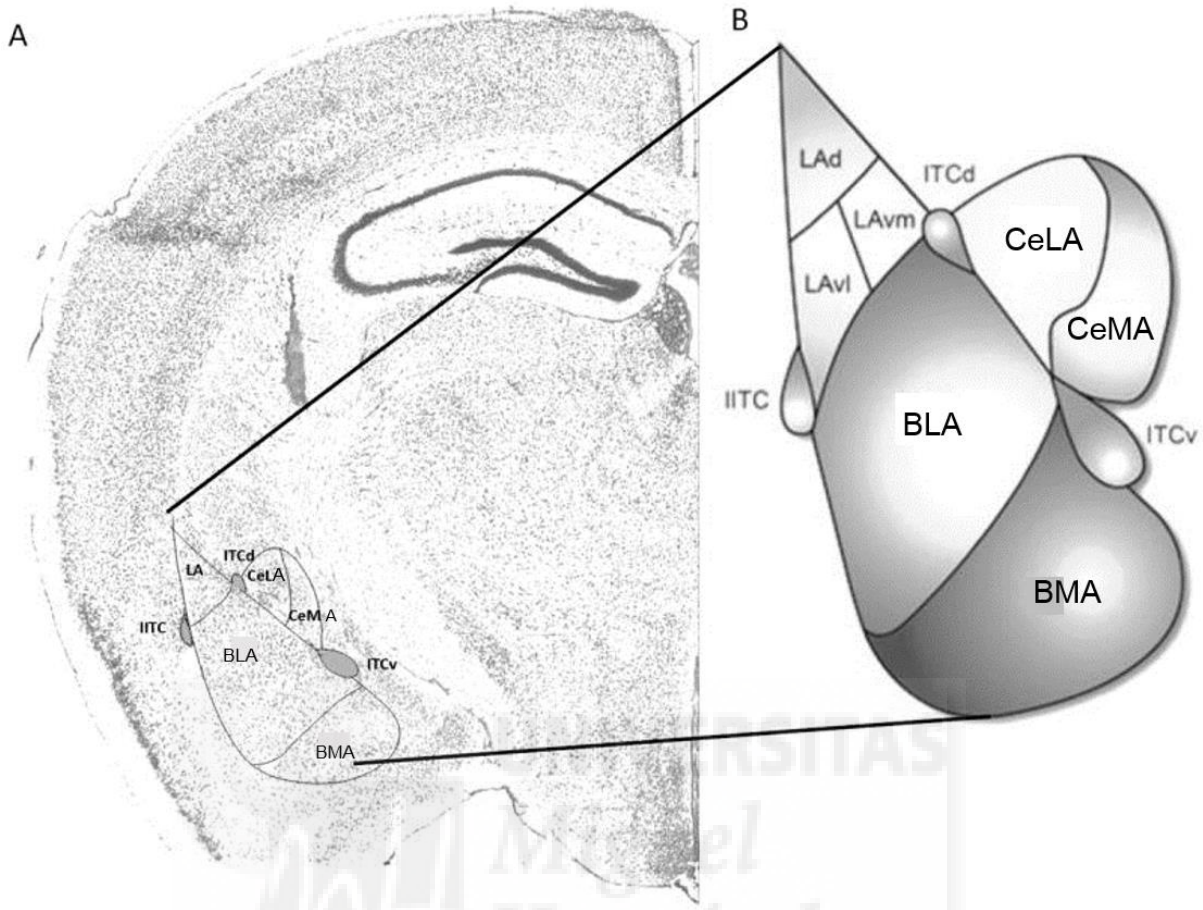

Figure 7: Location of different subregions of the amygdala.

A. Nissl stain of transverse brain section from mouse (Image Credit: Allen Brain Atlas). B. Schematic diagram of amygdala complex. Abbreviations: Lad (Lateral amygdala dorsal), LAvm (Lateral amygdala ventromedial), BMA (Basomedial amygdala), IITC (Lateral Intercalated cells), LAvl (Lateral amygdala ventrolateral), ITCd (Intercalated cells dorsal), ITCv (Intercalated cells ventral), BLA (Basolateral amygdala), CeLA (Centrolateral amygdala), CeMA (Centromedial amygdala). Adapted from Lee et al., (2013); Gafford and Ressler et al., (2017)

1.5.1 CYTOARCHITECTURE AND PHYSIOLOGY OF BASOLATERAL AMYGDALA

The BLA is bordered by two fibre bundles: the external capsule (EC) laterally, separating BLA from cortex, and the internal capsule medially, separating the BLA from the CeA. Both BLA subdivisions, BA and LA consist of 80% excitatory large spiny pyramidal shaped PNs regulated for changes in excitatory activity by 20% smaller in size, sparsely spiny GABAergic inhibitory INs (McDonald, 1992, Spampanato et al.,2011). Ex vivo, when depolarized with current injections, PNs

display adaptive firing and broad (~1 ms half-width in whole-cell mode) action potentials (APs; Sosulina et al., 2006). A minority of PNs are intrinsically bursting neurons (Paré et al., 1995) while the majority are regular spiking neurons with a variable adaptation patterns prevalent due to different K^+ conductances owing to differential expression of voltage and Ca^{2+} dependent K^+ channels (Faber and Sah et al., 2002).

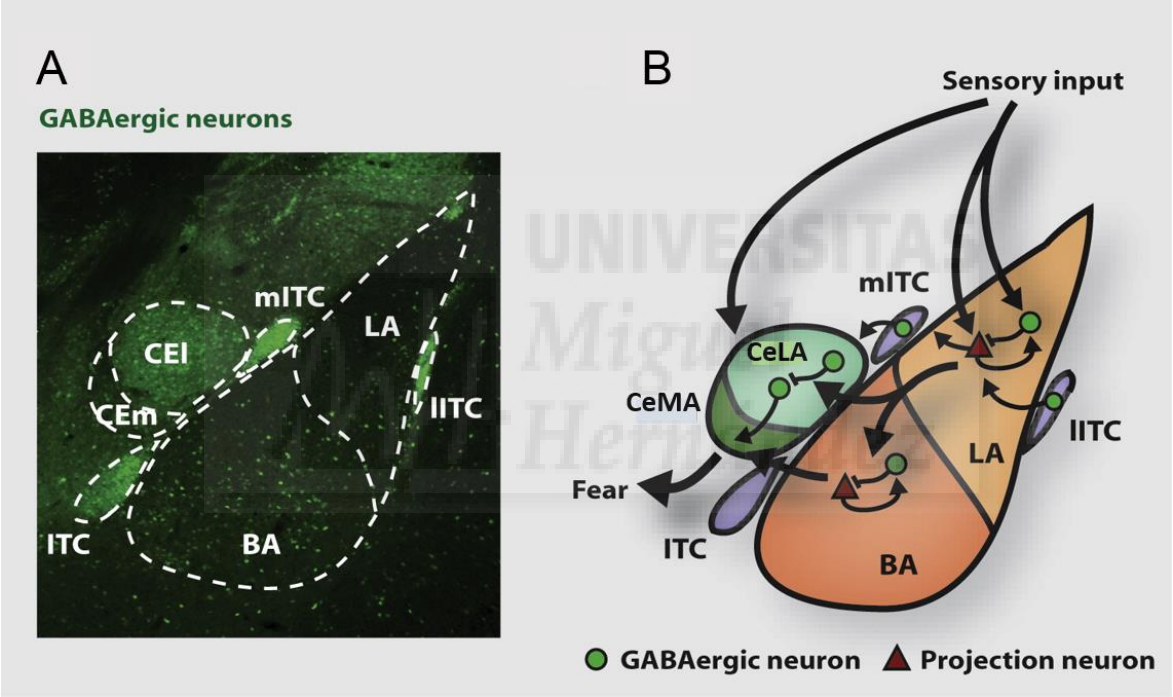

Figure 8*:* Subdivisions, basic organisation, and flow of information in the amygdala of the mouse. Scheme of the different subregions and overall information transfer within the amygdala. (A) Transverse brain slice stained for the enzyme glutamic acid decarboxylase (GAD67) depicting GABAergic INs distribution across the amygdaloid complex. (B) Simplified scheme of the organization and function of projection neurons PNs and inhibitory INs in amygdaloid nuclei. In the lateral nuclei and Basal nuclei of the amygdala, local INs control outputs of the projection neurons. lITCs and mITCs relay feedforward inhibition to the BLA and CeA, respectively. Output projections of neurons of the CeLA has inhibitory control over CeMA neurons. CeLA output is regulated by intrinsic CeLA inhibition mediated between LFCs and RFCs. Adapted from Ehrlich (2009).

The amygdala has quite abundant intranuclear and internuclear network connections. For instance, axons of PNs in the BLA innervate other brain regions distally (McDonald, 1982; Millhouse and DeOlmos, 1983) whereas locally, PNs are connected via multiple axon collaterals forming 100-200 synapses per mm of axon to other BLA neurons including both PNs and INs (Smith and Paré, 1994). The activity of PNs is tightly regulated by the release of GABA from BLA INs, which are characterized by mostly aspiny dendrites and widely branching local axons (McDonald, 1982; Millhouse and DeOlmos, 1983). BLA INs are critical neurons as they release GABA to cause feedforward inhibition of PNs. The depression of this feedforward inhibition leads to expression of LTP at excitatory synapses onto PNs, hence INs function as regulators of synaptic plasticity (Watanabe et al., 1995).

BLA INs are heterogeneous like the INs of other brain regions like cortical INs (Ascoli et al., 2008) and HPC INs (Klausberger and Somogyi, 2008), and they have different categories depending on shape and size of soma, dendritic branching, expression of different Ca^{2+} binding proteins or neuropeptides and electrophysiological properties (McDonald and Mascagni, 2001). Thus, INs have distinct intrinsic membrane properties owing to different expression of neuropeptides and they fire according to the brain states (Muller et al., 2006; see also Woodruff and Sah, 2007). The majority of BLA INs are local neurons contacting different compartments of their postsynaptic targets but a subset are also projection neurons having connections to basal forebrain (McDonald et al., 2012). Two BLA IN populations are prominent in the BLA, the parvalbumin (PV)-expressing INs, accounting for ~50% of the BLA INs (McDonald and Mascagni, 2001), and somatostatin (SOM)-expressing, accounting for 11-18% (McDonald and Mascagni, 2002). BA has majority of PV^+ INs (McDonald and Mascagni, 2001) which innervates the PNs perisomatic region (Wolff et al., 2014). In vivo, PV^+ INs display higher frequency of firing APs as compared to PNs (Muller et al., 2006). Ex vivo, PV^+ INs are fast spiking INs having very little adaptation and high frequency (up to ~100 Hz) of short (~0.5 ms half-width) APs (Rainnie et al., 2006).

PV^+ INs receive strong inputs from PNs, but less inputs from cortical regions. They are of two types, 1) Basket cells are fast spiking INs innervates the perisomatic region of the PNs (Wolff et al., 2014) and 2) Non-Basket cells, which have boutons contacting distal dendrites and axon initial segments of PNs (Sorvari et al., 1995). The major function of basket cells and non-basket cells is to control the activity and output of PNs (Veres et al., 2014). PV^+ INs play a very important role in controlling anxiety related behaviour (Hale et al., 2010).

SOM^+ INs form synapses with distal dendrites of PNs (Muller et al., 2007) and play a role in feedback inhibition of PNs (Wolff SB, et al., 2014). Strong evidence through cFos immunohistochemistry indicates activation of SOM^+ INs under anxiogenic conditions (Butler RK et al., 2012). Also, in other behavioural studies activation of SOM^+ neurons increases the time spent by mice in open arms of Elevated plus maze, thus having an anxiolytic effect (Fuchs et al., 2016). All this data confirms the role of SOM^+ INs in anxiolysis.

Other types of INs are the CB^+ INs representing the largest class of BLA INs, accounting for ~60% of all GABAergic cells (McDonald and Mascagni, 2001) and calretinin (CR) expressing INs, which include cells that also express vasointestinal peptide (VIP), together with small CCK^+ neurons (most of which are also VIP^+; Mascagni and McDonald, 2003).

Importantly, as compared to cortex or HPC, the diversity of INs in BLA is not very well understood (Capogna, 2014).

1.5.2 AFFERENT CONNECTIVITY OF THE BLA

Several studies involving tracer experiments in rats, cats and non-human primates have shed light on afferent connectivity of the BLA. The BLA receives wide range of sensory glutamatergic afferents carrying visual, auditory, gustatory, olfactory and visceral information. The majority of these afferents come from higher order association areas of the cerebral cortex (McDonald, 1998) and

sensory thalamus (Sah et al., 2003). Auditory information comes to the LA from both the temporal association cortex (TeA) and the medial geniculate nucleus (MGN) of the thalamus (LeDoux et al., 1990; 1991). Information regarding taste (gustatory) and internal hormonal state (visceral) is relayed to the BLA from the insular cortex (Shi and Cassell, 1998). Information regarding smell makes its way to the BLA from the piriform cortex and the anterior olfactory nucleus (Luskin and Price, 1983).

The somatosensory information (pressure sensations, pain, warmth, etc) is relayed to the BLA from the parietal insular cortex (Shi and Cassell, 1998) and also from the thalamus (Linke et al., 2000).

Along with sensory and somatosensory information that reaches LA, memory information is also received in the BA of the amygdala from glutamatergic projections of the PNs in perirhinal (Shi and Cassell, 1999) and entorhinal (McDonald and Mascagni, 1997) cortices, together with the ventral CA1 (vCA1) region of the HPC and the subiculum (Kishi et al., 2006). INs of vCA1 region of the HPC also send GABAergic projections to the BLA but their role needs further investigation (Müller et al., 2012).

Thus, LA and BA perform different computations of the signals depending upon the environmental cue faced by the organism and integrates sensory, somatosensory and memory information, a process known as flexible gating (Paré et al., 2003 see also Duvarci and Paré., 2014).

1.5.3 EFFERENT CONNECTIVITY OF THE BLA

Efferent connections of the BLA includes intra-amygdala outputs and extra-amygdala outputs.

1.5.3.1 Intra-amygdala outputs of the BLA

Thus, processed sensory, somatosensory and memory information from the LA and BA of the amygdala is forwarded through intraamygdala projections to the CeA. The LA PNs sends projections to the BA, and both LA and BA PNs targets, among other brain regions, the CeA (Krettek and Price, 1977) thus projections from BLA are relayed to CeA dorsoventrally. There is either a direct connection from BA to CeA or information is feedforwarded to CeA through Intercalated GABAergic cell clusters (ICMs). The PNs in LA appear to innervate the CeLA, but not the CeMA. In contrast, the PNs at the BA project to both CeLA and CeMA (Savander et al., 1995). This is important because the majority of output of CeA neurons is relayed from the CeMA to the brain stem regions like BNST, PAG, Periventricular thalamus (PVT), etc and these projections depending on excitation or inhibition of CeMA cells are able to trigger fear, anxiety and reward behaviours (Ciocchi et al., 2010; Duvarci and Paré, 2014).

1.5.3.2 Extra-amygdala outputs of the BLA

The BLA in addition to receiving extensive inputs relating to different sensory modalities, also targets multiple brain areas. Different extra-amygdaloid outputs from the BLA facilitate distinct behaviour responses hence knowledge of functional connectivity of each of these projections is very important and is still under investigation (Felix-Ortiz et al., 2013; Senn et al., 2014). Both BA and LA, but mostly LA projects to entorhinal, insular and perirhinal cortices (Krettek and Price, 1977). The BA PNs also innervate mPFC including both prelimbic and infralimbic cortical regions.

The BLA projections also reach the HPC. The PNs at BA mostly project to vCA1 while the LA have sparser projections to vCA1. These projections from the BA PNs synapsing onto vCA1 are critical to anxiety related behaviours as evidenced from optogenetic manipulations (Felix-Ortiz et al., 2013). In fact, activation of BLA

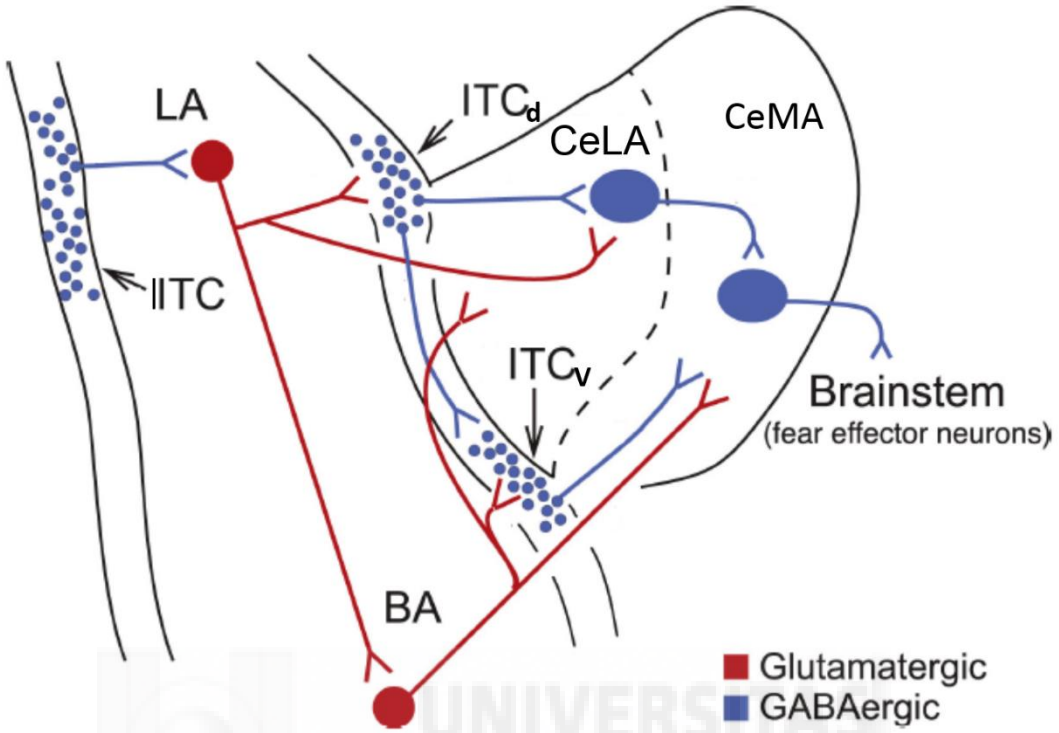

Figure 9: BLA and CeA connectivity. LA communicates dorsoventral information to CeMA. LA PNs sends projections to BA PNs. LA PNs also innervates CeLA, but not CeMA. Both CeLA and CeMA receives inputs from BA PNs. Lateral IITCs via assistance of glutamatergic inputs from the external capsule mediate feedforward inhibition of BLA neurons, while feedforward inhibition to CeA neurons is mediated by medial ITCs (ITCd and ITCv). Source: Duvarci and Pare, (2014).

projections to the vHPC increases anxiety-related behaviours for instance, mice spend less time in the open arms of elevated plus maze (EPM), and less time in the center of open field during open field test (OFT). On the other hand, inhibition of the BLA projections to the vHPC decreases anxiety-related behaviours, thus increasing the time spent by the mice in the open arms of EPM, and in the center of open field during OFT (Felix-Ortiz et al., 2013). The BA PNs also innervates directly subcortical regions namely the mediodorsal thalamus (Krettek and Price, 1977; McDonald, 1991), and BNST (Krettek and Price, 1978) and these connections provide additional support to the processing of physiological and behavioural responses underlying emotional information like anxiety and fear (Walker et al., 2003; Tovote, 2015) And specifically the projections from BA PNs innervating ventral striatum (ventral caudate-putamen and NAc) is involved in reward learning (Stuber et al., 2011).

1.5.4 INTERCALATED CELL MASSES (ICMs)

This encompasses GABAergic cells, which are dorsal intercalated cell masses (ITCd), ventral intercalated cell clusters (ITCv) and medial intercalated cell clusters (ITCm) situated in the internal capsule at the interface between BLA and CeA. ITCd divides LA and dorsal CeLA, ITCv separates BA and ventral CeLA, while ITCm borders the CeMA and is located at the boundary between BA and CeMA (Knapska et al., 2009). Also found in the EC, lateral intercalated cells (IITc) are located at the interface between Cortex and BLA. These densely packed clusters of inhibitory neurons at the interface of Cortex-BLA and BLA-CeA, contributes as a critical source of inhibition in the cortico-amygdala and intra-amygdala circuits (Ehrlich et al., 2009; Marowsky et al., 2005). Therefore, in addition to local INs in the BLA described above, feedforward inhibition onto BLA PNs and CeA INs is driven by ICMs located in external and internal capsules that surround the BLA (Millhouse, 1986; Asede et al., 2015). Most prominent type of cell in all these ICMs is a regular spiking neuron having a high input resistance and high intrinsic excitability while it shows a modest adaptation (Marowsky et al., 2005; Geracitano et al., 2007).

1.5.5 CYTOARCHITECTURE AND PHYSIOLOGY OF CENTRAL AMYGDALA

CeA, a striatal like structure is the main output nuclei of the amygdaloid complex that has exclusively GABAergic cells including local and projection neurons having distinct functional roles (Jolkkonen and Pitkänen,1998; Ciocchi et al., 2010; Haubensak et al., 2010; Lee et al., 2013). CeA is subdivided into CeLA and CeMA both of which project to different regions. CeLA receives glutamatergic inputs from the BLA. CeMA on the other hand receives 85% GABAergic inputs from CeLA and 15% glutamatergic inputs from BLA and it projects mainly to the brain-stem but also to Hyp and striatal regions (Hopkins and Holstege 1978). The predominant population of neurons in the entire CeA is GABAergic interneurons.

Cells in the CeLA are medium-sized, densely spiny neurons medium resembling spiny neurons of the Striatum (Hall et al.,1972). Based on electrophysiological properties, the CeLA mainly consists of four types of neurons: late firing cells (LFCs), regular firing cells (RFCs), low threshold bursting and fast spiking INs (PV^+ INs). LFCs account for up 50-60% of the CeLA population and fire with a delay of about 200 ms when depolarized. LFCs fire with a delay due to their voltage dependent outward rectification properties, accordingly they are sensitive to low µM concentrations of 4-Aminopyridine (4-AP; McCormick 1991; Storm et al., 1988). LFCs also exhibit slowly inactivating delayed rectifier type K^+ conductance which shows rapid activation kinetics at around -65 mV while hyperpolarization below -100 mV is necessary for full inactivation (Gabel and Nisenbaum, 1998).

In the CeLA, 30-40% cells are RFCs that fire regularly without the characteristic delay. Also present in the CeLA are fast spiking PV^+ INs with almost negligible adaptation, high input resistance and high firing frequency. Low threshold bursting neurons is the fourth type of cells present in the CeLA which are similar to thalamocortical neurons in their firing properties. They show spike burst of two to seven APs followed by silent period and this sequence is repeated again. This pattern is due to the presence of a calcium conductance that is inactivated at resting membrane potentials and goes back to normal upon hyperpolarization.

On the basis of immunohistochemical expression of proteins, the INs in the CeLA are mainly classified into either Protein Kinase C-δ^+ (PKC-δ^+) or Protein Kinase C-δ^- (PKC-δ^-). Most of PKC-δ^- cells are also Somatostatin-positive (SOM^+) as they express Somatostatin (Yu et al., 2016; Lee et al., 2013). The PKC-δ^- type and PKCδ^+ are also classified as CeLA ON cells and CeLA OFF cells, respectively based on increased and decreased activity following fear conditioning and they are known to mutually inhibit each other. CeLA ON cells or PKCδ^- cells are mainly RFCs and respond to fear conditioning with an increased activity (Yu et al., 2016). But CeLA OFF cells or are predominantly LFCs and respond to fear conditioning with a decreased activity (Haubensak et al., 2010). Also, PKC-δ^+ cells form monosynaptic connections with PAG projecting cells of

the CeMA (Veening et al. 1984). CeMA neurons have moderate to sparse spine density unlike CeLA neurons (Cassel and Gray 1989; Kamal and Tömböl 1975). A prominent population (95%) in CeMA are LFCs, which display a marked voltage- and time-dependent outward rectification. Consequently, CeMA LFCs depolarize slowly following a ramp lasting hundreds of milliseconds (Martina et al., 1999) because of delayed rectifier type K^+ conductance, that is sensitive to 4-AP.

1.5.6 AFFERENT AND EFFERENT CONNECTIVITY OF THE CENTRAL AMYGDALA

The glutamatergic projections from BLA reach the CLA neurons. There are either direct excitatory projections from the BLA pyramidal cells to the INs of the CeLA or the axons from BLA pyramidal cells form disynaptic inhibitory connections through the ICMs cluster to the cells in the CeLA (Royer et al., 1999, Jüngling et al., 2008) The disynaptic connectivity facilitates feedforward inhibition of CeLA neurons thus maintaining the excitatory and inhibitory balance in the CeLA neurons (Paré and Smith, 1993, Royer et al., 1999, 2000). Topographical organization makes PNs in the LA to connect to cells in the dorsal cluster ITCd while the BA PNs connect to cells in the ventral cluster (ITCv) (Geracitano et al., 2007).

Further PKC-δ^+ cells and PKC-δ^- INs of the CeLA mutually inhibit each other and provide a circuit level control through the inhibition of CeMA neurons. PKC-δ^+ cells are major effector neurons of CeLA targeting mainly CeMA LFCs which further send inhibitory projections to the PAG, Striatum (mainly to NAc), BNST and PVT in the thalamus, Hyp and dorsal vagal complex (Viviani et al., 2011). And there exist projections going directly from PKC-δ^- INs to extra-amygdala areas like the PVT of the thalamus and PAG of the midbrain (Penzo et al., 2014) but brainstem has connections more strongly from CeMA than from CeLA.

Hence, the CeLA and CeMA innervate several brain stem nuclei to promote defensive responses (Penzo et al., 2014). For example, CeMA projections to the nucleus reticularis pontis caudalis mediate acoustic startle reflexes (Davis et al., 1982), whereas CeLA and CeMA projections to the BNST, PAG and PVT mediate freezing responses (LeDoux et al., 1988; Amorapanth et al., 1999). The CeLA, CeMA and effector regions of the brain stem, Hyp and striatum decide the animal behaviour (fear, anxiety and reward related responses) depending on the afferent sensory, somatosensory and memory inputs followed by physiological processing in the synapses between BLA and CeA neurons.

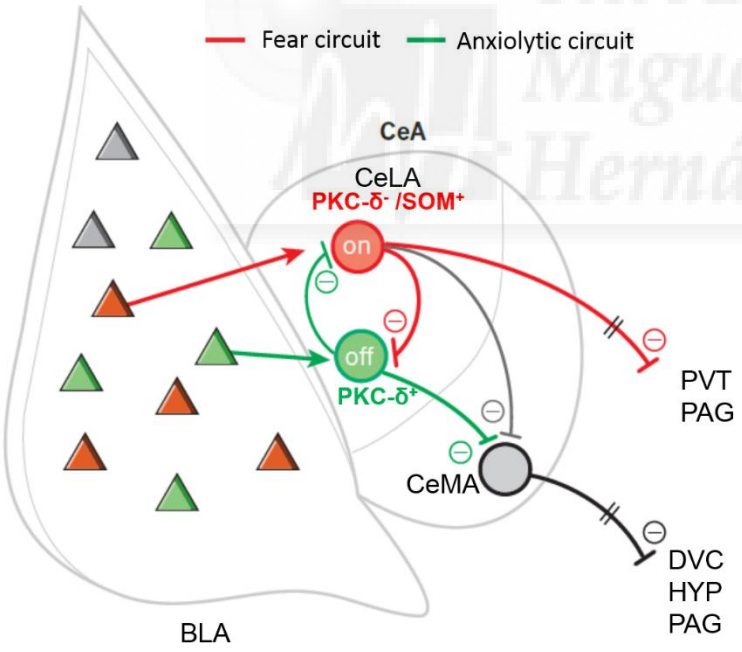

Figure 10: Intrinsic and extrinsic connectivity of CeA.

Different populations of BLA PNs activate CeLA INs like PKC-δ⁺ cells and PKC-δ⁻ (most of which are also SOM⁺) cells to either increase fear expression or increase anxiolysis based on the activation or inhibition of downstream targets of both CeLA and CeMA. DVC, dorsal vagal complex; PAG, periaqueductal grey; PKC, protein kinase C; PVT, paraventricular nucleus of the thalamus; HYP, hypothalamus; SOM, somatostatin (From Janak and Tye, 2015)

1.6 ROLE OF AMYGDALA IN ANXIETY AND REWARD RELATED BEHAVIOURS.

Processing of anxiety related information in the amygdala involves different mechanisms and neural ensembles. Anxiety can be defined as a sustained unpleasant emotional state of hyperactivity or mental distress persisting for a longer term in a response to an uncertain and diffuse threats.

Anxiety results in a variety of defensive behaviours and is essential to survival of an organism. Anxiety related disorders can lead to emotional burdens like state of fear and apprehension owing to a perceived threat, or reluctance to pleasurable and social activities known as anhedonia or even can lead to physiological aberrations like increased respiratory rate or cardiovascular problems. The neuronal circuit detecting and processing anxiety related behaviour is much more complex than the circuit dedicated to the processing of fearful stimuli, still both exhibits decent overlap (Janak and Tye., 2015). The circuits underlying defensive behaviours especially anxiety, is conserved across humans and rodents. Optogenetic investigations in last few years targeting specific subsets of neuronal populations have been successful in resolving novel circuits underlying anxiety mediated behaviour.

Hyperactivity or increased excitatory transmission through stimulation of amygdala leads to perception of anxiety in humans and rodents (Forster, 2012). Lesions in the amygdala in humans and rodents cause imperception of anxiety. Hyperexcitability of amygdala, especially BLA, is a common finding in patients with generalized anxiety disorders, social anxiety disorders, panic disorders, etc (Forster, 2012). This is supported by studies in the mice using optogenetics, where PNs of the BLA (PNs) were activated with expression of Channelorhodopsin (ChR2) (Tye et al., 2011). Consistent with this observation, Intra-BLA Injections of GABA agonist and antagonist in rodents leads to modulation of anxiety phenotypes with the former leading to an anxiolytic effect while the latter being involved in anxiogenic effect (Prager et al., 2016; see also Nuss., 2015). So, the INs in the amygdala circuits play a key role in constraining

the excitatory output of the PNs in the BLA and consequently reduces anxiety response (Spampanato, 2011). Further, acute administration of anxiogenic drugs leads to hyperexcitability in the BLA. This happens because of increased basal activity of PV^+ INs that inhibits SOM^+ INs thus disinhibiting PNs in the BLA. The increased basal activity of PV^+ INs following administration of anxiogenic drugs is evident in cFos immunolabelling studies (Hale et al., 2010). This hypothesis is supported by the fact that brain-wide activation or disinhibition of SOM^+ INs by PV^+ INs had anxiolytic consequences in the open arms exposure in EPM, hence mice is more exploratory and less anxious (Fuchs et al., 2016).

In addition to the BLA, the CeLA plays a crucial role in decreasing the activity of anxiogenic CeMA projection neurons and hence causing anxiolysis (Ciocchi et al., 2010). When the BLA→CeL pathway was selectively activated, mice were shown to be less anxious through increased open arm explorations in behaviour tests (Tye et al., 2011). So excitatory projections from BLA to CeLA has a role in anxiolysis. Later studies using selective photoactivation of $PKC\delta^+$ cells confirmed the identity of cells in the CeLA that were responsible for this anxiolysis and hence these were CeLA OFF cells or $PKC\delta^+$ cells, most of which are LFCs (Haubensak et al., 2010). The reason implicated here is decreased firing of anxiogenic CeMA neurons leading to disinhibition of adBNST (antero-dorsal BNST) neurons (Tye et al., 2011; see also Janak and Tye 2015). On the contrary, inactivation of the direct excitatory projections from BLA to adBNST leads to increased avoidance of open arms and increased respiratory rate hence increased anxiety. This indicates that BLA glutamatergic projections to adBNST is anxiolytic. Whereas, there exist other output projections from the BLA such as the excitatory projections to vHPC that promote anxiety and decreases social interaction (Allsop et al., 2014).

Depending on the valance of the stimulus whether it's rewarding or threatening, BLA PNs target specific regions that execute reward or threat related behaviours. The precise mechanisms of matching rewarding threat or reward related stimuli to specific behaviour is currently under investigation. Different populations of BLA

PNs change their firing rates during presentation of stimuli of positive or negative valances representing rewarding and aversive situations respectively (Beyeler et al., 2016; Kim et al., 2017). There are valance specific, independent sets of PNs in the BLA that display differential activation depending on the sensory stimulus that is either aversive or rewarding. The PNs of the BLA that projects to NAc are activated by a rewarding stimulus and therefore are called reward related neurons, while the PNs projecting to CeMA neurons gets activated in response to a threat and hence are referred to as anxiety and fear related cells So, an aversive stimulus such as threat will stimulate projection cells that are CeMA projectors leading to increased anxiety levels in the animal.

Table 1.1: Link of inhibitory INs of the amygdala in anxiety related behaviours. Source: Babaev (2018)

Region	Cell type	Link to anxiety
BLA	PV^+	The number of neurons tends to be negatively correlated with avoidance in the OF
		Activated by the acute delivery of anxiogenic drugs
		Optogenetic stimulation/suppression during the acquisition phase of fear conditioning bidirectionally modulates conditioned freezing
	SOM^+	Optogenetic activation during the acquisition phase of fear conditioning reduces conditioned freezing
	$CALB^+$ PV^-	Suppressed by exposure to innately aversive stimuli
CeLA	$PKC\delta^+$	Partial silencing enhances conditioned freezing following fear conditioning
		Optogenetic stimulation reduces avoidance in OF, EPM and LDB
		Optogenetic stimulation reduced the discrimination between CS+ and CS- in fear conditioned animals
		Optogenetic stimulation increases avoidance in EPM and OF
	SOM^+	Chemogenetic and optogenetic suppression during fear conditioning and fear retrieval reduces conditioned freezing
		Optogenetic stimulation induces freezing in naïve mice
	CRF^+	Optogenetic stimulation decreases freezing and promotes flight during exposure to US following fear conditioning
		Optogenetic stimulation of CRH^+ terminals projecting from the CeA to the Locus Coereleus increases avoidance
CeM	$Tac2^+$	Chemogenetic suppression prior to fear conditioning reduces conditioned freezing
		Optogenetic stimulation induces immobility-like behavior in naïve mice

In summary, distinct populations of PNs exist in the BLA controlling anxiety and reward related behaviours. BLA projections to CeLA ON cells, PKCδ^{-} most of which are RFCs get activated in response to anxiogenic stimuli, while the ones to PKCδ^{+} cells which are mainly LFCs gets activated to cause anxiolytic like behaviour. Lastly the activation of direct projections of BLA PNs to NAc mediates reward related behaviours, whereas the increased activity of direct projections from BLA to CeMA leads to anxious phenotype.

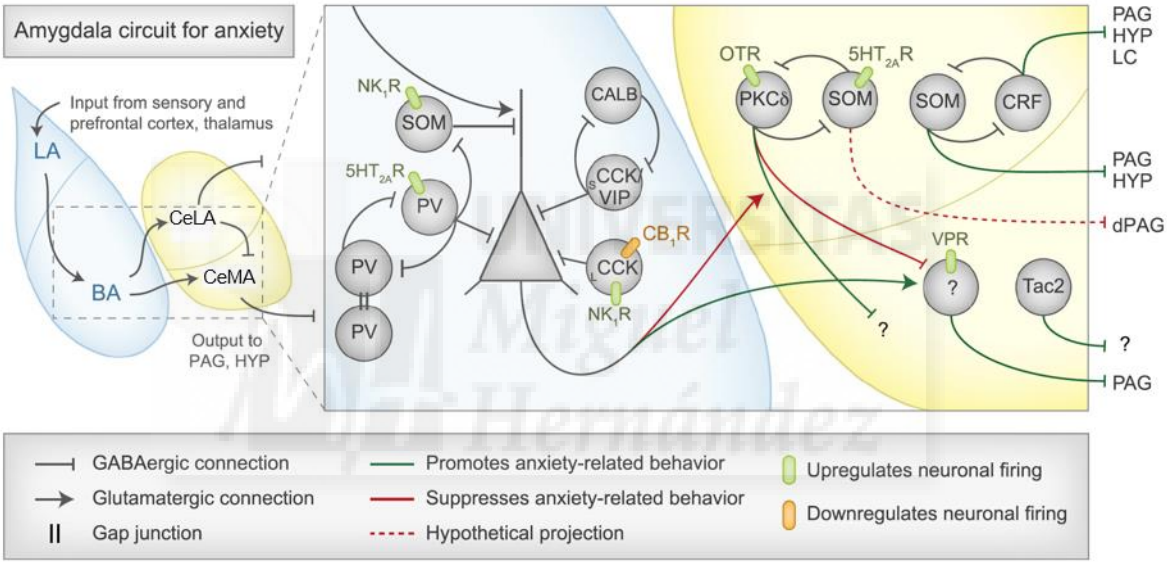

Figure 11: Inhibitory connections of the amygdala that are involved in the control of anxiety-related behaviour. BLA receives sensory information from the cortex and thalamus which depending on source and valance, bifurcates to enter either CeMA or CeLA. For simplicity, all of the afferents to the CeA apart from the BLA afferents are omitted, as well as some of the CeA downstream targets, including the dorsal vagal complex and the hypothalamus (which receives input from the CeMA). Abbreviations: BLA basolateral amygdala; CALB calbindin; LCCK large cholecystokinin; SCCK small cholecystokinin; CeA central amygdala; CeL centrolateral amygdala; CeMA centromedial amygdala; CRF corticotropin releasing factor; dPAG dorsal periaqueductal gray; HTR2A serotonin receptor 2 A; HYP, hypothalamus LC, locus coeruleus; NK1R neurokinin 1 receptor; OTR, oxytocin receptor; PAG periaqueductal gray; PV parvalbumin; SOM somatostatin; Tac2 tachykinin 2; VIP vasoactive intestinal peptide; VPR vasopressin receptor. Source: Babaev (2018)

1.7 PHYSIOLOGICAL ROLE OF KAINATE RECEPTORS

KARs play an important role in fast excitatory neurotransmission in the CNS by contributing to postsynaptic depolarization. In most of the brain regions, the postsynaptic current mediated by KARs is a small fraction of absolute EPSC amplitude (mediated by AMPARs and KARs) and has slow activation and deactivation kinetics (Castillo et al., 1997).

KARs also locate presynaptically and are involved in bidirectional regulation of the synaptic release of neurotransmitters such as glutamate and GABA. Hence presynaptic KARs helps to maintain excitation-inhibition balance through modulation of neurotransmitter release at both excitatory and inhibitory synapses (Lerma, 2003). For instance, KARs contribute to regulate inhibition in the HPC (Rodriguez-Moreno et al., 1997; Vignes et al., 1998), intra-amygdala synapses (Braga et al., 2004), synapses in the neocortex (Ali et al., 2001), globus pallidus (Jin and Smith, 2007) and other brain regions. The modulation of GABA inhibition in the HPC is mediated by metabotropic action of presynaptic KARs as the inhibitory action of these presynaptic KARs was successfully reversed by Pertussis Toxin (PTx) and inhibitors of PKC and PLC, indicating the involvement of a metabotropic signaling cascade (Rodriguez-Moreno and Lerma, 1998: Rodriguez-Moreno et al, 2000).

KARs are also involved in the development of neuronal synapses and circuits. A number of studies have indicated the role of KARs in maturation of neuronal circuits. For instance, KARs keeps glutamate release under check in immature hippocampal CA1 synapses (Lauri et al., 2006), through most probably non-canonical metabotropic signaling mechanism. KARs also control firing rate of INs by suppression of AHPs in CA3 INs during the first postnatal week (Segerstrale et al., 2010). Also, KARs can bidirectionally modulate neuronal maturation and neurite outgrowth of sensory neurons (Marques et al., 2013). In the HPC, KARs control network activity by bidirectional modulation of glutamate input from MFs to CA3 PNs (Frerking and Nicoll, 2000) and through increasing GABA release from INs (Lauri et al., 2005).

This is very critical for development of neuronal circuits in the HPC. So, these are just few of the examples and recent investigations are aimed at exploring such role of KARs in other circuits including amygdala and prefrontal cortex, regions critical to controlling neural excitability in order to prevent neuropsychiatric disorders.

A major fraction of postsynaptic excitatory transmission in the BLA is mediated by AMPARs although a part (8- 30%) may be mediated by postsynaptic by KARs in the PNs of the BLA. This was shown by recording evoked EPSCs (eEPSCs) in the BLA PNs with the use of bipolar stimulation electrode placed in the EC (Li et al., 1998). The responses mediated by KARs were isolated through the application of selective AMPAR blocker GYKI 53655 and further this was confirmed by application of antagonist of GluK1 containing KARs that is LY293558 (Li et al., 1998). Also, part of excitatory postsynaptic current in the BLA INs was due to presence of postsynaptic GluK1 containing receptors (Braga et al., 2003). Therefore, it could be concluded that GluK1 containing postsynaptic receptors in the BLA INs and PNs mediates a part of excitatory postsynaptic component of synaptic transmission.

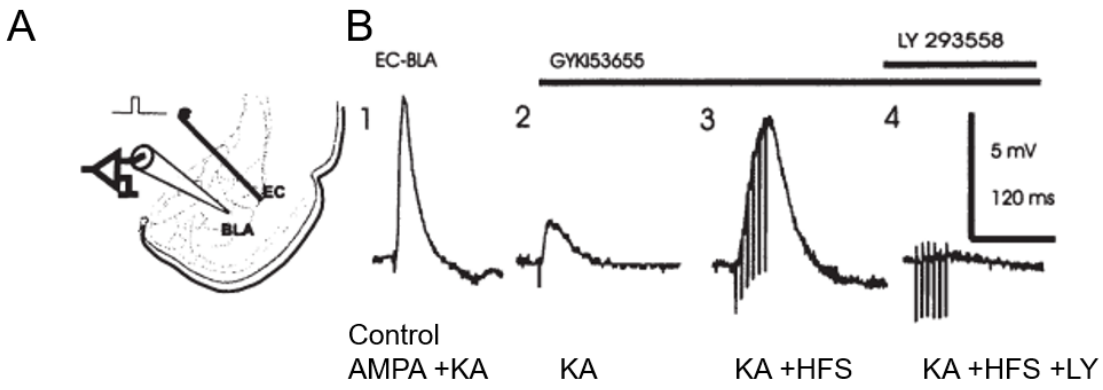

Figure 12: KAR mediated excitatory postsynaptic transmission in the amygdala. (A) Scheme of amygdala showing bipolar stimulation electrode placed in the external capsule and recording electrode in the BLA. (B) A component (30%) of excitatory glutamatergic postsynaptic potential-EPSP (1) is mediated by GluK1 containing KARs (2). KAR mediated EPSP is isolated by application of AMPAR antagonist GYKI53655 (2). High frequency stimulation (six pulses at 100 Hz) significantly increased the response (3) that was further abolished by GluK1 specific antagonist 10 µM LY 293558 (4). The slice medium contained the NMDA receptor antagonist APV (100 µM) and the $GABA_A$ receptor antagonist bicuculline (10 µM). The recording electrode contains 50 mM of QX-314. EC, External capsule BLA, Basolateral amygdala; HFS: High frequency stimulation; KA Kainate mediated response (Li and Rogawski, 1998)

1.7.1 KAR MEDIATED MODULATION OF NEUROTRANSMITTER RELEASE IN THE BLA

Further GluK1 containing receptors were also shown to exist on the presynaptic terminals of BLA interneurons. These presynaptic GluK1 containing KARs were shown to increase the presynaptic release of GABA to cause the inhibition of BLA PNs (Braga et al., 2003). The release modulation by presynaptic GluK1 containing KARs in the INs was further shown to be dependent on agonist concentrations and also on subunit composition and depending on these factors it can increase or decrease synaptic release. Lower concentrations of KAR agonist ATPA stimulates presynaptic GluK1 containing KARs on INs of the BLA increasing the release of GABA onto BLA PNs. Higher concentrations of ATPA have the contrary effect, decreasing GABA release onto BLA PNs and likely increasing excitability in the BLA. Although it has been proposed that these receptors may be low affinity homomeric KARs GluK1/2, this is not entirely clear (Braga et al., 2003).

Hence presynaptic intraneuronal KARs regulate and maintain excitatory synaptic transmission in the BLA through different mechanisms, which may involve or not distinct KARs. This might involve both ionotropic and metabotropic signaling upon KAR activation as demonstrated in other brain regions and synapses such as the HPC (Rodriguez-Moreno and Lerma, 1997; Contractor et al., 2001; Cossart et al., 2001). Hence it is hypothesized in the current model that different functions of amygdala in fear related memories and anxiety behaviour may involve this fine tuning of presynaptic GluK1 containing KARs to either promote or dampen GABAergic transmission. For instance, intense emotional stimuli might trigger hyperexcitability of amygdala circuits by increased glutamate concentrations extrasynaptically. The increased glutamate further activates presynaptic homomeric low affinity GluK1/2 containing KARs in the BLA INs which causes suppression of GABA release and increased EPSCs in the BLA PNs (Braga et al., 2004). In this case overexcitation can lead to synaptic plasticity, and also promote development of stress related mood disorders, like autism and schizophrenia. While on the other hand, weak or moderate emotional input might trigger suppression of amygdala circuits, through low concentrations of extrasynaptic glutamate activating high affinity KARs (GluK4/5 containing) present on presynaptic sites of INs. This facilitates GABA release from the INs consequently decreasing EPSCs in the BLA PNs. So, GluK1 containing KARs in the INs may have an important role in converting emotional valance to either increased or decreased excitatory activity in the BLA.

1.8 ROLE OF KARS IN NEUROPSYCHIATRIC DISORDERS

The KARs not only participate in postsynaptic excitatory neurotransmission but also influences the integrative properties of the synapses through proper tuning and modulation of presynaptic release of neurotransmitters at the excitatory and inhibitory contacts in the brain (Lerma, 2003; Sachidhanandam et al., 2009; Frerking et al.,1999). KARs participate in the latter function in the brain through their metabotropic nature of signaling (Rozas et al., 2003; Lerma , 2003; see also

Valbuena and Lerma, 2016). Several chromosomal and genetic abnormalities like insertions, deletions, duplications and inversions of KAR genes lead to their loss or gain of function. This could change the number of synaptic contacts or density of KARs in synapses hence modulating the binding and release of neurotransmitters such as glutamate and GABA. As a consequence, differential activation of KARS may convey an imbalance of excitation and inhibition in neural circuitry likely leading to neuropsychiatric disorders in humans.

1.8.1 ROLE OF KARS IN MOOD DISORDERS

GluK1

GluK1 subunit encoded by gene *GRIK1* localized on human chromosome 21q22.1 has been implicated in Down´s syndrome because genetic mapping places *GRIK1* is in the vicinity of genes coding for APP and super oxide dismutase (SOD1; Gregor et al., 1994). Owing to the trisomy, the extra copy of *GRIK1* on this chromosome encodes for excess of GluK1 protein that might be involved in pathogenesis of Down´s syndrome but this needs further investigation and is being studied extensively in our lab.

GluK2

The role of KARs in mood disorders have been studied more recently. Decreased *GRIK2* mRNA was detected postmortem in HPC, parahippocampus and the prefrontal cortex in the brains of patients with known schizophrenia and bipolar disorder (Scarr et al., 2005). A de novo mutation in *GRIK2* (A657T) have recently been shown to cause higher lever cognitive dysfunction and ataxia in a young girl (Guzmán et al., 2017). Interestingly, recombinant KARs incorporating the mutation have altered channel gating and are constitutionally active (Guzmán et al., 2017). *Grik2* KO mice on the other hand produces social behaviour deficits and autism related phenotypes (Micheau et al., 2014).

Deletion of exons 7 and 8 localized in ATD and transmembrane domain in *Grik2* gene has been reported in patients with intellectual disability (Motazacker et al., 2007). Several single nucleotide polymorphism (SNPs) association studies in different populations have found *GRIK2* in linkage disequilibrium with autism (Shuang et al., 2004; Griswold et al., 2012). But some studies failed to detect this association of SNPs in *GRIK2* with autistic patients (Lerma and Marques, 2013) as the case in Indian population (Dutta et al., 2007)

GluK3

Some SNPs, like SNP T298G, have been reported in *Grik3* gene that leads to serine being replaced by Alanine at 310th position in the extracellular domain of GluK3 (Schiffer et al 2000). This SNP has been significantly associated to patients with major depression and schizophrenia (Begni et al., 2002; Minelli et al., 2009; Lai et al., 2005). A microdeletion was reported in *GRIK3* gene in a patient with severe developmental delay affecting her language and fine motor skills (Takenouchi et al., 2014). Consistent with this, GluK3 knock out mice displayed markedly reduced short- and long-term synaptic potentiation processes that are important for learning and memory (Pinheiro et al., 2007).

Table 1.2: KAR subunits implicated in Mood disorders. Adapted from Lerma and Marques 2013

Gene	Data	Linked Disease	Behavioral Test in KO	References
Grik1	Upregulated expression	Epilepsy	No	Sander et al., 1997, Izzi et al., 2002, Li et al., 2010, Lucarini et al., 2007
Grik2	Modest linkage	Autism	No	Jamain et al., 2002, Shuang et al., 2004, Szatmari et al., 2007, Freitag, 2007; but see Dutta et al., 2007
Grik2	Deletion of exons 7 and 8	Mania, mild mental retardation	No	Motazacker et al., 2007, Shaltiel et al., 2008, Lanore et al., 2012
Grik2	Mapping susceptibility locus	Schizophrenia	Yes	Beneyto et al., 2007, Shaltiel et al., 2008; but see Shibata et al., 2002, Shibata et al., 2006
Grik2	mapping	Huntington	No	MacDonald et al., 1999, Chattopadhyay et al., 2003; but see Lee et al., 2012 and Diguet et al., 2004
Grik3	SNP T928G (rs6691840)	Schizophrenia	No	Begni et al., 2002, Kilic et al., 2010, Ahmad et al., 2009;
Grik3	SNP T928G (rs6691840)	Major depression	No	Schiffer and Heinemann, 2007, Wilson et al., 2006
Grik4	Treatment response	Depression	No	Paddock et al., 2007
Grik4	14 bp deletion/insertion variant	Bipolar disorder	Yes	Pickard et al., 2008, Catches et al., 2012, Lowry et al., 2013
Grik4	SNPs rs2282586 and rs1944522	Protection against Schizophrenia	Yes	Pickard et al., 2006

1.9 ROLE OF GLUK4 IN NEUROPSYCHIATRIC DISORDERS

The *GRIK4* gene is shown to exhibit consistent pleiotropic associations in independent case-control genome wide linkage studies across multiple endophenotypes of schizophrenia hence establishing *GRIK4* as a risk gene for schizophrenia disorder (Greenwood et al., 2016). More studies have shown that knock out of *Grik4* produces symptoms of bipolar disorders, like hyperactivity and disruption of spatial memory acquisition and recall in a Morris water maze test (Lowry et al., 2013; Catches et al, 2012). This suggests a role of *Grik4* in spatial memory.

The haplotype consisting of three genetic determinants or SNPs within the gene have been related to schizophrenia susceptibility, while the other haplotype with two genetic determinants or SNPs had a protective effect against bipolar disorder (Pickard et al., 2006). Subsequent studies identified a 13 base pair insertion deletion (indel) variant in the 3' UTR of the *GRIK4* gene. In subjects carrying deletion variant, a negative association with the bipolar disorder was demonstrated, which coincided with the generation of stable transcripts of *GRIK4* mRNA in normal subjects (Pickard et al., 2008). These subjects carrying the deletion variant further showed enhanced hippocampal activation in fMRI studies (Whalley et al., 2009); something that has been replicated recently in a mouse model (Aller et al., 2015). Hence excess of GluK4 has a link to increased activation in hippocampal circuits and thus altered information processing. This was consistent with higher GluK4 protein in frontal cortex and HPC in post-mortem brains in patients with deletion variant (Knight et al., 2012). Also, CNV in GluK4 subunit has been implicated in neuropsychiatric disorders as the duplication of the 11q23.3-q24.1 locus in which *GRIK4* lies was recently identified in a case of autism (Griswold et al., 2012). This observation forms the basis of this work aimed at exploring significance of GluK4 containing KARs in context of neuropsychiatric disorders.

1.10 AIMS AND OBJECTIVES OF THIS THESIS PROJECT

Recent studies have implicated CNVs in the chromosomal locus where *GRIK4* maps in ASDs (Griswold et al., 2012). To understand the physiological consequences it may have, it is mandatory to study the role of GluK4 subunits in synaptic information processing by modelling GluK4 related aberrations in rodents. Recent investigations have started to assess how the absence or the overexpression of KAR subunits like GluK4 in rodents affect behaviour of the animals in the context of neuropsychiatric anomalies like autism (Aller et al., 2015). The objective of this study was to follow a similar gain of function strategy and reproduce the case of autistic patients in mice with de novo duplication of

Grik4 (Griswold et al., 2012), and further study altered behaviour and synaptic alterations underlying such behaviour in amygdala circuits.

To study the function of GluK4 protein and the role it may play in mental disorders, our lab has generated mice overexpressing *Grik4* gene (C57BL/6J-Tg (camk2-grik4)3 mice) in the PNs of the forebrain. The mice were named GluK4^{Over} mice for simplification. Similar to patients having *de novo* duplication of 11q23.3-q24.1 locus, the mouse displayed several behavioural deficits such as increased anxiety, depression, anhedonia and impaired social interaction (Aller et al., 2015), closely mimicking the situation of patients suffering from ASDs (Griswold et al., 2012; White et al., 2009; Gillott et al., 2001).

The amygdala has long term association with autistic symptoms like hyperactivity, depression, altered social behaviour, anhedonia, as it is known to be the prominent center for processing fear anxiety and social behaviour. This motivated us to study the presynaptic and postsynaptic effects of *Grik4* overexpression in the pyramidal cells of the BLA, late firing and regular firing cells of the CeLA. The *Grik4* overexpression in GluK4^{Over} mice was significant in PNs of the forebrain including amygdala circuits.

Thus, specific aims of the thesis projects were

1. Is *GriK4* expressed in amygdala circuits and how does the overexpression of GluK4 reveal its function?
2. What is the function of GluK4 in synaptic transmission in amygdala circuits (BLA and CeL$_A$)?
3. How does *Grik4* overexpression affects behaviour and basal activation in amygdala circuits?
4. Does normalizing the dosage of *Grik4* in the transgenic mice rescue synaptic and behaviour abnormalities observed after overexpression?

UNIVERSITAS
Miguel
Hernández

CHAPTER 2. MATERIALS AND METHODS

2.1 ANIMAL HANDLING

For experimental procedures, mice were kept in ventilated cages on a 12 hours light/dark cycle in a temperature controlled, standard pathogen free environment (23°C) at humidity between 40% and 60%. 328 male and female mice in total belonging to wild type and transgenic siblings (with altered *Grik4* expression) were reared and subjected to environmental procedures following the Spanish and EU regulations (2010/63/EU), Approval was taken from both the Bioethical committee at the Instituto de Neurociencias (INA) and the Consejo Superior de Investigaciones Cientificas (CSIC) for the use of animals for various procedures including molecular biology, electrophysiology and standard behaviour paradigms. All the mice had ad libitum access to food and water and cages were replaced weekly. The electrophysiology experiments were performed on postnatal P18-P20 animals. Immunocytochemistry procedures involving anti-myc and anti-cFos immunofluorescence studies of coronal sections of the brain, western blotting procedures involving cortical and hippocampal protein lysates and behavioural procedures were carried out on > 4 weeks-old mice. All the experiments and analysis of measured parameters were done in a blind manner with genotypes being unknown to the experimenter.

2.2 GENERATION OF MOUSE LINES

To generate the mouse lines, Rat *Grik4* c DNA was tagged with 5 myc epitopes, just after the signal peptide consisting of first 20 amino acids. The resulting plasmid which is pcDNA3 myc *Grik4* was accessed for proper function through electrophysiological experiments in HEK293 cells. To generate the transgenic mice, myc-*Grik4* construct was cloned as an EcoRV-SmaI fragment into the pNN265 plasmid already having an intron sequence required for proper functioning of CaMKII promoter. This was followed by introduction of a NotI fragment containing myc-*Grik4* and the intronic sequence into the PMM403

plasmid which had the CaMKII promoter inserted in pBluescript (Mayford et al., 1996). Finally, the SfI 1 restriction enzyme was used to remove the pBluescript backbone from the construct and this was followed by its injection into the pronucleus of fertilized eggs. The latter experiment was performed at the Unitat Animals Transgènics Centre de Biotecnologia Animal i Teràpia Gènica, Universitat Autònoma de Barcelona. The levels of myc-*Grik4* expression was analysed in the F1 generation by immunohistochemistry and in western blots. GluK4 KO mice were obtained from Dr. Anis Contractor from Northwestern University.

2.3 GENOTYPING

DNA was isolated from tail samples of wild type and GluK4^{Over} animals and *Grik4* recombination in transgenic mice lines was accessed using the PCR method followed by gel electrophoresis technique. PCR conditions used were: 3 minutes at 94°C; 30 seconds at 94°C, 30 seconds at 62°C, and 30 seconds at 72°C repeated for 35 consecutive cycles; and finally, 8 minutes at 72°C. PCR product was run in 2% agarose gel. After electrophoresis, the gel was placed on a UV light box and a standard photograph of the fluorescent ethidium bromide-stained DNA separation pattern is taken indicating bands corresponding to the myc fragment under detection.

2.4 IMMUNOFLUOROSCENCE

Twelve mice (5 GluK4$^{+/+}$ and 7 GluK4^{Over}) were transcardially perfused with PBS for 2-3 minutes (5-10ml) followed by fixative (4 % PFA in PBS, pH 7.4) for 10 minutes (– 20 ml). After perfusion brains were removed from skull and immersed in the same fixative for 4 hours at 4ºC. After fixation, the brains were left in PBS overnight. For each brain 50 µM coronal sections were collected in PBS using Leica VT 1000S vibrotome and rinsed 3 x 10 minutes with PBS (pH 8 at room

temperature). For myc detection, 20 µM sections were used instead. Further the sections were transferred to a blocking solution containing 10% Normal Goat serum and 0.2 % Triton X in for 1 hour. Sections were then subjected to overnight incubation at - 20 ºC with 1:1000 rabbit anti cFos polyclonal IgG (1:1000; Synaptic Systems, Germany) in the same blocking solution. For myc immunocytohistochemistry, sections were incubated in a rabbit anti Myc antibody (1:500 Abcam) in a blocking solution (PBS-0.2% Triton X-100 and 10% NGS). The following day, the sections were rinsed with PBS and c Fos and myc revealing was done by incubation with 1:1000 goat anti-rabbit secondary antibodies (Jackson) tagged with Alexa 555 in the solution containing 5% NGS and 0.2 % Triton X in 0.1 M PBS. Sections were rinsed with 0.1 M PBS and mounted on the slides with DAPI solution (H-1200 Vectashield with DAPI – Palex Medical SA). Immunofluoroscence stainings were evaluated on a Leica DMLFSA confocal microscope and analysed using Imaris image analysis software (Bitplane). A low pass filter was applied to subtract the background.

Quantitative analysis of Leica images was performed by an observer blind to experimental conditions. For c-Fos quantification we used 10x objective and measured c-Fos activity by using image J software. Circular ROI was drawn over BLA, CeLA and CeMA and the background of the images was removed with a rolling ball radius of 40 pixels. Further the threshold was set at 12 pixels for cells to be visible. Three to five sections were considered for a given mouse and cells were counted per area unit for all sections and were averaged for a given mouse. Mean immunofluorescence intensity was also calculated for each section and was similarly averaged for a given mouse.

In a few instances while performing electrophysiology experiments, BLA PNs and INs were also visually identified taking advantage of their typical morphology, by filling the cell with biocytin after break-in the cell, once tight Gigaseal (>1GΩ) was made. Thus, biocytin was dissolved in the recording pipette solution at 1 mg/ml. Cells were recorded for an average of 30 min, and the recorded slices were immediately fixed in 4% paraformaldehyde followed by 3 washes each of 10 minutes in PBS. Slices were left overnight in PBS. In the morning, slices were again washed for 3 times (10 minutes each) in PBS and further they were

processed for immuno-histochemistry by permeabilizing in 0.2% Triton X-100, PBS for 2 min. After one hour, slices were again washed 3 times with PBS and further incubated with Alexa 488-conjugated streptavidin (Molecular Probes) diluted in the blocking buffer (Selak et al., 2006). Following each incubation step, slices were washed 3×15 min in PBS. After the last wash, slices were mounted onto slides in DAPI-supplemented mounting medium (Vectashield: Vector Laboratories, Burlingame, CA, USA) and viewed using a Leica Laser Confocal Microscope.

2.5 WESTERN BLOTTING

Cortical and hippocampal protein lysates were analyzed in Western blots probed with the following primary antibodies: mouse anti-α-tubulin (1:1000; Abcam), mouse anti-myc (1:500; Santa Cruz Biotechnology), Rabbit anti-GluK4 (1:1000; Abcam). Antibody binding was detected on a luminescent image analyzer (LAS-1000PLUS, Fuji) and quantified with Quantity One 1D Analysis Software (Bio-Rad Laboratories). For quantifications, all densities were normalized to the respective tubulin signal.

2.6 NON-RADIOACTIVE *IN SITU* HYBRIDIZATION

In situ hybridization was performed on free-floating sections (Acloque et al., 2008, Paternain et al., 2000). Mouse brains were dissected out from animals previously perfused with 4% paraformaldehyde. Two different *Grik4* probes were hybridized to transverse vibratome brain sections (50 µm): (1) a sequence encompassing the 3′ UTR (333 bp); and (2) a sequence corresponding to exons 13, 14, and 15 of the *Grik4* gene (356 bp). The first probe was generated by PCR with the primers 5′-TGGCAGCAGCGAAGGACCATG and 5′-TAGGGGGAATTCAACTGATGAC, while the second probe was generated with primers located between exons 13 and 15 of *Grik4*, 5′-ATCCCTTTTCTCCAGGAGTC and 5′-CAGGTCATCCACAGACTCAA (Fernandes et al., 2009). Probe specificity was assessed by using the sense probe and/or brain tissue from GluK4-deficient mice. Both probes produced similar labelling.

2.7 ELECTROPHYSIOLOGICAL RECORDINGS OF BRAIN SLICES

2.7.1 SET-UP

Electrophysiological recordings were performed in a dedicated rig with the following parts

Set up contained Inverted microscope, mechanical and piezoelectric manipulators mounted on a pneumatic anti-vibration table to prevent vibrations. An Axopatch 200A patch clamp amplifier was used for making electrophysiological recordings. Slices were visualised using Sony CCD- Iris camera and Sony Monitor. Regions were identified by infrared (IR)-DIC (differential interference contrast) microscopy with a 40× water immersion objective. Data acquisition was carried out using Digidata 1400A Axon Instruments and pClamp10 acquisition software on a personal computer. Brain regions were stimulated in Slices using a stimulation system (Cibertec CS20 and ISU165). Internal Noise in the setup was eliminated as much as possible using Noise eliminator (HumBug Quest Scientific) while Faraday cage was used to remove the surrounding electrical noise.

2.7.2 SLICE PREPARATION FOR ELECTROPHYSIOLOGY

Mice (18 to 21 days old) was anaesthetized using isoflurane (IsoVet®) and decapitated. Intact brains were carefully removed and immediately transferred to ice cold high sucrose Ringer buffer (in mM: 124 NaCl, 8 $NaHCO_3$, 10 Glucose, 3 KCl, 1.25 NaH_2PO_4, 1 $MgSO_4$, 2 $CaCl_2$, saturated with 95% O_2/5%CO_2). Hind brain region of the brain consisting of Cerebellum/Pons/Medulla Oblongata was removed by sharp blade and rest of the brain was glued to a holder which was later attached to the vibrotome slicer (LeicaVT 1200S) base in order to cut coronal/horizontal slices. Coronal slices (350µm) were cut at the level of amygdala. About 2 slices were cut and later separated into four slices, 2 slices containing the left amygdala and the other 2, the right amygdala.

Slices were preserved until recording in a chamber kept in a 37°C bath of extracellular artificial cerebrospinal fluid (ACSF) or ringer solution. Slices were left for 45 minutes to an hour in the chamber to recover before recording session was started. ACSF had the following composition in millimolar 124 NaCl, 3 KCl, 1.25 KH2PO4, 1 MgSO4, 2 CaCl2, 26 NaHCO3, and 10 glucose, equilibrated with 95% O2/5% CO2 (pH 7.3; 300 mOsm).

2.7.3 INTRACELLULAR PATCH CLAMP RECORDINGS

Electrophysiological recordings were performed for up to 6 hours after slices were obtained. For recordings, slices were transferred to a recording chamber regularly perfused with ACSF or extracellular solution and supplemented constantly with 95% O_2/5% CO_2 and different drugs. The slices were perfused and supplemented with drugs using a fast perfusion system renewing the solution at a speed of 1ml/minute and consisting of 4 tubes which allowed changes between different bathing solutions. Drugs were applied by gravity, switching between four perfusion lines using a switch valve (Valve Driver II, General Valve). We calculated that full exchange of the solutions required approximately 3 min, and, for this reason, cells were recorded for at least 5 min before the effect of the drug was assessed. A platinum grid was kept over the slice, while recording to keep the slice fixed during measurements and avoid any movement artefacts. Amygdala regions, both BLA and CeLA was identified using infrared (IR)-DIC (differential interference contrast) microscopy with a 10× normal objective and cells namely PNs and INs were identified using 40× water immersion objective.

EPSCs were recorded using the Tight seal (>1GΩ) whole cell configurations and different cells were identified with their physiological properties under current clamp. Both evoked and miniature synaptic EPSCs were recorded from identified PNs in the BLA and interneurons such as late firing and regular firing interneurons from the CeLA. Cells were patched using borosilicate glass pipettes (Kwik-Fil^{TM},WPI) of 4-5 MΩ resistance.

2.7.3.1 CURRENT CLAMP RECORDINGS.

Electrophysiological Characterization of BLA cells

PNs were distinguished from interneurons in the BLA through current clamp recordings. For distinguishing PNs from INs, input resistance and firing rate was measured for both types of cells. Firstly, the rheobase current was determined and then 400 ms-long depolarizing current injection of 2x rheobase current was applied to obtain the instantaneous firing rate. PNs were always <20 Hz, while interneurons presented a higher firing frequency. Secondly, after break-in the cell, we looked at the input resistance (measured by a hyperpolarizing current injection or I/V). PNs had low input resistances (~100 MΩ), while input resistance of interneurons was generally >200 MΩ.

Patch pipettes were filled with following intracellular solution while making current clamp recordings for amygdala neurons, 120 KMeSO3, 20 KCl, 2 MgCl2, 10 HEPES, 0.2 EGTA, 0.2 Na2ATP, 7 Na2-phosphocreatine (pH 7.2; 290 mOsm).

Electrophysiological Characterization of CeLA cells

For characterizing late firing and regular firing cells of the CeLA, same protocol was used as for BLA neurons: 400ms-long depolarizing current injection of 2x the rheobase was applied to obtain the instantaneous firing rate, that was checked for delay, if any before the cell starts firing. Late firing cells had a delay ≥ 200ms before firing APs corresponding to their voltage dependent outward rectification properties, while regular firing cells started firing as soon as the current was injected. Other properties were also checked like Resting membrane potential (mV), Input resistance (MΩ), Rheobase Current (pA), Firing Frequency (Hz) and AP amplitude (mV) to make the full characterisation of PNs and INs in the BLA and LFCs and RFCs in the CeLA.

2.7.3.2 VOLTAGE CLAMP RECORDINGS.

Miniature AMPARs/KARs-mediated excitatory currents

$mEPSC_{AMPARs}$ were recorded from PNs of the BLA and late firing and regular firing interneurons of the CeA after at least 3 minutes from break-in, so to let the intracellular solution to fill the cell completely. This was done as we calculated that full exchange of the solutions needed at least 3 minutes and hence cells were recorded for at least 5 minutes before the drug was applied and the effect was accessed. Recordings were performed at -60 mV holding potential with the extracellular bath solution (ACSF) as above but using a cocktail of compounds to isolate $mEPSC_{AMPARs/KARs.}$ The cocktail of compounds consisted of 25µM D-APV to antagonize NMDARs, 100 µM picrotoxin to inhibit GABA-A receptors and 0.5 µM TTX to record AP independent miniature postsynaptic currents $mEPSC_{AMPARs/KARs.}$

UBP310 (10µM) a GluK1 selective antagonist (Dolman et al., 2007) but also an antagonist of heteromeric receptors such as GluK2/5 was dissolved in ACSF with the cocktail of compounds described above and applied by gravity. The exchange from ACSF to ACSF with UBP310 was by using switch valve as described above. $mEPSC_{AMPARs/KARs}$ were recorder for at least 5 minutes before the switchover was made. Following switchover, 1 minute was allowed for UBP310 to reach the recording chamber and another 2-3 minutes for stabilization of the drug effect. Further $mEPSC_{AMPARs/KARs}$ with the effect of UBP310 were recorded for 3 minutes.

The intracellular solution in the recording electrode for recording miniature AMPARs/KARs-mediated excitatory currents had the following composition.

120 KMeSO3, 20 KCl, 2 MgCl2, 10 HEPES, 0.2 EGTA, 0.2 Na2ATP, 7 Na2-phosphocreatine (pH 7.2; 290 mOsm)

Evoked excitatory postsynaptic currents (eEPSCs) from cortico-amygdala synapses and BLA-CeLA synapses.

To measure EC evoked eEPSCs from BLA PNs, electrical pulses were applied through a monopolar electrode (made from a glass pipette) carefully placed in the EC to stimulate cortical fibers that innervate PNs of the BLA. The $eEPSC_{AMPARs/KARs}$ were recorded at supramaximal intensity from BLA PNs in the presence of 25 µM D-APV to antagonize NMDARs, 100 µM picrotoxin to inhibit GABA-A receptors. Each evoked response was repeated for 20 times with an interstimulus interval of 10 sec (0.1Hz). BLA PNs were clamped at -60 mV for ~ 6-7 minutes to ensure stable response. Similarly, $eEPSC_{AMPARs}$ were recorded from late firing and regular firing INs of CeLA after stimulating via monopolar electrode placed in the BLA. The stimulation was performed at multiple intensities starting at 6 mA until 10 mA followed by recording of $eEPSC_{AMPARs}$ for 20 sweeps at 0.1 Hz at intensities ranging from 6-10 mA.

Recording of NMDAR-mediated eEPSC were performed by switching the holding potential to +40 mV for additional 5 minutes and repeating the same protocol with each evoked response being repeated for 20 times with an interstimulus interval of 10 sec (0.1Hz) for all the BLA cells recorded. Hence $eEPSC_{AMPARs/KARs}$ were recorded at -60 mV and $eEPSC_{NMDARs}$ at +40 mV. Averaged NMDARs mediated eEPSC was measured at 50 ms after the onset of the eEPSC. The ratio of $eEPSC_{AMPARs/KARs}$ to $eEPSC_{NMDARs}$ was measured by dividing the peak of AMPARs current over NMDARs current.

To measure KAR mediated $eEPSC_{KARs}$ or KAR mediated evoked excitatory postsynaptic currents from cortico-amygdala synapses, LY303070 (25µM) was added to the bath, and eEPSCKARs was recorded in the same way as above, at supramaximal intensity from BLA PNs in the presence of 25µM D-APV to antagonize NMDARs, 100 µM picrotoxin to inhibit GABA-A receptors. BLA PNs were clamped at -60 mV for ~ 6-7 minutes to ensure stable response.

For recording paired pulse ratios of (PPRs) of $eEPSC_{AMPARs}$, EC was stimulated twice at 0.1 Hz (every 10 s) using 50 ms interstimulus interval. PPRs were recorded at supramaximal intensity stimulation of EC from BLA PNs in the presence of 25µM D-APV to antagonize NMDARs, 100 µM picrotoxin to inhibit GABA-A receptors. BLA PNs were clamped at -60 mV for ~ 6-7 minutes to ensure stable response.

The intracellular solution in the recording electrode for recording AMPARs/KARs mediated evoked excitatory currents had the following composition.
120 KMeSO3, 20 KCl, 2 MgCl2, 10 HEPES, 0.2 EGTA, 0.2 Na2ATP, 7 Na2-phosphocreatine (pH 7.2; 290 mOsm)

Simultaneous recording of spontaneous AMPAR mediated EPSCs and GABA-A mediated IPSCs

Simultaneous sEPSC/sIPSC were recorded from CeLA late firing and regular firing neurons with a help of special intracellular solution consisting of 5 mM Cl^- to make the reversal potential go back to around -90 mV, thus holding potential was optimized to around -50 mV to record sEPSCs as inwardly downward deflections while sIPSCs were outward currents. For these recording picrotoxin was omitted from the extracellular solution to avoid blocking GABA-A receptors, while 25µM D-APV was added to antagonize NMDARs.

The intracellular solution in the recording electrode for recording simultaneous spontaneous AMPAR mediated EPSCs and GABA-A mediated IPSCs had the following composition.

135 $KMeSO_4$, 0.5 $CaCl_2$, 2 $MgCl_2$, 10 HEPES, 5 EGTA, 0.1 Na_3GTP, 2 MgATP (pH 7.2, 286 mOsm) (Zhou et al., 2009)

2.8 DATA ANALYSIS

Electrophysiological data was acquired using Clampex 10.6. While evoked EPSCs were analysed by Clampfit 10.6, miniature EPSCs were analysed using mini-analysis software (Synaptosoft Inc.). For the analysis of kinetics of EPSCs such as the decay, an exponential was fitted to the decay phase of the EPSC curve. Statistical analysis was performed using the statistical tools provided by the Sigmaplot 12.5 software, which incorporates built in statistical tests to analyse data and make the comparisons. Advisor wizard in this software guides to select the appropriate tests based on the type of distribution of the data (whether normal or non-normal). Mainly one-way ANOVA (Analysis of variance) test was used to compare more than two groups of data, two tailed paired or unpaired t test (confidence interval 95%) was used for comparing two groups (eg. Wild type and transgenic) when the data distribution was normal. If the distribution was not normal, non-parametric test such as Mann Whitney Rank Sum test was used. The results were presented as box plots where the bottom and top of the box are the first and third quartiles, respectively, and the whiskers above and below indicate the 95^{th} and 5^{th} percentiles. The median (grey line) and the mean (white line) are indicated.

UNIVERSITAS
Miguel
Hernández

CHAPTER 3. RESULTS

3.1 Increased *Grik4* Gene Dosage Causes Imbalanced Circuit Output and Human Disease-Related Behaviors

This work has been published in Cell Reports Journal (an open access Q1 journal from Cell Press) by two co-first authors namely Vineet Arora and Valeria Pecoraro in collaboration with other members of our laboratory that are co- authors of the article. Here I described the author contribution for each of the co-authors: Juan Lerma conceived the idea. Vineet Arora performed the electrophysiology experiments in amygdala circuits in the GluK4^{Over} mouse model and also collected data from in-vivo cFos assays to explore the basal activation in amygdala circuits in relation to GluK4 overexpression. Valeria Pecoraro performed the electrophysiology experiments on hippocampal slices in the GluK4^{Over} mouse model. Maria Isabel Aller created the GluK4 ^{Over} mouse model and checked for the overexpression of GluK4 using antibody against myc and also performed behaviour studies of the GluK4^{Over} mouse. She also performed *in situ* hybridization experiments on coronal slices of the brain to reveal the native expression of the GluK4 in amygdala circuits. The latter studies were performed with assistance of Celia Román. Vineet Arora, Valeria Pecoraro, Maria Isabel Aller, and Ana Valero Paternain conducted the data analysis and Juan Lerma wrote the paper.

The article presented here is open access and it contain supplementary figures that are attached here and also available online in this link:

https://www.cell.com/cell-reports/fulltext/S2211-1247(18)30867-2

Article

Cell Reports

Increased *Grik4* Gene Dosage Causes Imbalanced Circuit Output and Human Disease-Related Behaviors

Graphical Abstract

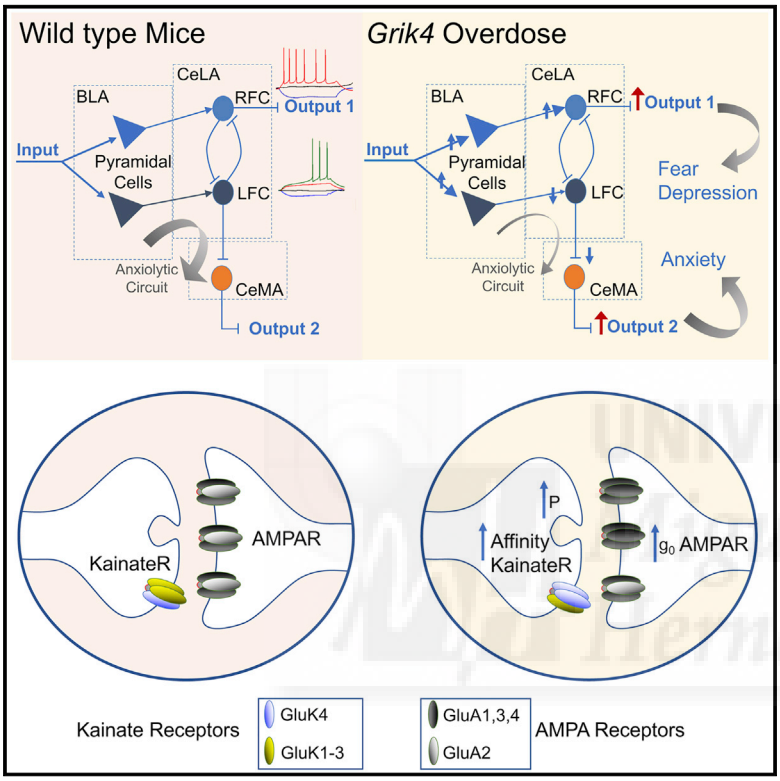

Highlights

- *Grik4* is widely expressed in the brain
- GluK4 enrichment increases glutamate release probability and AMPAR conductance
- *Grik4* overexpression leads to persistent unbalanced inhibitory and excitatory activity
- GluK4 gain of function alters behaviors common to human disease

Authors

Vineet Arora, Valeria Pecoraro, M. Isabel Aller, Celia Román, Ana V. Paternain, Juan Lerma

Correspondence

jlerma@umh.es

In Brief

Arora et al. show that an increase in *Grik4* gene dose enhances the efficiency of synaptic transmission, causing a persistent circuit disequilibrium that alters the main amygdala outputs. This may account for the behavioral abnormalities observed in disorders like autism and schizophrenia.

Arora et al., 2018, Cell Reports *23*, 3827–3838
June 26, 2018
https://doi.org/10.1016/j.celrep.2018.05.086

CellPress

Cell Reports
Article

Increased *Grik4* Gene Dosage Causes Imbalanced Circuit Output and Human Disease-Related Behaviors

Vineet Arora,[1,2] Valeria Pecoraro,[1,2,3] M. Isabel Aller,[1] Celia Román,[1] Ana V. Paternain,[1] and Juan Lerma[1,4,*]
[1]Instituto de Neurociencias CSIC-UMH, 03550 San Juan de Alicante, Spain
[2]These authors contributed equally
[3]Present address: UMR5297 Institut Interdisciplinaire de Neurosciences (IINS), University of Bordeaux, Bordeaux, France
[4]Lead Contact
*Correspondence: jlerma@umh.es
https://doi.org/10.1016/j.celrep.2018.05.086

SUMMARY

Altered glutamatergic neurotransmission is thought to contribute to mental disorders and neurodegenerative diseases. Copy-number variation in genes associated with glutamatergic synapses represents a source of genetic variability, possibly underlying neurological and mental disease susceptibility. The *GRIK4* gene encodes a high-affinity kainate receptor subunit of essentially unknown function, although *de novo* duplication of the 11q23.3-q24.1 locus to which it maps has been detected in autism and other disorders. To determine how changes in the dose of *Grik4* affect synaptic activity, we studied mice overexpressing this gene in the forebrain. A mild gain in *Grik4* enhances synaptic transmission, causing a persistent imbalance in inhibitory and excitatory activity and disturbing the circuits responsible for the main amygdala outputs. These changes in glutamatergic activity reverse when *Grik4* levels are normalized; thus, they may account for the behavioral abnormalities in disorders like autism or schizophrenia.

INTRODUCTION

Throughout the CNS, excitatory and inhibitory synaptic transmissions are tightly regulated to sustain proper brain function. The correct activity of circuits depends not only on their appropriate wiring but also on the concerted interactions between presynaptically released transmitters and their postsynaptic receptors. Notably, establishing the adequate receptor number and type at synapses is fundamentally important to fine-tune neuronal communication.

While changing the number of synaptic contacts and/or the density of synaptic receptors is a physiological mechanism that underlies the brain plasticity associated to learning and memory (e.g., Nicoll, 2017), pervasive brain pathologies can also emerge because of variations in the dosage of certain genes (Kenny et al., 2014; Poot et al., 2010; Sebat et al., 2007). Insertions, deletions, inversions, and duplications may result in loss or gain of gene function, and when this affects genes that are active at synapses, these alterations will modify normal circuits and their performance. This may be the case of *GRIK4*, a gene encoding a high-affinity kainate receptor (KAR) subunit, GluK4, whose function remains largely unknown. One known *GRIK4* insertion or deletion (indel) variant has an altered 3′ UTR (3-UTR), and this variant is negatively associated with bipolar disorder, reducing the likelihood that a carrier of the deletion will develop this disease (Pickard et al., 2008). Interestingly, *GRIK4* mRNA transcripts carrying the deletion generate more stable RNA transcripts in normal subjects and, thus, more GluK4 protein (Pickard et al., 2008; Knight et al., 2012). This situation is associated with enhanced hippocampal activation (Whalley et al., 2009), indicating that GluK4 abundance may significantly affect hippocampal processing. Similarly, a *de novo* duplication of the chromosome 11q23.3-q24.1 locus in which *GRIK4* lies has been identified in a case of autism (Griswold et al., 2012), and, more recently, a genome-wide linkage analysis found this gene to be associated to different endophenotypes in schizophrenia (Greenwood et al., 2016).

Understanding brain diseases relies on defining the molecular, synaptic, and cellular alterations that underlie the behavioral features of each disease, although some more general rules may exist. At certain glutamatergic synapses, KARs mediate a small part of the synaptic response, although they are critically important molecules that impart emergent integrative properties on the synapse (Sachidhanandam et al., 2009; Frerking et al., 1999). In addition, KARs participate in complex signaling pathways at both excitatory and inhibitory synaptic contacts in the brain (Lerma, 2003). The five KAR subunits are encoded by five separate genes (*GRIK1–GRIK5*), and they assemble into heteromeric receptors. KARs not only mediate fast synaptic transmission but also modulate synaptic properties and other events through canonical and non-canonical (metabotropic) signaling pathways (Rozas et al., 2003; Marques et al., 2013; for a review, see Valbuena and Lerma, 2016). Accordingly, these receptors play an instrumental role in the function and activity of neurons in many areas of the brain (Segerstråle et al., 2010; Lerma and Marques, 2013).

To further understand how neuronal communication is altered in cases of *GRIK4* gene overdose, particularly in relation to the aforementioned human brain diseases, synaptic transmission was evaluated in C57BL/6J-Tg(camk2-*grik4*)3 mice. This mouse line overexpresses GluK4 in principal cells of the forebrain, and

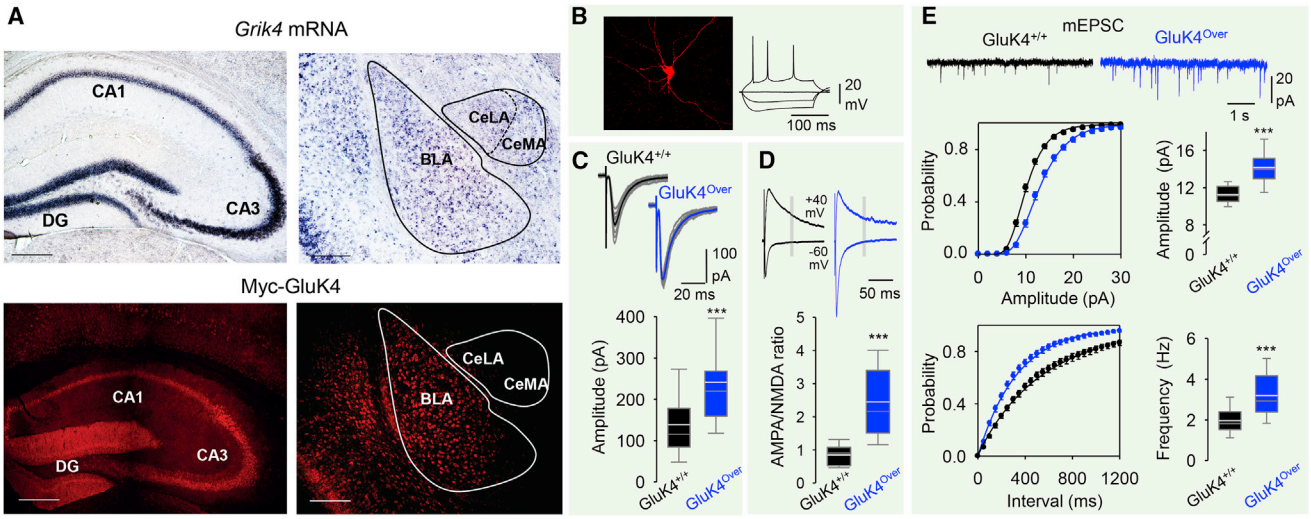

Figure 1. Synaptic Effects of GluK4 Overexpression in Basolateral Amygdala

(A) Top: *in situ* hybridization showing the expression of *Grik4* mRNA in the hippocampus and basolateral amygdala (BLA), centrolateral amygdala (CeLA) and centromedial amygdala (CeMA) of a GluK4$^{+/+}$ animal. Bottom: the immunocytochemical detection of transgenic myc-GluK4 in similar coronal slices (full images are the montage of four high-power images) (see also Figure S1). Scale bars: 100 μm.

(B) Pyramidal cells were identified in BLA by their morphology, after labeling with biocytin from the patch pipette, and by their firing properties. The panels show the morphology and the response to 50 pA hyper- or depolarizing current pulses of a typical BLA pyramidal neuron, reflecting spike adaptation.

(C) Synaptic currents evoked by supramaximal stimulation of the external capsule in GluK4$^{+/+}$ and GluK4^{Over} mice. The boxplot below represents the pooled data from n = 49 neurons (8 GluK4$^{+/+}$ mice) and n = 54 neurons (10 GluK4^{Over} mice). ***p<0.001. Mann-Whitney rank-sum test.

(D) The amplitude of external-capsule-evoked AMPAR-mediated EPSCs were also referred to the amplitude of NMDA receptor (NMDAR)-mediated EPSCs, which were measured 50 ms after the peak response at +40 mV (gray band) ($p < 0.001$, Mann-Whitney rank-sum test; n = 30 neurons).

(E) Representative AMPARs and/or KARs mediated mEPSCs at a membrane potential of −60 mV recorded from BLA pyramidal cells from each genotype, their quantification using cumulative probability distributions and boxplots showing the higher amplitude and the frequency for GluK4^{Over} mice relative to GluK4$^{+/+}$ mice. The data from n = 37 neurons from 7 slices from 6 GluK4$^{+/+}$ and 7 GluK4^{Over} mice are indicated.

***$p < 0.001$, Mann-Whitney rank-sum test.

See also Figures S1–S3.

these animals display signs of depression, anxiety, and social impairment (Aller et al., 2015), closely reflecting the human endophenotypes associated with autism and schizophrenia (e.g., White et al., 2009; Gillott et al., 2001). We found that modest increases in GluK4 protein are associated with synaptic gain at selected synapses in the amygdala complex, resulting in unbalanced circuit outputs. This effect is attained not only by increasing the synaptic release probability but also by enhancing the postsynaptic α-amino-3-hydroxy-5-methyl-4-isoxazolepropionic-receptor (AMPAR)-mediated component. Indeed, an excess of GluK4 seems to delay the maturation of synapses as they remain enriched in the GluA2-lacking AMPARs typical of young synapses. Interestingly, both the synaptic and behavioral phenotypes recover upon normalization of the *Grik4* gene dose. Overall, this remarkable effect on synaptic transmission may account for the behavioral abnormalities evident in diseases like autism spectrum disorders or schizophrenia.

RESULTS

The brain areas where genes encoding KAR subunits are expressed have been rudimentarily described in radioactive *in situ* hybridization studies (e.g., Wisden and Seeburg, 1993). While this approach allows the expression of intensely expressed KAR subunits to be defined, the expression of the *Grik4* gene remains poorly documented (e.g., the Allen Brain Atlas). Similarly, no specific antibodies are available that recognize KAR subunits—in particular, the high-affinity subunits—further hindering the completion of a comprehensive expression map in the brain, especially in mice. Perhaps, for this reason, KARs made up of GluK5 and GluK2 subunits are considered the most abundant in the brain (Wisden and Seeburg, 1993; Fisher and Fisher, 2014). To explore the expression of *Grik4* in the mouse brain, we took advantage of the higher sensitivity of non-radioactive *in situ* hybridization (Acloque et al., 2008; Paternain et al., 2000). Contrary to what is believed, *Grik4* was abundantly expressed in all fields of the hippocampal formation, including the CA1, CA2, and CA3 fields and the dentate gyrus (DG), as well as in the neocortex and the amygdala (Figures 1A and S1). Interestingly, the amygdala has classically been related to anxiety and depression, two of the phenotypes observed in the transgenic mice that overexpress *Grik4* (Aller et al., 2015).

Synaptic Transmission in the Basolateral Amygdala

We examined the influence of GluK4 overexpression in the amygdala. Although *Grik4* was abundantly expressed in the amygdala complex, recombinant GluK4 was mostly detected in pyramidal neurons, particularly in the basolateral amygdala (BLA) (Figure 1A). Pyramidal neurons in the BLA were recorded, where they were identified by their low firing frequency and the

large spike frequency adaptation upon membrane depolarization. Their identity was further verified anatomically by filling the recorded neurons with biocytin (Figure 1B). The KainateR-mediated excitatory postsynaptic currents ($EPSCs_{KAR}$) in BLA pyramidal neurons were larger and presented faster decay kinetics (Figure S2), demonstrating the presence of functional KARs that contain the GluK4 subunit in these neurons. We also noted an increase in the number of neurons in which $EPSCs_{KAR}$ could be resolved (10/41 neurons in the wild-type [WT] as opposed to 13/32 neurons in the transgenic mice: 24.4% versus 40.6%). Moreover, the AMPAR-mediated EPSC ($EPSCs_{AMPAR}$) evoked by supramaximal stimulation of the external capsule were 75% larger in the GluK4-overexpressing mice (138.7 ± 12.14 pA versus 241.2 ± 18.9 pA; ns = 49 and 54 neurons, respectively; $p < 0.001$; Figure 1C). To further verify that this increase in $EPSC_{AMPAR}$ amplitude was specific, we measured the ratio of $EPSCs_{AMPAR}$ to NMDAR-mediated EPSCs ($EPSCs_{NMDA}$), which certified the enhancement of synaptic AMPAR-mediated responses in transgenic mice (Figure 1D).

We then analyzed how GluK4 overexpression affected presynaptic parameters, such as the miniature EPSC (mEPSC) frequency in the presence of tetrodotoxin (TTX). Analysis of these elementary synaptic events revealed a higher frequency in $GluK4^{over}$ mice (1.96 ± 0.15 Hz versus 3.19 ± 0.26 Hz for the WT and $GluK4^{over}$ mice, respectively; $p < 0.001$), compatible with the presence of KARs at presynaptic boutons, where they could enhance the release probability (e.g., Pinheiro et al., 2007). As mEPSCs are of an unknown source, we looked at the paired-pulse ratio of responses evoked by external capsule stimuli and found that it was significantly decreased (Figure S3), further certifying an increase of the probability of release, at least from these terminals. However, to our surprise, the cumulative plots clearly revealed that the $mEPSC_{AMPAR}$ amplitude was also larger in the transgenic mice (11.26 ± 0.95 pA versus 14.14 ± 0.47 pA for WT and $GluK4^{over}$ mice, respectively; $p < 0.001$; Figure 1E). Hence, GluK4 overexpression in principal cells would appear to have a dual effect. On the one hand, it increases the amplitude of EPSCs mediated by KARs, while on the other, it enhances both the amplitude and frequency of the AMPAR-mediated mEPSCs.

Synaptic Effect on Neurons of the Centrolateral Amygdala

While BLA is the main entry point of sensory inputs to the amygdala (LeDoux et al., 1990), the central nuclei are the main source of amygdala outputs; particularly, the centromedial amygdala (CeMA) (Duvarci and Pare, 2014). BLA pyramidal cells project to the centrolateral amygdala (CeLA), where they contact two different types of GABA neurons, one projecting outside the amygdaloid nucleus (the regular-spiking cells) while the other contacts CeMA neurons (late-spiking cells: for reviews, see Duvarci and Pare, 2014; Janak and Tye, 2015). These neurons did not overexpress GluK4 (see Figure 1A), because expression of the *Grik4* transgene is under the control of the CaMKII promoter in these mice, which is only active in principal cells. To determine how these connections were modulated by an excess of GluK4, the two different types of GABA neurons in the CeLA were identified by their firing pattern and studied separately (Figure 2A). Regular-spiking cells developed larger excitatory responses in the transgenic mice in response to stimuli applied to the BLA (Figure 2B). While the $mEPSC_{AMPAR}$ amplitude was altered slightly (12.0 ± 0.45 pA in WT versus 13.8 ± 0.45 pA in $GluK4^{over}$; ns = 26 and 36 neurons, respectively; $p = 0.027$), their frequency was dramatically enhanced (2.1 ± 0.16 Hz in WT versus 3.3 ± 0.11 Hz in $GluK4^{over}$ mice; $p < 0.001$; Figure 2C). By contrast, the evoked EPSC $(eEPSC)_{AMPAR}$ amplitude remained fairly constant in late-spiking cells, although there was a tendency for it to be smaller than in mice overexpressing GluK4 (Figure 2D). Accordingly, the $mEPSC_{AMPAR}$ frequency diminished by 40% (3.0 ± 0.21 Hz versus 1.8 ± 0.16 Hz for WT and $GluK4^{over}$ mice, respectively; $p < 0.001$), while the amplitude decreased only mildly (14.2 ± 0.45 pA versus 12.8 ± 0.50 pA for WT and $GluK4^{over}$ mice, respectively; $p = 0.042$; Figure 2E).

These data indicate that excess of GluK4 has two different effects in the amygdala. While it increases the release probability at BLA pyramidal boutons that contact regular-spiking cells in the CeLA, it also reduces the release probability at contacts established by BLA pyramidal neurons with CeLA late-spiking cells. The overall result of these changes may be a dramatic alteration in the excitatory-inhibitory balance within this structure.

Since regular- and late-spiking neurons inhibit each other (Lopez de Armentia and Sah, 2004), imbalances in the input to these cells is likely to strongly affect their activity in these transgenic mice (Figure 3A). To further assess this hypothesis, we simultaneously recorded spontaneous EPSCs (sEPSCs) and spontaneous inhibitory postsynaptic currents (sIPSCs) from both types of CeLA neurons, adjusting the intracellular chloride concentration to 5 mM during recordings at a −50-mV holding potential (Zhou et al., 2009). Under these conditions, the sIPSCs were outward currents, while the sEPSCs were inwardly directed deflections (Figure 3B). As expected, the frequency of sEPSCs, but not that of sIPSCs, increased by 39% in regular-spiking cells (2.3 ± 0.14 Hz versus 3.2 ± 0.21 Hz for WT and $GluK4^{over}$ mice; ns = 17 and 18 neurons, respectively; $p < 0.001$; Figure 3B). By contrast, late-firing neurons had a larger frequency of sIPSCs in the transgenic mice (1.5 ± 0.14 Hz versus 2.6 ± 0.22 Hz for WT and $GluK4^{over}$ mice; ns = 19 and 20 neurons for WT and $GluK4^{over}$ mice, respectively; $p < 0.001$) and a slightly reduced excitatory input (2.8 ± 0.28 Hz versus 2.0 ± 0.22 Hz for WT and $GluK4^{over}$ mice, respectively; $p = 0.041$; Figure 3C). We did not detect any changes in sEPSCs or in the sIPSC amplitudes in these cells (Figures 3C and 3D).

Basal Neuronal Activity Is Altered in the Amygdala Nuclei *In Vivo* in the Transgenic Animals

To further test whether this imbalance occurs during an *in vivo* situation, we undertook experiments using activity-dependent, immediate-early gene (*c-Fos*) expression to track ongoing neuronal activity in behaving animals. This method has been reliably used to detect changes in neuronal activation in the amygdala and several other brain structures (e.g., Tye et al., 2011). We quantified the proportion of neurons in the BLA, CeLA, and CeMA in WT (5 mice) and GluK4-overexpressing (7 mice) animals (Figure 4). Consistent with the electrophysiological data, we found not only a significantly 75% higher proportion

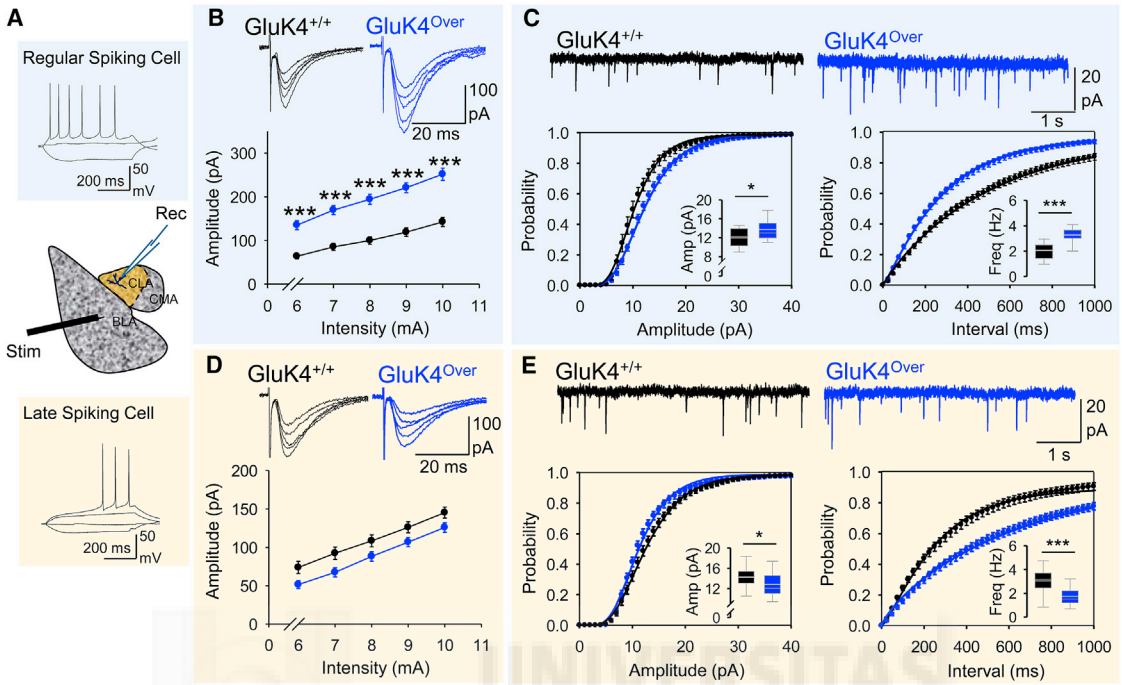

Figure 2. GluK4 Overexpression in BLA Pyramidal Cells Produces Dissimilar Effects on Excitatory Synaptic Input to the CeLA Principal Neurons

(A) CeLA neurons were distinguished according to the firing properties as regular-spiking (top) and late-spiking (bottom) neurons. The intermediate cartoon shows a scheme of position of stimulation and recording electrodes.

(B) Top: typical examples of eEPSCs recorded from CeLA regular-spiking cells after stimulating the BLA in the GluK4$^{+/+}$ and GluK4^{Over} mice. Bottom: the stimulus-response curves were obtained by applying stimuli from 6 mA to 10 mA (n = 11 neurons from 9 slices from 4 GluK4$^{+/+}$ mice and n = 9 neurons from 8 slices from 5 GluK4^{Over} mice. ***p < 0.001, Student's t test with Bonferroni correction for pairwise multiple comparisons).

(C) AMPAR-mediated mEPSCs recorded from regular-firing neurons (V_m = −60 mV). Below are the cumulative probability distributions and boxplots (insets) of the frequency and amplitudes of mEPSCs$_{AMPAR}$ (n = 60 neurons from 60 slices from 13 GluK4$^{+/+}$ and 17 GluK4^{Over} mice; *p < 0.05; ***p < 0.001; Student's t test).

(D) eEPSCs recorded from CeLA late-spiking neurons after stimulating the BLA of the GluK4$^{+/+}$ and GluK4^{Over} mice (top) and the corresponding stimulus response curves (bottom).

(E) AMPAR-mediated mEPSCs recorded from late-firing neurons (V_m = −60 mV). Below are the cumulative probability distributions and boxplots (insets) for the mEPSC$_{AMPAR}$ frequency and amplitudes (n = 63 neurons from 63 slices from 12 GluK4$^{+/+}$ and 15 GluK4^{Over} mice; *p < 0.05; ***p < 0.001, Student's t test).

of c-Fos-positive BLA cells but also a slightly but significantly higher c-Fos immunoreactivity average intensity in transgenic animals (Figure 4C). Although barely significant (p = 0.06, two-tailed t test), c-Fos-positive cells were also more abundant in CeLA (53%). In contrast, c-Fos-positive neurons were largely increased in CeMA (73%) (Figures 4D–4F), as could be expected from electrophysiological *ex vivo* data.

Altogether, these data indicate that the excess of GluK4 sets a new level of ongoing activity in the different types of amygdala neurons, which permanently alters the intra-amygdala circuit processing and output.

Larger Postsynaptic Responses Are Not Only the Result of a Higher Release Probability

The increased frequency of events can be accounted for by an enhanced release probability at presynaptic terminals where high-affinity KARs are overexpressed, producing larger evoked postsynaptic responses. However, the larger amplitude of elementary mEPSCs$_{AMPAR}$ is more difficult to explain. More abundant and/or different types of AMPARs at postsynaptic sites where GluK4 subunits are expressed could account for these effects. However, a significantly higher frequency of elementary events leading to multiquantal responses could contribute to, if not explain, the larger average amplitude of mEPSCs$_{AMPAR}$ observed in transgenic mice. To determine whether the increase in the mEPSC$_{AMPAR}$ amplitude was simply the consequence of an increased release probability, we performed a quantal analysis of these responses in both hippocampal CA3 and BLA neurons. When we classified the events according to their amplitude, and we constructed frequency histograms, a typical distribution was evident, with an initial peak and then a skewed tail over larger amplitudes (Figure S4A), particularly for the GluK4^{over} mice. To avoid the influence of the skewed distribution when determining the amplitude of the minimum quantal events, we fitted a Gaussian curve to the initial peak by using the initial half of the distribution together with those bars after the peak that showed symmetrical values. In this way, the quantal content in CA3 pyramidal cells was seen to be 10.4 ± 0.50 pA (18 cells, 3 mice) in GluK4 WT mice and 12.7 ± 0.44 pA in GluK4^{over} mice (22 cells, 3 mice; p < 0.005), consistent with the average increase observed

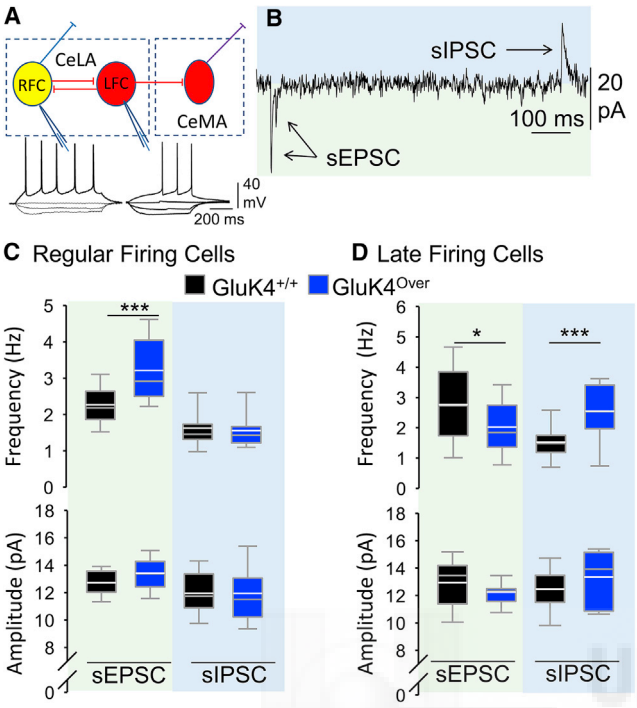

Figure 3. Unbalanced Inhibitory to Excitatory Activity in CeLA Principal Neurons

(A) Scheme of the intrinsic amygdaloid circuit showing the mutual inhibition of CeLA principal neurons (regular- and late-firing cells; RFC and LFC, respectively) and their output and electrode arrangements. The neurons were identified according to their firing in response to current pulses (insets).

(B) Spontaneous IPSCs and EPSCs were recorded simultaneously by arranging the intracellular chloride concentration so that the sIPSCs were seen as outward currents and the sEPSCs were directed inwardly (see Experimental Procedures).

(C) The frequency of sEPSCs, but not of sIPSCs, was increased in regular-firing cells from GluK4^{Over} mice (top). The amplitude remained unaltered (bottom) (***$p < 0.001$, Student's t test, ns = 17 and 18 neurons from WT and transgenic mice, respectively).

(D) The frequency of sIPSCs was increased in late-firing cells from GluK4^{Over} mice (***$p < 0.001$, Student's t test), while that of the sEPSCs fell slightly (*$p = 0.041$, Student's t test; ns = 19 and 20 neurons from each type of mouse). The amplitudes of sEPSC and sIPSCs did not change (plot shown at the bottom).

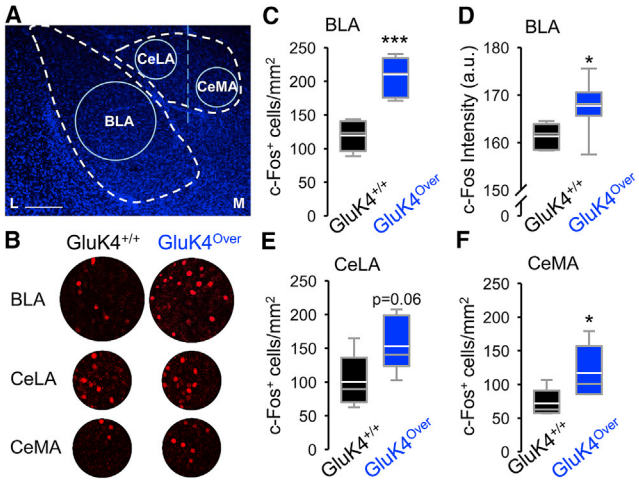

Figure 4. c-Fos Expression in Basolateral Amygdala, Centrolateral Amygdala, and Centromedial Amygdala Neurons in GluK4^{Over} Mice

(A) Coronal section through the amygdala complex showing DAPI-positive cells and regions of interest used for quantification of c-Fos immunoreactivity (M, medial; L, lateral).

(B) Representative examples of regions used for quantification arranged in a column per genotype.

(C) Density of DAPI-identified neurons positive for c-Fos immunoreactivity in BLA.

(D) The average c-Fos intensity in cells measured in (C) was slightly (4%) but significantly ($p = 0.039$) increased in transgenic mice.

(E and F) The density of c-Fos-expressing cells in (E) CeLA and (F) CeMA in both genotypes are shown. Data were obtained from averaging 4–5 section counts per mouse from 5 (GluK4$^{+/+}$) and 7 (GluK4^{Over}) animals.

*$p < 0.05$; ***$p < 0.001$, two-tailed Student t test. Scale bar: 100 μm.

after the more conventional mEPSC$_{AMPAR}$ analysis. To further reduce the probability of multiquantal events, we reduced the concentration of extracellular Ca^{2+} to 0.1 mM (Figure S4B), and there were dramatically fewer larger events, allowing the initial peak to be more accurately estimated. The minimum peak amplitudes were consistently higher in overexpressing cells (10.4 ± 0.52 pA and 12.5 ± 0.54 pA for GluK4 WT and GluK4^{over}, respectively; $p < 0.01$), indicating that the larger amplitude of elementary events in GluK4^{over} mice must be due to some other phenomenon, one probably related to postsynaptic alterations in the number and/or the type of AMPARs. Similar outcomes were obtained when BLA neurons were analyzed, with the quantal size in BLA pyramidal cells estimated to be 8.4 ± 0.3 pA in WT neurons (n = 16) and 11.3 ± 0.2 pA in transgenic cells (n = 16; $p < 0.001$), representing a 23% increase in amplitude (Figure S4C).

Overexpression of GluK4 Alters the Type of AMPARs at the Synapse

Once the summation of more frequent mEPSCs$_{AMPAR}$ had been ruled out as the cause of the larger postsynaptic events, we wanted to determine whether the increased event amplitude observed in GluK4^{over} mice was due to more Ca^{2+}-permeable AMPARs (CP-AMPARs) present at the postsynaptic membrane. CP-AMPARs have larger single-channel conductance (Swanson et al., 1997), so that their enrichment at synapses provokes synaptic responses of larger amplitudes. A hallmark of these CP-AMPARs is their strong inward rectification, which allows them to be detected by simply looking at the rectification index, calculated as the ratio of the responses measured at membrane potentials of +40 and −65 mV. We studied this issue at mossy fiber (MF)-to-CA3 synapses, and since the abundance of these CP-AMPARs varies with neuronal maturation, we looked at two different developmental stages (post-natal day [P]13–P14 and P17–P21), which displayed clear plastic changes in the WT animals (Figure 5A) but not in the transgenic animals overexpressing GluK4 (Figure 5B). Hence, more CP-AMPARs exist at synapses overexpressing GluK4 at both ages. To further substantiate this conclusion, we assessed the effects IEM1460, a CP-AMPAR and KAR open channel blocker (Schlesinger et al., 2005), and while we found this blocker had no effect on WT P17–P21 mice (8.0 ± 7.8% blockade), it largely blocked AMPARs in GluK4^{Over} mice (34.1 ± 4.8%; p = 0.009) (Figure 5C).

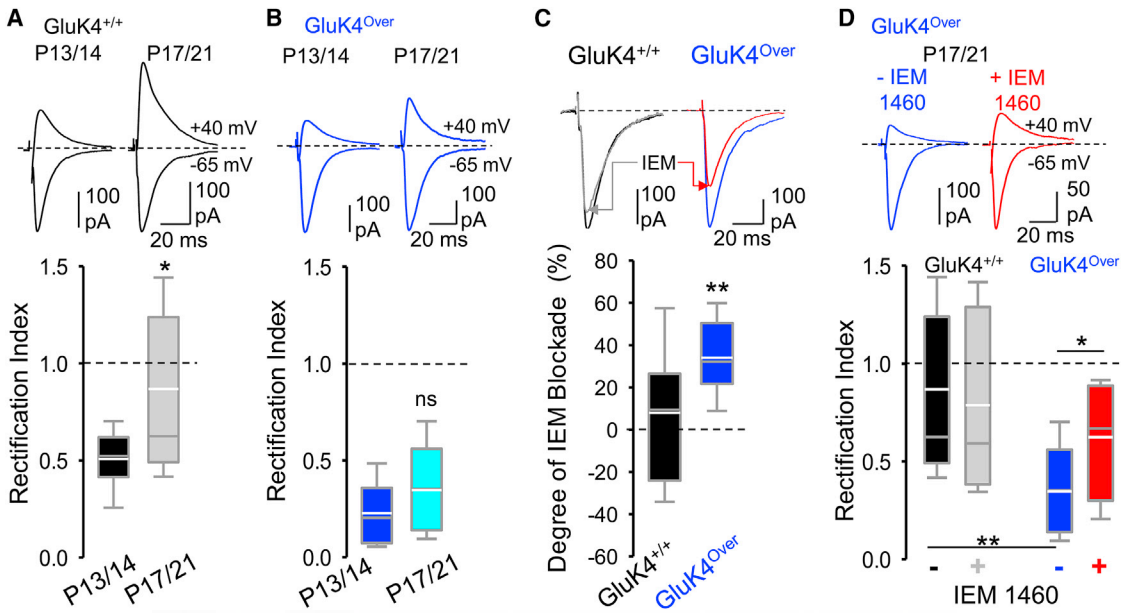

Figure 5. Ca^{2+}-Permeable AMPARs Are Enriched in GluK4-Overexpressing Synapses

(A) Representative AMPAR eEPSCs recorded from CA3 pyramidal neurons at the indicated holding potentials from P13–P14 (juvenile) and P17–P21 (adult) WT mice. The RI was calculated as the peak response at +40 mV relative to the peak response at −65 mV (bottom), and it was significantly different between the two stages of maturation: P13–P14, 0.51 ± 0.04 (13 neurons from 13 slices); and P17–P21, 0.87 ± 0.12 (22 neurons from 22 slices).

(B) Same analysis in $GluK4^{Over}$ mice revealed no difference at the two developmental stages: 0.23 ± 0.04 (18 neurons from 18 slices) and 0.35 ± 0.06 (16 neurons from 16 slices).

(C) Representative recordings of individual EPSCs evoked by stimulation of mossy fibers at −65 mV in CA3 neurons from $GluK4^{+/+}$ and $GluK4^{Over}$ mice, before and after application of IEM 1460 (upper panel). The bottom panel presents data showing the larger blocking effect of IEM 1460 (50 μM, gray bar) on $GluK4^{Over}$ mice. The data derive from 15 neurons from 15 slices for WT and 18 neurons from 18 slices for $GluK4^{Over}$ recorded from 3 adult mice from each genotype.

(D) Representative recordings of individual EPSCs evoked by MF stimulation at −65 mV and +40 mV in neurons from $GluK4^{Over}$ mice, with and without IEM 1460 (upper). The bottom panel presents data showing the lack of effect of IEM 1460 (50 μM, grey bar) on the rectification index of WT neurons yet it decreased the rectification in $GluK4^{Over}$ neurons (red bar). The data from 22 neurons/22 slices for WT and 15 neurons/15 slices for $GluK4^{Over}$ recorded from 3 adult mice from each genotype.

*$p < 0.05$; **$p < 0.01$; Mann-Whitney rank-sum test was used in (A)–(C) and ANOVA on ranks with Dunn's method was used in (D).

Accordingly, IEM1460 significantly reduced the rectification in neurons from $GluK4^{over}$ mice (Figure 5D) but did not totally remove it.

Together, these data suggest that the presence of more GluK4 subunits increases the ratio of calcium-permeable to -impermeable AMPARs at synapses, which could account for the altered amplitude of $EPSCs_{AMPAR}$ beyond the increase in transmitter release. This led us to hypothesize that GluK4 could regulate synaptic transmission at excitatory synapses beyond its role as an ion channel receptor.

The Increased Probability of Release in $GluK4^{over}$ Mice Is due to a Change in the Affinity of Presynaptic KARs

At the presynaptic level, the overexpression of GluK4 increased the release probability, as revealed by a higher mEPSC frequency. This phenomenon might reflect a higher affinity of the presynaptic KARs due to the incorporation of more high-affinity GluK4 subunits into the functional receptors. Such higher affinity KARs would eventually become activated by ambient glutamate, stimulating quantal glutamate release. To address this possibility, we recorded mEPSCs from BLA pyramidal cells in the presence of the KAR antagonist UBP310. This treatment attenuated the mEPSC frequency in WT animals and, as expected, reverted the increase in the mEPSC frequency in $GluK4^{over}$ mice (Figures 6A and 6B). Experiments carried in CA3 pyramidal cells yielded similar results (Figure S5). Furthermore, the greater release probability in $GluK4^{Over}$ mice attenuated the short-term plasticity measured as the degree of frequency facilitation in MF-to-CA3 synapses (Figures 6C and 6D), and blocking KARs with UBP310 restored the magnitude of frequency facilitation to values observed in WT mice (Figure 6D). These results led us to conclude that enhanced GluK4 expression enriches presynaptic boutons with higher affinity KARs, making them sensitive to ambient glutamate and facilitating quantal glutamate release.

Normalizing the *Grik4* Dose Rescues the Synaptic and Behavioral Phenotypes of $GluK4^{over}$ Mice

The data presented earlier strongly suggest that the synaptic phenotypes associated with a higher dose of *Grik4* in the transgenic mice are the direct consequence of excess of GluK4 protein. To demonstrate this, we generated $GluK4^{Over}$ mice with a normal copy number of the *Grik4* gene ($GluK4^{Res}$) by crossing $GluK4^{Over}$ mice with $GluK4^{-/-}$ mice, generating animals in which the amount of GluK4 protein was normalized. In western blots

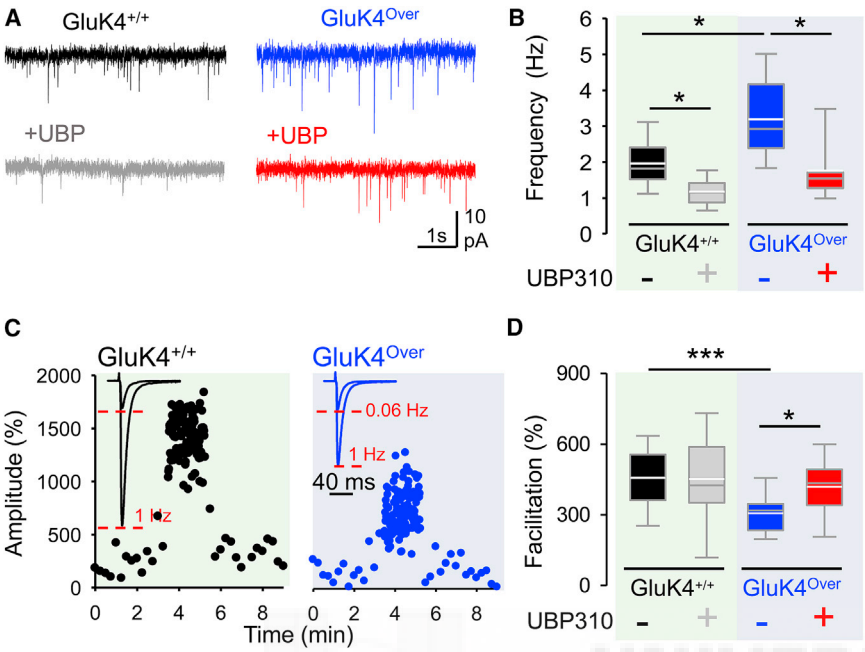

Figure 6. Enhanced Glutamate Release Is Caused by the Tonic Activity of Presynaptic High-Affinity KARs

(A) The antagonism of KARs by UBP310 (10 μM) depressed the increased frequency of mEPSC in BLA synapses.

(B) Quantification of the effects of UBP310 on the frequency of mEPSC in GluK4$^{+/+}$ and GluK4-overexpressing mice. While the frequency in GluK4$^{+/+}$ mice was reduced from 1.96 ± 0.15 Hz to 1.17 ± 0.09 Hz in GluK4^{Over} mice, it was reduced from 3.20 ± 0.25 Hz to 1.75 ± 0.21 Hz (n = 18 neurons; *p < 0.05, one-way ANOVA on ranks with Dunn's method).

(C) In the CA3 field of the hippocampus, short term plasticity measured as 1-Hz frequency facilitation (FF) was attenuated in GluK4-overexpressing mice: 456 ± 39.3% (n = 10 neurons from 10 slices) and 307 ± 29.2% (n = 8 neurons from 8 slices) in WT and GluK4^{Over} mice, respectively (p = 0.01, two-tailed Student's t test). The insets show the representative averaged (n = 30) synaptic responses in each case.

(D) Effect of UBP310 on FF in CA3 pyramidal cells. Note how the degree of facilitation is restored upon KAR antagonism in GluK4^{Over} mice: 419 ± 41.8% (n = 8 neurons from 8 slices). ***p < 0.001, *p < 0.05, two-tailed Student's t test).

See also Figure S5.

(WBs) of brain tissue, there was a clear lack of endogenous GluK4, with these animals exclusively expressing the protein product of the *Grik4* transgene (i.e., myc-GluK4: Figure 7A). The amplitude of the miniature and evoked EPSCs from BLA neurons reverted to the normal WT amplitude (Figure 7B). Interestingly, the release probability—which was increased in GluK4^{Over} and depressed in GluK4$^{-/-}$ mice, as estimated by the paired-pulse ratio—returned to those values observed in WT animals (Figure 7B). The frequency of mEPSCs recorded from both regular- and late-spiking cells in the CeLA recovered to normal values (Figure 7C). Similarly, in the hippocampus, the amplitude of eEPSCs$_{AMPAR}$ recorded from CA3 pyramidal neurons in these mice was similar to that of WT, and the sEPSCs$_{KAR}$ had normal values, too. Paired-pulse ratio and frequency facilitation returned to typical values at mossy-fiber-to-CA3 synapses (Figure S6).

GluK4^{over} mice display several behavioral phenotypes, like anxiety, depression, reduced locomotor activity, etc. (see Aller et al., 2015). We confirmed these altered behaviors in new experiments carried out in WT siblings and GluK4$^{-/-}$ animals and observed that normalization of GluK4 protein levels also reversed these altered behaviors, as is evident in a series of tests that characterize social interactions (Figure 7D), depression (Figure 7E), and anxiety (Figures 7F and 7G) in mice. Interestingly, the locomotor activity of these animals was also normalized (see Figure 7F).

DISCUSSION

In this study, we found that the over-dosage of *Grik4*, which encodes a high-affinity KAR subunit and results in a mild increase of GluK4 protein levels, alters the efficacy of synaptic transmission in the amygdala circuits. This consisted of a remarkably persistent enhancement of synaptic gain at selected synapses, which caused a clear imbalance between the inhibitory and excitatory activity at the amygdala output cells. As *de novo* duplication of this gene has been described in cases of autism (Griswold et al., 2012) and was associated with different endophenotypes in schizophrenia (Pickard et al., 2006; Greenwood et al., 2016), the synaptic alterations described in this study as a result of enriched GluK4 expression may also occur in these pathologies, possibly accounting for some of the abnormal behaviors observed. Thus, our data reveal that mild, yet reliable, alterations to the properties of particular synapses affect the overall performance of neuronal circuits and, hence, the individual's behavior. Although great caution needs to be applied when trying to extrapolate from animal models to human diseases, these data highlight that persistent aberrant activity within defined circuits may underlie the abnormal behaviors associated with mental disease.

KARs Modify the Circuit Balance in the Amygdala

Previous studies circumscribed the expression of *Grik4* mostly to the CA3 field in the hippocampus (Wisden and Seeburg, 1993; see also the Allen Mouse Brain Atlas). However, we revisited the expression of *Grik4* by non-radioactive *in situ* hybridization and found *Grik4* transcripts to be more widely distributed than anticipated, with strong *Grik4* expression in the CA3 and dentate gyrus, as well as in the CA1 field of the hippocampus. Similarly, we also found significant expression in the neocortex and amygdala nuclei. Accordingly, the expression of this gene in this structure and the remarkable effects that its overexpression has on

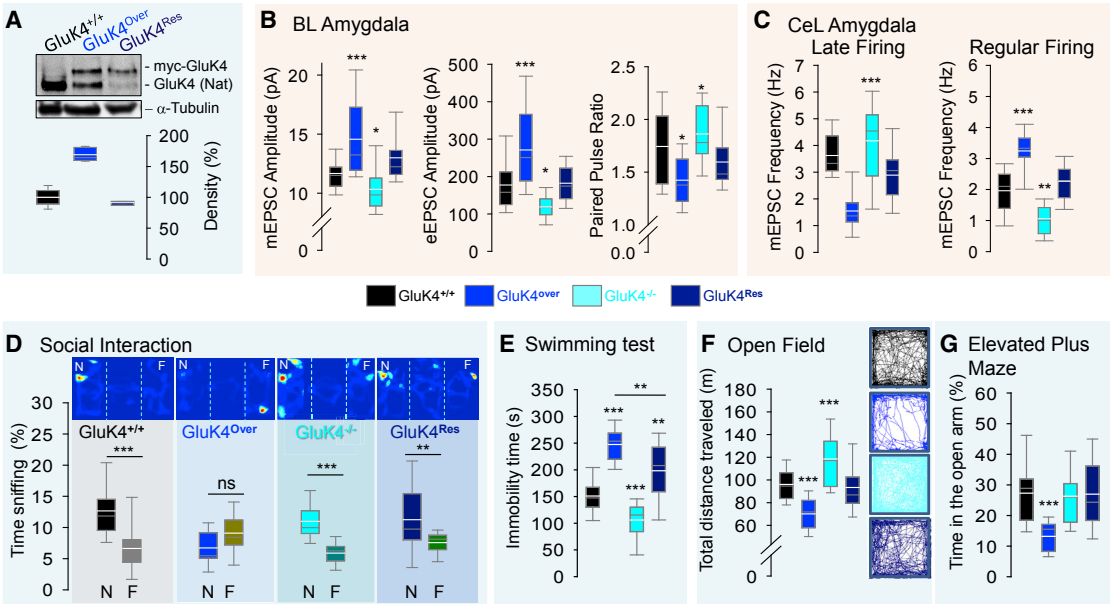

Figure 7. Rescue of GluK4^{Over} Synaptic and Behavioral Phenotypes by Restoring Levels of *Grik4* Expression

(A) Western blot analysis showing the recovery of the total amount of GluK4 protein after crossing GluK4^{Over} and GluK4$^{-/-}$ mice (i.e., GluK4^{Res}). Note that normal GluK4 protein levels are established in these mice at the expense of the native GluK4 protein (Nat). The boxplot shows data obtained from 3 different sets of animals.

(B) Amplitudes of AMPAR-mediated mEPSCs (ns = 31, 21, 15, and 27 neurons for each phenotype, respectively from 4–9 mice) and external-capsule-eEPSCs (ns = 26, 17, 15, and 16 neurons from 5–9 mice) in BLA pyramidal neurons in the four different mouse genotypes, including GluK4 deficient. The right panel shows the paired-pulse ratio values from BLA neurons observed in the four genotypes, showing recovery in mice with normalized levels of GluK4 (ns = 29, 17, 19, and 16 neurons, respectively, from 5–9 mice).

(C) Frequencies of mEPSCs at late-firing cells (ns = 13, 16, 15, and 19 neurons from 8–9 mice) and regular-firing cells from the CeLA from mice (ns = 11, 20, 11, and 12 neurons from 7–11 mice) of the four genotypes.

For (B) and (C): *p < 0.05; **p < 0.01; ***p < 0.001, one-way ANOVA on ranks with Dunn's method.

(D) GluK4^{Over} mice do not discriminate between novel (N) and familiar (F) mice in social interaction tests, while restoring GluK4 protein levels restores social interaction to normality. Insets are representative heat plots from a 3-chamber social test for each type of mouse, in which mice were confronted with familiar and novel mice. Student's t test: **p < 0.01; ***p < 0.001, from 14 GluK4$^{+/+}$, 11 GluK4^{Over}, 9 KO, and 14 GluK4^{Res} mice).

(E) In the forced swimming test, GluK4^{Over} mice remained immobile for longer periods than WT and KO mice, which is compatible with depressive behaviors. These symptoms were attenuated, but not eliminated, after normalizing the GluK4 protein levels.

(F and G) Mice overexpressing GluK4 show indications of severe anxiety in the open field test (F) and elevated plus maze (G) that were eliminated when GluK4 levels were normalized (GluK4^{Res}). Insets show the animal's tracks with different phenotypes. In the open field test, the deficit of total distance walked by GluK4^{Over} mice was recovered upon normalization of the GluK4 protein levels.

For (E)–(G): *p < 0.05, **p < 0.01; ***p < 0.001 one-way ANOVA analysis of 21 GluK4$^{+/+}$, 19 GluK4^{Over}, 19 KO and 19 GluK4^{Res} mice.

See also Figure S6.

the synaptic efficiency at the level of the amygdala, a structure classically related to depression and anxiety, are of particular interest. Cortico-amygdala synaptic transmission was enhanced through two main actions: the increase in the probability of release; and the enhancement of postsynaptic responses through an increase in quantal size, which drives an increase in the activity of BLA neurons in the transgenic animals. This concurs with the observation that most forms of human anxiety disorders are associated with BLA hyperactivity (Felix-Ortiz et al., 2016), and BLA hyperexcitability (or hypertrophy) in rodents is associated with enduring facilitation of anxiety-like behaviors (Roozendaal et al., 2009). In addition, BLA interactions with downstream targets like the central amygdala and ventral hippocampus are sufficient to alter anxiety (Tye et al., 2011; Felix-Ortiz and Tye, 2014).

Perhaps the most striking effect of GluK4 overexpression was found in the intra-amygdala circuits, where transmission from the BLA to CeLA was clearly altered. Interestingly, the CeLA contains GABA neurons, and as such, they do not overexpress *Grik4*. Therefore, the enhanced GluK4 activity could be ascribed exclusively to the enrichment of GluK4-containing presynaptic KARs in BLA pyramidal neuron terminals that contact CeLA neurons. The mEPSC$_{AMPAR}$ frequency increased in synapses contacting CeLA regular-spiking cells, but it was reduced in synapses with the other type of CeLA neuron, the late-spiking cells, which represent the main source of inhibition of CeMA inhibitory neurons (LeDoux et al., 1990; Duvarci and Pare, 2014; Janak and Tye, 2015). Consequently, the evoked responses in the CeLA were enhanced in regular-spiking cells and depressed in late-spiking cells. The mEPSC$_{AMPAR}$ amplitudes were also slightly larger or reduced, respectively, probably reflecting the altered frequency of multiquantal release in each case.

This intrinsic circuit disequilibrium might dramatically alter the main amygdala ouptputs. This hypothesis was further confirmed

by looking at the spontaneous occurrence of IPSCs and EPSCs at CeLA principal neurons and was confirmed *in vivo* by measuring the number of neurons expressing the c-Fos, an indirect marker of neuronal activity. There was a remarkable imbalance in excitatory to inhibitory inputs, particularly in late-spiking cells. These neurons belong to an anxiolytic circuit, the activation of which reduces anxiety by inhibiting CeMA neurons (Tye et al., 2011). On the other hand, regular-spiking cells have been said to promote fear (Amano et al., 2011). According to our data, the basal activity of the fear-promoting circuit would be enhanced in the GluK4-overexpressing mice, while the anxiolytic circuit is basally depressed. This interpretation was further supported by *in vivo* c-Fos assays, which indicated a significantly higher proportion of active neurons in BLA as well as in CeMA, the origin of an anxiogenic circuit. In terms of behavior, GluK4^{over} mice do display a severe anxiety and have signs of fear (Aller et al., 2015), all compatible with the imbalances in the activity of these circuits. Accordingly, the intra-BLA injections of UBP302, a KAR antagonist, and ablation of GluK4 have anxiolytic effects in the open field and the acoustic startle response tests (Aroniadou-Anderjaska et al., 2012; Catches et al., 2012). Therefore, our data support the idea that the stable and balanced transmission between the BLA and the central amygdala regulates anxiety-related behaviors and that *Grik4* duplication may be relevant to such behaviors in humans, given that the amygdala is structurally and functionally conserved across species.

Postsynaptic Effects of GluK4 Gain of Function

The excess of GluK4 protein resulted in enhanced synaptic KAR-mediated responses, something that would be expected. Not only was the amplitude increased but the decay kinetics was also altered, indicating that exogenous GluK4 took part of functional synaptic KARs in BLA neurons from overexpressing mice. However, to our surprise, the amplitude of the AMPAR-mediated responses was also increased. Although an increased release probability would be enough to explain this result, the larger amplitude of mEPSCs$_{AMPAR}$ suggested that an additional effect was produced, likely involving an increase in synaptic content of glutamate receptors. We ruled out the possibility that the more frequent release events in GluK4^{over} mice artifactually increased the mean mEPSCs$_{AMPAR}$ calculated as the average of all events. Experiments where we measured the minimal quantal content of postsynaptic responses indicated that this was not the case. The quantal content estimated after reducing the release probability by lowering the extracellular Ca^{2+} concentration, where multiquantal release was minimized, still revealed a larger elementary response in transgenic mice. This strongly suggests that a postsynaptic change in the receptor number and/or type took place in GluK4-enriched synapses. One possible explanation for this change in amplitude was found in that overexpressing mice had more CP (inwardly rectifying)-AMPARs than the WT mice. CP-AMPARs (i.e., those lacking GluA2 subunits) have a significantly larger single-channel conductance than Ca^{2+}-impermeable (CI) (no rectifying)-AMPARs (Swanson et al., 1997), which may account for the increase in the amplitude of elementary synaptic responses. We showed this to be the case indirectly by assessing the rectification coefficient in both situations, which estimates the ratio of CP-AMPARs to CI-AMPARs at the synapse. However, we cannot rule out that more AMPARs were also present at overexpressing synapses.

The enlarged KAR-mediated synaptic response as a consequence of GluK4 incorporation could also contribute to larger postsynaptic responses. However, if any, this influence was minimal, since the KAR component represents only a small part of the overall AMPAR-mediated current: ~18% in amygdala recordings (see data in the present study); and ~10% in CA1 interneurons (Frerking et al., 1999). Hence, the possible contribution to the overall amplitude could probably be disregarded. In addition, we did not observe a clear contribution of the slow KAR component to the overall mEPSCs in mice, contrary to what has been reported in rats (Cossart et al., 2002). Interestingly, these data indicate that KARs (at least those containing GluK4) have synaptic effects beyond their role as ion-channel-forming receptors. The metabotropic non-canonical signaling also triggered by KARs (for a review, see Valbuena and Lerma, 2016) could offer a further explanation for this phenomenon, although this remains to be determined.

Presynaptic Effects

Overexpression of GluK4 led also to more frequent elementary synaptic events, indicating increased release probability. Accordingly, short-term plasticity, measured as paired-pulse or frequency facilitation, was attenuated. These results indicate not only that exogenous GluK4 subunits integrated into functional presynaptic KARs but also that these receptors probably changed their affinity, becoming tonically activated by ambient glutamate. Although no potent and specific antagonists of KARs are available, experiments carried out with UBP310, a competitive antagonist that recognizes heteromeric KARs (e.g., those incorporating high-affinity KAR subunits; Pinheiro et al., 2013), supported this tonic activation. Indeed, the frequency of mEPSCs$_{AMPAR}$ and the magnitude of frequency facilitation were both recovered upon exposure to UBP310. These data further clarify a function of KARs, such as the facilitation of glutamate release at particular synapses, a role that is somewhat controversial (Kwon and Castillo, 2008). Our data further extend this function to external capsule and to BLA pyramidal cells contacting CeLA regular-spiking cells.

Rescue of Synaptic and Behavioral Abnormalities in GluK4^{over} Mice

Interestingly, all the synaptic and behavioral anomalies observed in the mice with a higher dose of GluK4 were rescued by normalizing the amount of GluK4 protein. We reasoned that, if the synaptic phenotypes observed were due to the increase in GluK4 protein, normalizing these amounts in neurons should restore normal function, regardless of the origin of the protein. Crossing the overexpressing mice with GluK4-deficient mice produced good protein compensation, with the only difference being that the active protein in the "rescued" mice was transgenic rather than native. In these so-called GluK4^{Res} mice, the spontaneous synaptic responses mediated by KARs were undistinguishable from those in WT mice in terms of both amplitude and kinetics. Furthermore, AMPAR-mediated transmission was normal; other characteristics, such as short-term plasticity, appeared to be normal in the hippocampus, and the synaptic activity in the

BLA pyramidal neurons returned to normality in terms of pre- and postsynaptic properties. The frequency of mEPSCs in CeLA neurons was also close to normality in these animals. Interestingly, these animals performed normally in behavioral tests, with no enhancement of anxiety or depression, and they recovered their walking activity; the loss of which was previously interpreted as a lack of motivation (Aller et al., 2015). Social interactions in the 3-chamber text also reverted to normal when GluK4 protein levels were restored, with these mice preferring to interact with novel rather than with familiar partners. Interestingly, some behaviors that we observed as abnormal in GluK4-deficient mice (see also Catches et al., 2012), were also normalized when the GluK4 protein normal levels were restored, which further indicates a causal relation between the amount of GluK4 protein and behavioral anomalies. Together these data indicate that an excess of GluK4 produces an increase in synaptic gain in behaviorally relevant circuits, provoking aberrant behaviors that appear to reflect disease states evident in mood disorders and autistic traits.

In summary, enhanced doses of *Grik4*, a gene encoding a high-affinity subunit of the KAR family, produces unanticipated effects on the synaptic efficiency of particular synapses, revealing subtle roles for KARs in the control of synaptic efficacy. This gene has been found duplicated *de novo* in cases of autism (Griswold et al., 2012), and there is cytogenetic and genetic evidence supporting a link of *GRIK4* with schizophrenia and bipolar disorders (Pickard et al., 2006; Greenwood et al., 2016). In addition, there is evidence that this gene has common forms that affect the final abundance of both its transcripts and the protein it encodes in humans (Pickard et al., 2008), altering hippocampal function (Whalley et al., 2009). Therefore, the synaptic effects of GluK4 overexpression described here recapitulate functional circuit activity in humans and may be significant for understanding the ethiopathology of human disorders, establishing new ways to approach their experimental understanding.

EXPERIMENTAL PROCEDURES

Male and female mice were used in these experiments (n = 328), either mice with altered *Grik4* expression or their WT siblings, which were used as controls. The mice were housed in ventilated cages in a temperature-controlled, standard, pathogen-free environment (23°C), at 40%–60% humidity and on a 12-hr:12-hr light:dark cycle. The mice had *ad libitum* access to food and water, and the cages were changed weekly. Experimental procedures involving the use of live mice were performed in accordance with Spanish and European Union regulations (2010/63/EU) and with the approval of the bioethics committees at the Instituto de Neurociencias and the Consejo Superior de Investigaciones Científicas. All experiments were performed on mice whose genotype was unknown to the experimenter, and the data were also analyzed in a blind manner.

Generation of Mouse Lines

The transgenic lines overexpressing *Grik*4 were generated as described elsewhere (Aller et al., 2015). Briefly, a NotI fragment that contained *myc-grik*4 and the intronic sequence was introduced into the PMM403 plasmid that has the CaMKII promoter inserted in pBluescript (Mayford et al., 1996). The levels of *myc-Grik4* expression were analyzed in the first generation by *in situ* hybridization, and GluK4 levels were assessed by immunohistochemistry and in WBs. For these experiments, two different lines with a similar degree of GluK4 overexpression (50%–100%) were used, and similar phenotypes were found. GluK4 knockout (KO) animals were kindly provided by Dr. A. Contractor, Northwestern University (Chicago, IL, USA).

Slice Preparation and Electrophysiology

Parasagittal brain slices (300 μm) prepared from P17–P21 mice, unless otherwise stated, were used for hippocampal recordings (e.g., Aller et al., 2015). The same procedure was used for amygdala recordings, but using horizontal slices. Electrophysiological recordings were obtained from neurons identified visually by infrared (IR)-DIC (differential interference contrast) microscopy with a 40× water immersion objective, and all the experiments were carried out at room temperature (22°C–25°C). The slices were continuously perfused with a solution consisting of (in millimolar) 124 NaCl, 3 KCl, 1.25 KH_2PO_4, 1 $MgSO_4$, 2 $CaCl_2$, 26 $NaHCO_3$, and 10 glucose, equilibrated with 95% O_2/5% CO_2 (pH 7.3; 300 mOsm), supplemented with antagonists as required. Patch pipettes were filled with one of the following solutions (in millimolar): for amygdala neurons, 120 $KMeSO_3$, 20 KCl, 2 $MgCl_2$, 10 HEPES, 0.2 EGTA, 0.2 Na_2ATP, 7 Na_2-phosphocreatine (pH 7.2; 290 mOsm); for hippocampal neurons: 130 $CsMeSO_3$, 4 NaCl, 10 HEPES, 0.2 EGTA, 10 TEA, 2 Na_2ATP, and 0.5 Na_3GTP, 5 QX314 (pH 7.3, 287 mOsm). When recording spontaneous activity from central amygdala neurons, the internal solution consisted of (in millimolar): 135 $KMeSO_4$, 0.5 $CaCl_2$, 2 $MgCl_2$, 5 EGTA, 0.1 Na_3GTP, 10 HEPES, 2 MgATP (pH 7.2, 286 mOsm) (Zhou et al., 2009). Drugs were applied by gravity, switching between four perfusion lines using a switch valve (Valve Driver II, General Valve). We calculated that full exchange of the solutions required approximately 3 min, and, for this reason, cells were recorded for at least 5 min before the effect of the drug was assessed. To evoke EPSCs, supramaximal stimulation was applied through a monopolar electrode made from a glass pipette situated in the mossy-fiber pathway, the external capsule, or the BLA. Tight-seal (>1 GΩ) whole-cell recordings were obtained from the cell body of neurons situated in the CA3 pyramidal layer, BLA, or CeLA. Mossy-fiber responses were identified by large paired-pulse facilitation. The specificity of mossy-fiber stimulation was further assessed by looking at the depression induced by L-CCG-I (10 μM), a group II mGluR agonist that specifically depresses mossy-fiber-induced synaptic responses. Neurons in the amygdala nuclei were identified by their firing patterns when they were depolarized by current passing through the patch pipette. In a few instances, the correlation between morphology and electrical responses was confirmed by filling the neurons with biocytin, which was then visualized with streptavidin (Selak et al., 2006). The perfusion solution was supplemented with picrotoxin (100 μM), D-2-amino-5-phosphonovalerate (D-APV) (50 μM), and LY303070 (25 μM) to isolate spontaneous KAR-mediated EPSCs. To record mEPSCs, TTX (1 μM) was added to the solution, and LY303070 was omitted. Other drugs, such as the KAR antagonist UBP310 or the AMPAR/KAR antagonist CNQX, were added to the recording solution as required.

To calculate the AMPAR rectification index (RI), AMPAR currents were recorded with a normal perfusion solution containing 100 μM picrotoxin and 25 μM D-APV. Each evoked response was repeated 30 times with an interstimulus interval of 15 s, and they were averaged. The cells were first clamped at −65 mV for ~5 min, and the holding potential was then switched to +40 mV for an additional 5 min. The RI was calculated by dividing the peak AMPAR current at +40 mV with the peak of those at −65 mV. Frequency facilitation (FF) was elicited by delivering 30 pulses at 0.06 Hz, followed by another 30 pulses at 1 Hz to afferent fibers, and facilitation was calculated as the percentage increase in the eEPSCs observed at 1 Hz relative to the eEPSCs recorded at low frequency. All electrophysiological data were acquired using Clampex 10.6, and while the eEPSCs and the sEPSCs were analyzed with Clampfit 10.6, mEPSCs were measured with the MiniAnalysis software (Synaptosoft).

Non-Radioactive *In Situ* Hybridization

In situ hybridization was performed on free-floating sections, as described previously (Acloque et al., 2008; Paternain et al., 2000). Briefly, mouse brains were dissected out from animals previously perfused with 4% paraformaldehyde. Two different *Grik4* probes were hybridized to transverse vibratome brain sections (50 μm): (1) a sequence encompassing the 3′ UTR (333 bp); and (2) a sequence corresponding to exons 13, 14, and 15 of the *Grik4* gene (356 bp). The first probe was generated by PCR with the primers 5′-TGGCAGCAGC GAAGGACCATG and 5′-TAGGGGGAATTCAACTGATGAC, while the second

probe was generated with primers located between exons 13 and 15 of *Grik4*, 5′-ATCCCTTTTCTCCAGGAGTC and 5′-CAGGTCATCCACAGACTCAA (Fernandes et al., 2009). Probe specificity was assessed by using the sense probe and/or brain tissue from GluK4-deficient mice. Both probes produced similar labeling.

WBs

Protein lysates were probed in WBs with the following primary antibodies: mouse anti-alpha-tubulin (1:1,000, Abcam), mouse anti-Myc (1:500, Santa Cruz Biotechnology), and rabbit anti-KA1 (1:1,000, a generous gift from Dr Melanie Darstein; see Darstein et al., 2003). Antibody binding was detected on a luminescent image analyzer (LAS-1000PLUS; Fuji) and quantified with Quantity One 1D Analysis Software (Bio-Rad Laboratories), normalizing all densities to the corresponding α-tubulin signal.

Immunofluorescence

Brain sections (20 μm) were processed for immunocytochemistry as described previously (Aller et al., 2015), and they were then incubated overnight at 4°C with a rabbit anti-Myc antibody (1:500, Abcam) in blocking solution (PBS-0.2% Triton X-100 and 10% normal goat serum [NGS]). For c-Fos analysis, 50-μM vibratome sections were collected and stained with rabbit anti c-Fos polyclonal immunoglobulin G (IgG) (1:1,000; SynapticSystems, Germany). Antibody binding was detected with Alexa Fluor 555-conjugated anti-rabbit secondary antibodies at 1:1,000. Immunofluorescence staining was evaluated on a Leica DMLFSA confocal microscope and analyzed using the Imaris image analysis software (Bitplane). A low-pass filter was applied to subtract the background.

c-Fos quantification was conducted in a blind manner by using ImageJ software. Circular regions of interest (ROIs) were drawn over BLA, CeLA and CeMA (see Figure 4), and the background was removed with a rolling ball radius of 40 pixels. Three to five sections were considered for each mouse (12 to 15 weeks old, male and female). Cells were counted per unit area for all sections, and counts were averaged for each mouse. Mean immunofluorescence intensity was also calculated for each section and was similarly averaged for each mouse.

Behavioral Tests

Behavioral tests were carried out on 8–12 male and female week-old mice, using two different groups containing 9–10 mice per phenotype, as described in Aller et al. (2015). The procedures and analyses were carried out blind, although sometimes the phenotype was evident to the experimenter. The number of animals used (sample size) was chosen according to the estimated measurement variability and a pre-specified effect (equal to or more than twice the SD), with $p \leqslant 0.05$ and a power of 90%, according to the equation provided by the Grants Evaluation Committee of the University Miguel Hernández. Animals were studied randomly, regardless of their genotype.

Statistical Analysis

Statistical analyses were performed using the statistical tools in the SigmaPlot 12.5 software (i.e., built-in statistical tests to analyze data), including the Advisor Wizard, which guides the process of selecting the appropriate test. We used one-way ANOVAs for comparisons among more than 2 groups of data. Comparison between groups was performed using two-tailed paired or unpaired t tests (confidence interval, 95%) as appropriate (i.e., data were normally distributed) or the Mann-Whitney rank-sum test when the data did not conform to a normal distribution or when variances were unequal. The results are presented as scatterplots, which represent the mean ± SEM, or boxplots where the bottom and the top of the box are the first and third quartiles, respectively, and the whiskers above and below the box indicate the 95th and 5th percentiles. The median (gray line) and the mean (white line) are indicated.

SUPPLEMENTAL INFORMATION

Supplemental Information includes six figures and can be found with this article online at https://doi.org/10.1016/j.celrep.2018.05.086.

ACKNOWLEDGMENTS

We thank Dr. A. Contractor (Northwestern University) for kindly providing the GluK4$^{-/-}$ mouse. The authors gratefully acknowledge the financial support received from the Spanish Agency of Research (AEI) under the grant BFU2015-64656-R (to J.L.), co-financed by the European Regional Development Fund (ERDF); the Generalitat Valenciana through the program Prometeo II/2015/012 (to J.L.); and the "Severo Ochoa" Programme for Centres of Excellence in R&D (SEV-2013-0317). V.A. holds an FPI fellowship from the AEI (SVP-2014-068519), and V.P. was supported by the Generalitat Valenciana Santiago Grisolía fellowship programme.

AUTHOR CONTRIBUTIONS

C.R., M.I.A., V.A., and V.P. performed research; A.V.P., M.I.A., V.A., and V.P. analyzed data; and J.L. designed and supervised research and wrote the paper.

DECLARATION OF INTERESTS

The authors declare no competing interests.

Received: March 9, 2018
Revised: April 19, 2018
Accepted: May 24, 2018
Published: June 26, 2018

REFERENCES

Acloque, H., Wilkinson, D.G., and Nieto, M.A. (2008). In situ hybridization analysis of chick embryos in whole-mount and tissue sections. Methods Cell Biol. *87*, 169–185.

Aller, M.I., Pecoraro, V., Paternain, A.V., Canals, S., and Lerma, J. (2015). Increased dosage of high-affinity kainate receptor gene grik4 alters synaptic transmission and reproduces autism spectrum disorders features. J. Neurosci. *35* (*40*), 13619–13628.

Amano, T., Duvarci, S., Popa, D., and Paré, D. (2011). The fear circuit revisited: contributions of the basal amygdala nuclei to conditioned fear. J. Neurosci. *31*, 15481–15489.

Aroniadou-Anderjaska, V., Pidoplichko, V.I., Figueiredo, T.H., Almeida-Suhett, C.P., Prager, E.M., and Braga, M.F.M. (2012). Presynaptic facilitation of glutamate release in the basolateral amygdala: a mechanism for the anxiogenic and seizurogenic function of GluK1 receptors. Neuroscience *221*, 157–169.

Catches, J.S., Xu, J., and Contractor, A. (2012). Genetic ablation of the GluK4 kainate receptor subunit causes anxiolytic and antidepressant-like behavior in mice. Behav. Brain Res. *228*, 406–414.

Cossart, R., Epsztein, J., Tyzio, R., Becq, H., Hirsch, J., Ben-Ari, Y., and Crépel, V. (2002). Quantal release of glutamate generates pure kainate and mixed AMPA/kainate EPSCs in hippocampal neurons. Neuron *35*, 147–159.

Darstein, M., Petralia, R.S., Swanson, G.T., Wenthold, R.J., and Heinemann, S.F. (2003). Distribution of kainate receptor subunits at hippocampal mossy fiber synapses. J. Neurosci. *23*, 8013–8019.

Duvarci, S., and Pare, D. (2014). Amygdala microcircuits controlling learned fear. Neuron *82*, 966–980.

Felix-Ortiz, A.C., and Tye, K.M. (2014). Amygdala inputs to the ventral hippocampus bidirectionally modulate social behavior. J. Neurosci. *34*, 586–595.

Felix-Ortiz, A.C., Burgos-Robles, A., Bhagat, N.D., Leppla, C.A., and Tye, K.M. (2016). Bidirectional modulation of anxiety-related and social behaviors by amygdala projections to the medial prefrontal cortex. Neuroscience *321*, 197–209.

Fernandes, H.B., Catches, J.S., Petralia, R.S., Copits, B.A., Xu, J., Russell, T.A., Swanson, G.T., and Contractor, A. (2009). High-affinity kainate receptor subunits are necessary for ionotropic but not metabotropic signaling. Neuron *63*, 818–829.

Fisher, M.T., and Fisher, J.L. (2014). Contributions of different kainate receptor subunits to the properties of recombinant homomeric and heteromeric receptors. Neuroscience *278*, 70–80.

Frerking, M., Petersen, C.C.H., and Nicoll, R.A. (1999). Mechanisms underlying kainate receptor-mediated disinhibition in the hippocampus. Proc. Natl. Acad. Sci. USA *96*, 12917–12922.

Gillott, A., Furniss, F., and Walter, A. (2001). Anxiety in high-functioning children with autism. Autism *5*, 277–286.

Greenwood, T.A., Lazzeroni, L.C., Calkins, M.E., Freedman, R., Green, M.F., Gur, R.E., Gur, R.C., Light, G.A., Nuechterlein, K.H., Olincy, A., et al. (2016). Genetic assessment of additional endophenotypes from the consortium on the genetics of schizophrenia family study. Schizophr. Res. *170*, 30–40.

Griswold, A.J., Ma, D., Cukier, H.N., Nations, L.D., Schmidt, M.A., Chung, R.H., Jaworski, J.M., Salyakina, D., Konidari, I., Whitehead, P.L., et al. (2012). Evaluation of copy number variations reveals novel candidate genes in autism spectrum disorder-associated pathways. Hum. Mol. Genet. *21*, 3513–3523.

Janak, P.H., and Tye, K.M. (2015). From circuits to behaviour in the amygdala. Nature *517*, 284–292.

Kenny, E.M., Cormican, P., Furlong, S., Heron, E., Kenny, G., Fahey, C., Kelleher, E., Ennis, S., Tropea, D., Anney, R., et al. (2014). Excess of rare novel loss-of-function variants in synaptic genes in schizophrenia and autism spectrum disorders. Mol. Psychiatry *19*, 872–879.

Knight, H.M., Walker, R., James, R., Porteous, D.J., Muir, W.J., Blackwood, D.H.R., and Pickard, B.S. (2012). GRIK4/KA1 protein expression in human brain and correlation with bipolar disorder risk variant status. Am. J. Med. Genet. B. Neuropsychiatr. Genet. *159B*, 21–29.

Kwon, H.-B., and Castillo, P.E. (2008). Role of glutamate autoreceptors at hippocampal mossy fiber synapses. Neuron *60*, 1082–1094.

LeDoux, J.E., Cicchetti, P., Xagoraris, A., and Romanski, L.M. (1990). The lateral amygdaloid nucleus: sensory interface of the amygdala in fear conditioning. J. Neurosci. *10*, 1062–1069.

Lerma, J. (2003). Roles and rules of kainate receptors in synaptic transmission. Nat. Rev. Neurosci. *4*, 481–495.

Lerma, J., and Marques, J.M. (2013). Kainate receptors in health and disease. Neuron *80*, 292–311.

Lopez de Armentia, M., and Sah, P. (2004). Firing properties and connectivity of neurons in the rat lateral central nucleus of the amygdala. J. Neurophysiol. *92*, 1285–1294.

Marques, J.M., Rodrigues, R.J., Valbuena, S., Rozas, J.L., Selak, S., Marin, P., Aller, M.I., and Lerma, J. (2013). CRMP2 tethers kainate receptor activity to cytoskeleton dynamics during neuronal maturation. J. Neurosci. *33*, 18298–18310.

Mayford, M., Bach, M.E., Huang, Y.Y., Wang, L., Hawkins, R.D., and Kandel, E.R. (1996). Control of memory formation through regulated expression of a CaMKII transgene. Science *274*, 1678–1683.

Nicoll, R.A. (2017). A brief history of long-term potentiation. Neuron *93*, 281–290.

Paternain, A.V., Herrera, M.T., Nieto, M.A., and Lerma, J. (2000). GluR5 and GluR6 kainate receptor subunits coexist in hippocampal neurons and coassemble to form functional receptors. J. Neurosci. *20*, 196–205.

Pickard, B.S., Malloy, M.P., Christoforou, A., Thomson, P.A., Evans, K.L., Morris, S.W., Hampson, M., Porteous, D.J., Blackwood, D.H.R., and Muir, W.J. (2006). Cytogenetic and genetic evidence supports a role for the kainate-type glutamate receptor gene, GRIK4, in schizophrenia and bipolar disorder. Mol. Psychiatry *11*, 847–857.

Pickard, B.S., Knight, H.M., Hamilton, R.S., Soares, D.C., Walker, R., Boyd, J.K., Machell, J., Maclean, A., McGhee, K.A., Condie, A., et al. (2008). A common variant in the 3'UTR of the GRIK4 glutamate receptor gene affects transcript abundance and protects against bipolar disorder. Proc. Natl. Acad. Sci. USA *105*, 14940–14945.

Pinheiro, P.S., Perrais, D., Coussen, F., Barhanin, J., Bettler, B., Mann, J.R., Malva, J.O., Heinemann, S.F., and Mulle, C. (2007). GluR7 is an essential subunit of presynaptic kainate autoreceptors at hippocampal mossy fiber synapses. Proc. Natl. Acad. Sci. USA *104*, 12181–12186.

Pinheiro, P.S., Lanore, F., Veran, J., Artinian, J., Blanchet, C., Crépel, V., Perrais, D., and Mulle, C. (2013). Selective block of postsynaptic kainate receptors reveals their function at hippocampal mossy fiber synapses. Cereb. Cortex *23*, 323–331.

Poot, M., Eleveld, M.J., van 't Slot, R., Ploos van Amstel, H.K., and Hochstenbach, R. (2010). Recurrent copy number changes in mentally retarded children harbour genes involved in cellular localization and the glutamate receptor complex. Eur. J. Hum. Genet. *18*, 39–46.

Roozendaal, B., McEwen, B.S., and Chattarji, S. (2009). Stress, memory and the amygdala. Nat. Rev. Neurosci. *10*, 423–433.

Rozas, J.L., Paternain, A.V., and Lerma, J. (2003). Noncanonical signaling by ionotropic kainate receptors. Neuron *39*, 543–553.

Sachidhanandam, S., Blanchet, C., Jeantet, Y., Cho, Y.H., and Mulle, C. (2009). Kainate receptors act as conditional amplifiers of spike transmission at hippocampal mossy fiber synapses. J. Neurosci. *29*, 5000–5008.

Schlesinger, F., Tammena, D., Krampfl, K., and Bufler, J. (2005). Two mechanisms of action of the adamantane derivative IEM-1460 at human AMPA-type glutamate receptors. Br. J. Pharmacol. *145*, 656–663.

Sebat, J., Lakshmi, B., Malhotra, D., Troge, J., Lese-Martin, C., Walsh, T., Yamrom, B., Yoon, S., Krasnitz, A., Kendall, J., et al. (2007). Strong association of de novo copy number mutations with autism. Science *316*, 445–449.

Segerstråle, M., Juuri, J., Lanore, F., Piepponen, P., Lauri, S.E., Mulle, C., and Taira, T. (2010). High firing rate of neonatal hippocampal interneurons is caused by attenuation of afterhyperpolarizing potassium currents by tonically active kainate receptors. J. Neurosci. *30*, 6507–6514.

Selak, S., Paternain, A.V., Fritzler, M.J., and Lerma, J. (2006). Human autoantibodies against early endosome antigen-1 enhance excitatory synaptic transmission. Neuroscience *143*, 953–964.

Swanson, G.T., Kamboj, S.K., and Cull-Candy, S.G. (1997). Single-channel properties of recombinant AMPA receptors depend on RNA editing, splice variation, and subunit composition. J. Neurosci. *17*, 58–69.

Tye, K.M., Prakash, R., Kim, S.Y., Fenno, L.E., Grosenick, L., Zarabi, H., Thompson, K.R., Gradinaru, V., Ramakrishnan, C., and Deisseroth, K. (2011). Amygdala circuitry mediating reversible and bidirectional control of anxiety. Nature *471*, 358–362.

Valbuena, S., and Lerma, J. (2016). Non-canonical signaling, the hidden life of ligand-gated ion channels. Neuron *92*, 316–329.

Whalley, H.C., Pickard, B.S., McIntosh, A.M., Zuliani, R., Johnstone, E.C., Blackwood, D.H., Lawrie, S.M., Muir, W.J., and Hall, J. (2009). Modulation of hippocampal activation by genetic variation in the GRIK4 gene. Mol. Psychiatry *14*, 465.

White, S.W., Oswald, D., Ollendick, T., and Scahill, L. (2009). Anxiety in children and adolescents with autism spectrum disorders. Clin. Psychol. Rev. *29*, 216–229.

Wisden, W., and Seeburg, P.H. (1993). A complex mosaic of high-affinity kainate receptors in rat brain. J. Neurosci. *13*, 3582–3598.

Zhou, F.W., Chen, H.X., and Roper, S.N. (2009). Balance of inhibitory and excitatory synaptic activity is altered in fast-spiking interneurons in experimental cortical dysplasia. J. Neurophysiol. *102*, 2514–2525.

Cell Reports, Volume *23*

Supplemental Information

Increased *Grik4* Gene Dosage Causes Imbalanced Circuit Output and Human Disease-Related Behaviors

Vineet Arora, Valeria Pecoraro, M. Isabel Aller, Celia Román, Ana V. Paternain, and Juan Lerma

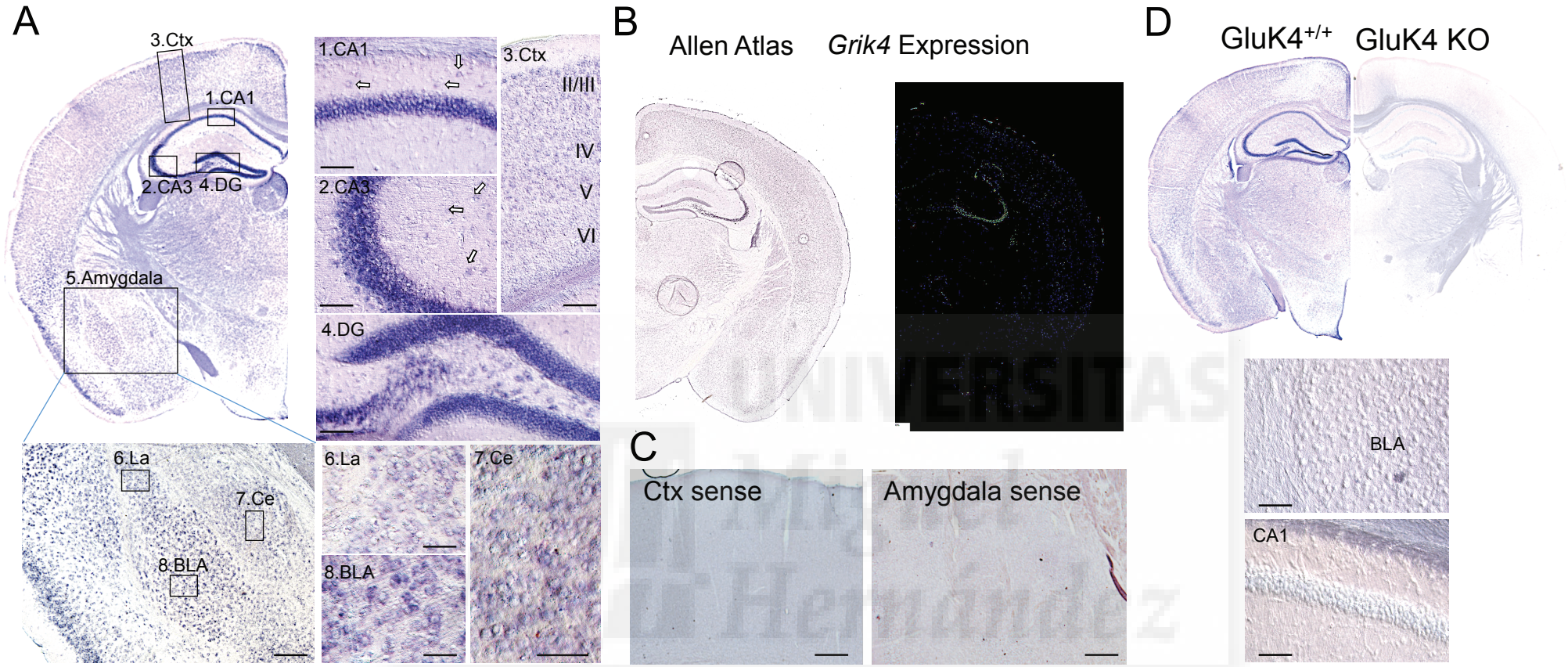

Figure S1. Related to Fig. 1. Expression of *Grik4* in the mouse brain. A, Non-radioactive in situ hybridisation using a probe encompassing the 3'UTR of mouse *Grik4* gene. Strong expression was observed in the CA3 area of the hippocampus, but also at the CA1 field (panel 1) and the Dentate Gyus (DG, panel 4). Expression was seen in putative interneurons at the Stratum Oriens (arrows in panel 1) and Stratum Lucidum (arrows in panel 2) as well as in all layers of the Neocortex (Ctx, panel 3). Interestingly, *Grik4* expression was also found in the Amygdala complex (panel 5) with significant signal in the Lateral (La, panel 6), Central (Ce, panel 7) and Baso-Lateral nuclei (BLA, panel 8). Calibration bars: 100 µm for panels 1-4; 500 µm for panel 5 and 50 µm for panels 7-8. **B**, Expression of mouse *Grik4* as reported in the Allen Mouse Atlas. On the right, the panel shows the net expression of this gene. Note that Dentate Gyrus, CA1 and other fields and structures appear devoid or near-devoid of *Grik4* expression. The section corresponds to a similar section as shown in A and D. **C,** As a first control of probe specificity, sections were hybridised with a sense probe, yielding total absence of signal. Calibration bars: 500 µm. **D**, As a second control, we used another probe encompassing the exon 11, which is not transcribed in the GluK4 deficient mouse (GluK4 KO). As can be seen, *Grik4* expression (top left panel) was found with a similar distribution as in A, which was totally absent in KO animals (top right panel). The bottom panels show detailed examples of lack of *Grik4* signal in the KO animal at amygdala and the CA1 field of the hippocampus. Calibration bars: 100 µm

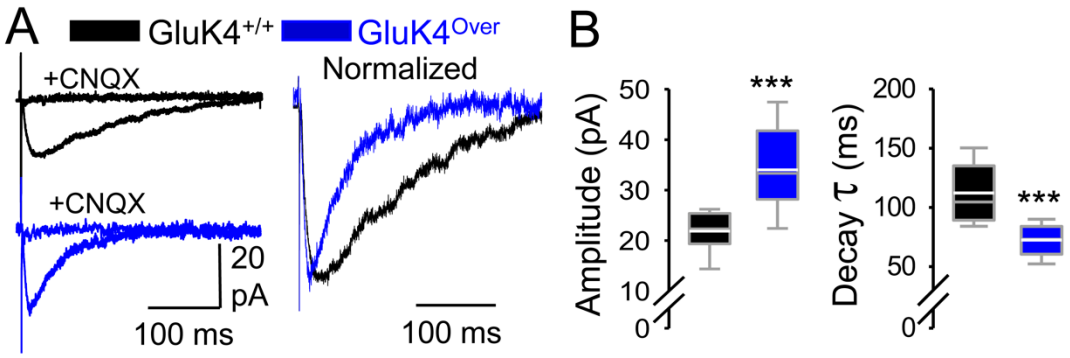

Figure S2, Related to Fig 1. $EPSC_{KAR}$ are enhanced in pyramidal cells of the Basolateral Amygdala in $GluK4^{over}$. **A**, KAR-mediated EPSCs in BLA cells evoked by external capsule stimuli in the presence of LY303070 (25 μM) and APV 50 μM), recorded at -60 mV of membrane potential (average of 10 responses). Note how the mixed KAR-AMPA antagonist, CNQX (50 μM), blocked KAR-mediated responses in $GluK4^{+/+}$ and $GluK4^{Over}$. On the right, both KAR-mediated responses have been normalized and superimposed. **B**, Population values for the amplitude and decay times of these responses are shown for each genotype (n=10 neurons/10 slices and n=14 neurons/14 slices from 8 $GluK4^{+/+}$ and 6 $GluK4^{Over}$ mice, respectively; ***p<0.001, Mann-Whitney Rank Sum test.

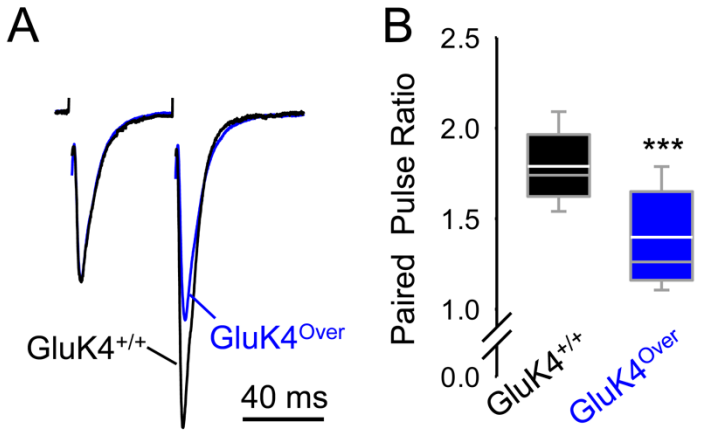

Figure S3, Related to Fig 1. GluK4 overexpression in BLA pyramidal cells increases release probability. A, Paired pulse responses (50 ms interval) from GluK4$^{+/+}$ and GluK4^{Over} mice have been normalized to the first amplitude to show a reduction of paired pulse facilitation, indicative of an increase in release probability in transgenic mice. **B**, Quantification of the ratio of second to first responses in both genotypes. Data from 28 (GluK4$^{+/+}$) and 35 (GluK4^{Over}) neurons (31 slices from 14 mice), ***p<0.001, Mann-Whitney Rank Sum Test.

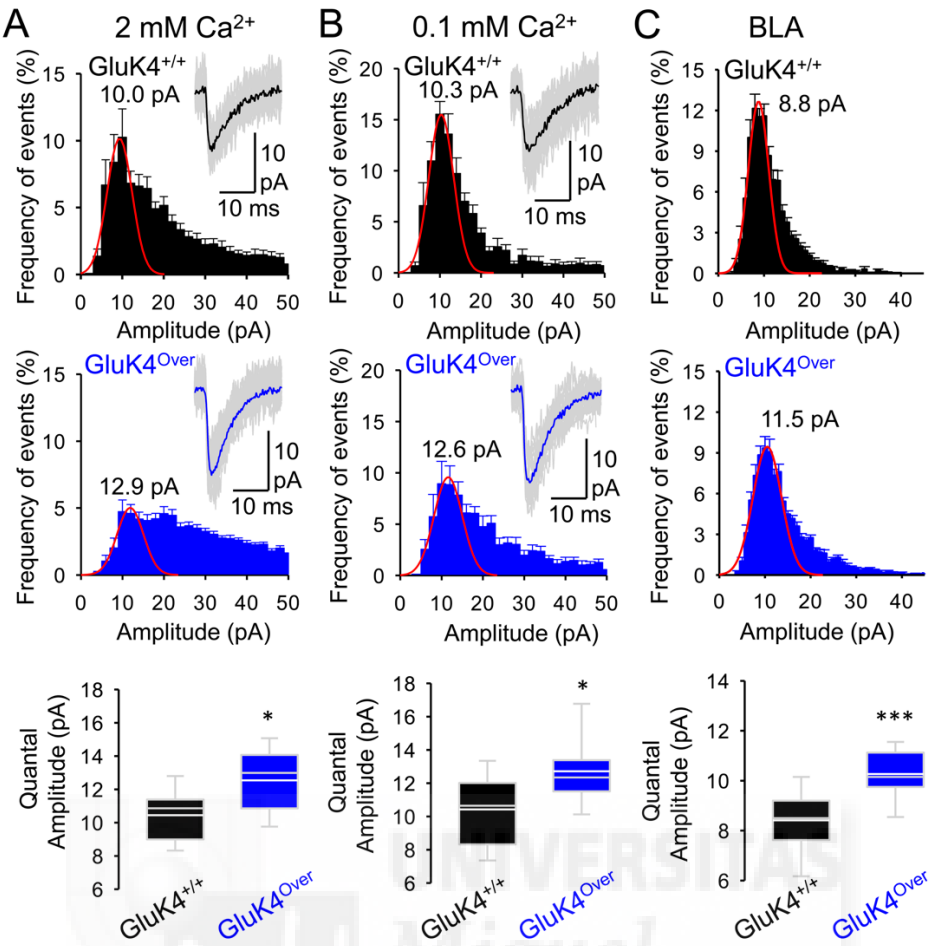

Figure S4, related to Fig 1 and 3. Amplitude histograms of mEPSCs demonstrate multiquantal events and higher quantal size in GluK4^{Over} mice. A, Average amplitude distributions of miniature events (2 pA bin size) in WT (top) and GluK4^{over} (bottom) mice, where a Gaussian curve has been fitted to the initial values. Note the broad and skewed amplitude distribution, suggesting that mEPSCs with larger amplitudes may represent multiquantal events. The values are the mean±SEM of 20 cells from WT and 22 cells from GluK4^{over} mice (3 mice). Single cell distributions were independently fitted with a Gaussian curve, considering only values from the beginning to those after the peak bars that were symmetrical, and the peak was computed. The third row shows the results of this analysis. The mean peak value was 10.4 pA ±0.50 pA for the GluK4$^{+/+}$ WT mice (18 cells from 3 mice), which was slightly shifted to the right compared to the mean value of 12.7±0.44 pA shown by GluK4^{Over} distributions (22 cells from 3 mice: *p=0.016, Student t-test). **B**, The same experiments and procedures were carried out in the presence of more limited extracellular Ca^{2+} (0.1 mM) to minimize the multiquantal events. The same analysis yielded mean amplitude values of 10.4 pA ±0.52 pA and 12.5 pA ±0.54 pA, for the neurons from GluK4$^{+/+}$ and GluK4^{Over} mice, respectively (data from 8 cells from 2 mice for WT, and from 12 cells from 2 mice for GluK4^{over}: **p=0.0015, Student t-test). Experiments in **A** and **B** are from CA3 pyramidal cells. The same analysis was carried out on BLA pyramidal neurons (normal Ca^{2+}) (**C)** and the peak amplitude was 8.9 ±0.37 pA and 11.3 ±0.3 pA for cells from GluK4$^{+/+}$ (16 cells from 6 mice) and GluK4^{over} (16 cells from 7 mice) mice, respectively: ***p<0.001, Student t-test. The insets are 30 single superimposed events and the average in each condition for both genotypes.

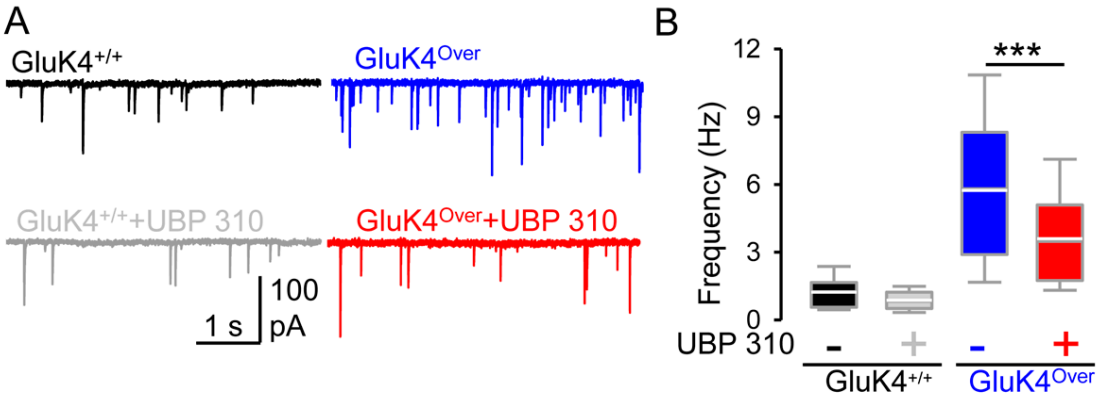

Figure S5, Related to Fig 6 and 7. Enhanced glutamate release is caused by the tonic activation of presynaptic high affinity KARs in mossy fiber to CA3 neurons. A, the antagonism of KARs by UBP310 (10 μM) depressed the increased frequency of mEPSC in CA3 synapses of GluK4 overexpressing mice (blue and red traces). **B**, quantification of the effects of UBP310 on the frequency of mEPSC in GluK4$^{+/+}$ and GluK4 overexpressing mice. The frequency in GluK4^{Over} mice was reduced from 5.7±0.78 Hz to 3.6±0.50 Hz, n=17 neurons (***p<0.001, two-tailed Student t-test) upon UBP310 treatment, while in the wild type it was marginally affected.

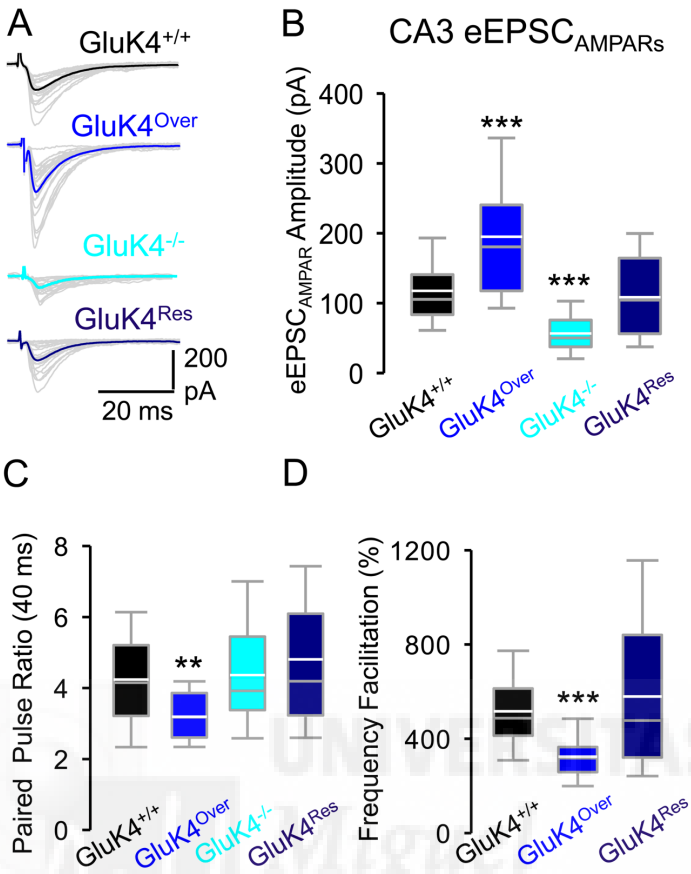

Figure S6, Related to Figure 7. A, **Representative examples of mossy fiber evoked EPSC in CA3 pyramidal neurons in the four different mouse genotypes**. **B**, Amplitudes of AMPAR-mediated evoked EPSCs in CA3 pyramidal cells from the four different genotypes (58 neurons/12 slices from 3 GluK4$^{+/+}$ and GluK4^{Over} mice, 39 neurons/15 slices from 3 KO mice and 22 neurons/8 slices from 3 GluK4^{Res} mice. **C**, Paired pulse ratio values observed in the four genotypes, showing recovery in mice with normalised levels of GluK4 (n=51/12, 29/10, 39/15 and 22/8 neurons/slices, respectively, from 3 mice in each case,). **D**, Degree of 1 Hz frequency facilitation in CA3 pyramidal cells of mossy fibre-induced responses was attenuated in GluK4^{Over} and fully recovered upon normalising GluK4 levels (37 neurons/12 slices, 3 mice, 20 neurons/8 slices, 2 mice, and 22 neurons/8 slices, 3 mice from GluK4$^{+/+}$, GluK4^{Over} GluK4^{Res} mice, respectively. **p<0.01, ***p<0.001, One-way ANOVA on ranks Dunn's method.

UNIVERSITAS
Miguel
Hernández

UNIVERSITAS
Miguel
Hernández

CHAPTER 4. DISCUSSION

In this study we looked at electrophysiological correlates of abnormal psychiatric phenotypes observed in GluK4^{Over} mice. To this end, we studied the effect of GluK4 overexpression on the presynaptic and postsynaptic excitatory activity in characterized cells of BLA and CeLA. Mild overexpression of GluK4 led to a drastic imbalance in glutamatergic transmission in the amygdala circuits, leading to enhanced spontaneous and EC evoked glutamate excitatory activity in the BLA and consequently increased excitatory inputs to the regular firing cells of CeLA. On the other hand, the input to the late firing cells of the CeLA was observed depressed and the inhibitory input to the late firing effector neurons of CeMA was therefore attenuated. This facilitates the increased synaptic gain in the direct synapses from BLA to CeMA as evident through shift of E-I balance towards excitation in the late firing cells of CeMA. In addition, the basal activity measured by c Fos expression in the BLA and CeLA, the origin of anxiogenic circuit was also found to be enhanced in the GluK4^{Over} mice suggesting that high affinity GluK4 subunit have a significant role in regulating synaptic transmission in the excitatory inputs from the prefrontal cortex to the BLA and in the intra-amygdala circuits encompassing BLA, CeLA and CeMA, which may account for the behaviour abnormalities that concur with diseases such as autism and schizophrenia.

In summary, the aberrant processing in the fear promoting and anxiolytic circuits in the amygdala underlined by complex and diversified alteration of synaptic function accounts for the behaviour abnormalities observed in GluK4^{Over} mice like increased anxiety, anhedonia, depression and altered social behaviour. As *GRIK4* duplication in humans has been already detected in patients with ASD (Griswold et al., 2012) and *GRIK4* gene is also in linkage disequilibrium with several endophenotypes of schizophrenia (Pickard et al., 2006; Greenwood et al., 2016), these amygdala alterations in GluK4^{Over} mice is a one step forward to unravelling the mechanisms behind such complex genetic diseases. Moreover, in previous studies, the mice lacking *Grik4* had anxiolytic and anti-depressant-like behaviours (Catches et al., 2012) further supporting our findings and indicating a positive correlation between dosage of *Grik4* and mood disorders.

Grik2 has been also implicated in autism (Shuang et al., 2004; Jamain et al., 2002), hence *Grik2* could also complement *Grik4* protein to alter synaptic processing in amygdala circuits which might account for behavioural abnormalities observed in *Grik4* enriched mice although this needs further investigation.

Hence the dosage of genes especially those encoding for glutamate receptors such as KAR subunits is critical to maintaining excitation inhibition balance in amygdala circuits, and GluK4 gain of function model reproducing autistic symptoms in mouse lines is ideal to study altered circuitry underlying human disease related behaviours given that these mice recapitulate the behaviour phenotypes of ASDs as showed in previous work (Aller et al., 2015).

4.1 *Grik4* IS EXPRESSED IN THE AMYGDALA CIRCUITS IN THE MOUSE BRAIN.

Until now in situ hybridization studies have reported the presence of mRNA coding for GluK1, GluK2 and GluK5 in the amygdala (Wisden and Seeburg, 1993; see also the Allen Brain Atlas). GluK1 subunit is enriched in the basolateral and medial nuclei, forming postsynaptic KARs in INs and PNs of the BLA and contributing to a small fraction of postsynaptic current. GluK1 also exists on the presynaptic terminals of INs in the BLA hence modulating the release of GABA in a bidirectional manner, probably through a metabotropic mode of action (Braga et al., 2003).

Previous studies using radioactive in situ hybridization failed to detect GluK4 mRNA in the amygdala circuits (Wisden and Seeburg, 1993; Li et al., 2001). *Grik4* mRNA expression was therefore accessed using highly sensitive non-radioactive in situ hybridization in the wild type mice as described in Acloque et al. (2008). Our data illustrated that *Grik4* mRNA was widely distributed through the brain, contrary to what it has been assumed: restricted expression to CA3 and DG granule cells and in Purkinje cells of the cerebellum. For our present data, we can conclude that GluK4 is remarkably present in amygdala circuits. Interestingly,

Grik4 mRNA was largely expressed in all amygdaloidal nuclei with a visible signal in the lateral, central and basolateral portions of the amygdala. As we know, GluK1 and GluK2 are highly expressed in amygdala especially in the BLA (Braga et al., 2003), we can assume the presence of GluK1/GluK4 and/or GluK2/GluK4 KARs in the pre- and/or postsynaptic sites in BLA PNs.

Our transgenic mouse line having significant overexpression of GluK4 protein in the forebrain, showed expression of exogenous GluK4 protein in PNs of the BLA but not in the neurons of CeMA. This is an expected observation because CamKII promoter under which *Grik4* was expressed is restricted to PNs and not expressed in GABAergic interneurons. The mouse line displayed anhedonia, enhanced anxiety and depressive states, as well as altered social interaction, common endophenotypes associated to ASDs (Aller et al., 2015). Hence the characterization of synaptic effects of overexpressing GluK4 in the amygdala circuits was of paramount importance because 1- Copy number variations of *Grik4* gene leads to ASDs in humans (Griswold et al., 2012) and 2- the amygdala complex is vital for processing information related to fear, anxiety and social behaviour (Ressler 2010; Forster 2012).

4.2 OVEREXPRESSED GLUK4 SUBUNITS CHANGE CORTICO-AMYGDALA INFORMATION TRANSFER VIA A PRESYNAPTIC EFFECT.

Presynaptic KARs are key players in regulating transmitter release in most of the central synapses (Lerma, 2003). A critical role exist for presynaptic KARs in excitatory neurotransmission as released glutamate activates presynaptic KARs at central synapses like MF-CA3 synapses leading to robust use-dependent facilitation of transmitter release (Kamiya and Ozawa, 2000; Schmitz et al., 2000; Lauri et al., , 2003.)

The overexpression of GluK4 led to increased probability of glutamate release in the BLA as seen through increased frequency of mEPSCs$_{AMPAR}$ and decreased paired pulse ratios of evoked EPSCs$_{AMPAR}$ measured after stimulating the EC at

different interstimulus intervals. These results were further supported by experiments showing that the increased frequency of mEPSCs in EC-BLA synapses was reversed through the application of UBP310. UBP310 is an antagonist of GluK1 subunits (Dolman et al., 2007) but also suppresses activity in heteromeric receptors such as GluK2/5 or those incorporating GluK4 subunits. So, the exogenous GluK4 subunits form functional presynaptic GluK4 containing KARs in cortico-amygdala synapses and seem to exert their effects by altering the release probability of glutamate. Hence this gives an indication that in addition to postsynaptic presence of KARs in the BLA PNs (Li and Rogawski et al., 1998), GluK4 containing KARs might also localize presynaptically.

The new presynaptic KARs with unknown stoichiometry have higher affinity for glutamate. Therefore, ambient glutamate could tonically activate these new receptors tonically increasing the release of glutamate from the presynaptic cortical terminals. We conclude that the heteromeric GluK4 containing KARs increases the glutamate release from the presynaptic terminals in GluK4 enriched EC- BLA synapses.

4.3 POST SYNAPTIC EFFECTS OF THE GLUK4 GAIN OF FUNCTION IN THE BLA

Using AMPARs selective allosteric antagonists such as GYKI 52466 and GYKI 53655 (Paternain et al., 1995), GluK1 containing KARs were shown in previous studies to be mediating a significant proportion (about 30%) of excitatory postsynaptic response in the BLA neurons of rats (Li and Rogawski et al., 1998). Using the same strategy by stimulating at EC, we checked for postsynaptic component mediated by KARs in mice overexpressing GluK4 and wild type mice. As expected, KARs mediated eEPSCs were found to be increased in amplitude and exhibited faster decay in BLA PNs of the GluK4^{Over} mice. Hence incorporation of GluK4 overexpressed subunits at the postsynaptic level led to increased KAR-mediated responses modifying the properties of heteromeric KARs. We found, however, that the overall postsynaptic response mediated by KARs in mice is

minimal (approximately 18%), in clear contrast with data from rats (Li and Rogawsky., 1998). Also we could not detect KARs mEPSC in mice overexpressing GluK4 subunits nor in in wild type, also in contrast to what it has been reported in rats (Cossart et al., 2002).

After overexpressing GluK4 subunits in BLA PNs, we also observed a significant increase in the amplitude of $mEPSCs_{AMPARs}$. We speculated that increased probability of release of glutamate from presynaptic sites (evident by increased frequency of mEPSCs) could account for increased mEPSC amplitude. However, we discarded this possibility by plotting the distribution of amplitudes of mEPSC events, following which we found that the elementary amplitude of single synaptic events was increased, which indicated an increase in quantal content. This increased mean amplitude of single synaptic events indicates an increased conductance of AMPARs at the postsynaptic site considering the fact that overall contribution of new postsynaptic GluK4-KARs to $mEPSCs_{AMPARs/KARs}$ was negligible and in $eEPSCs_{AMPARs/KARs}$ was only 18 %. The observation of increased $mEPSC_{AMPARs}$ amplitude could therefore be due to a larger number of postsynaptic AMPARs or a larger conductance of post synaptic AMPARs/KARs. These speculations were confirmed by checking AMPARs/NMDARs EPSC ratios and rectification index in BLA PNs. The increased AMPARs/NMDARs EPSC ratios at Gluk4 enriched synapses in the BLA indicated the presence of more AMPARs at the postsynaptic site. Furthermore, we saw more inwardly rectifying AMPARs in mice overexpressing GluK4. This was quantified through measuring the rectification index (RI; $EPSC_{-60mV}/EPSC_{+40mV}$), a measure to test the proportion of Ca^{2+} permeable to Ca^{2+} impermeable AMPARs at the postsynaptic site. Consequently, decreased RI for AMPARs indicated more GluA2 lacking AMPARs, which are more permeable to Ca^{2+} and have larger single channel conductance.

4.4 ALTERATION IN THE EXCITATORY INPUT FROM BLA TO CELA PATHWAY LEAD TO ANXIETY LIKE BEHAVIOUR

Intra-amygdala circuits such as BLA projections to CeLA has a critical role in anxiety like behaviour (Tye et al., 2011). Activation of distinct populations of CeLA neurons either promote fear or anxiolysis. For instance, activation of CeLA PKCδ^{+} population or mainly LFCs leads to reduced anxiety like behaviour (Haubensak et al., 2010; see also Janak and Tye 2015 for review) while activation of CeLA PKCδ^{-} cell population or RFCs promotes fear related responses (Janak and Tye 2015: Haubensak et al., 2010). It is also known that PKCδ^{+} cell population comprising of mainly late firing cells is the main source of inhibition of CeMA neurons (Stoop 2015; Viviani et al., 2011). Hence the prediction was that increased synaptic efficacy in the BLA in GluK4^{Over} mice might affect these mutually inhibiting LFCs and RFCs in contrasting ways. Indeed, GluK4 overexpression in the BLA PNs led to a striking imbalance in the LFCs and RFCs of CeLA which was concurrent with the behaviour abnormalities in the GluK4^{Over} mice. On one hand, the excitatory synaptic terminals from the BLA PNs had increased spontaneous glutamate release on RFCs while the BLA PNs contacting onto LFC showed significantly reduced glutamate release. The eEPSCs evoked in RFCs via electrical stimulation in the BLA also had significantly increased amplitudes likely owing to increased release probability in BLA synapses contacting CeLA RFCs. On the contrary, the amplitudes of eEPSCs evoked in LFCs via stimulation in the BLA had a tendency to be reduced (although statistically non-significant).

As discussed before, LFCs and RFCs from CeLA do not overexpress GluK4. Therefore, synaptic imbalance in these interneurons was due to the enrichment of GluK4-containing KARs exclusively at presynaptic terminals from the BLA PN that contact CeLA neurons. It would be interesting to know whether same BLA PN with increased presynaptic GluK4-KARs contact different CeLA cells, exerting opposing modulatory action on LFCs and RFCs or whether different populations of PNs send their segregated projections to LFCs and RFCs.

Since different populations of BLA neurons have already been reported to drive aversive and appetitive behaviours (Kim et al., 2016), likely different cell types in the BLA would have different targets in CeLA, but this needs to be confirmed by further experiments.

Hence synaptic transmission from BLA to CeLA reflected a major imbalance as evident by increased activation of RFC and decreased excitation of LFC. This was also assessed and further confirmed in c-Fos expression experiments, which indicated that this result can be extended to the in vivo situation. The intrinsic circuit disequilibrium in CeLA causing inhibition of LFCs leads to dis-inhibition of CeMA cells which will likely result in their increased firing and downstream inhibition of targets such as BNST, PAG and PVT. Increased ongoing activity of CeMA neurons as detected in mice overexpressing GluK4 leads to increased anxiety like behaviour according to previous studies (Ciocchi et al., 2010 see also Tovote., 2015) and is consistent with the behaviour abnormalities observed in GluK4^{Over} mice model.

4.5 GLUK4 OVEREXPRESSION LEAD TO CIRCUIT IMBALANCE IN INTRA-AMYGDALA CIRCUITS.

CeLA consists of mutually inhibiting cells, PKCδ^{-} which are mainly RFCs and PKCδ^{+} which are predominantly LFCs. Both the populations mutually inhibit each other (Haubensak et al., 2010) and they are antagonistic at electrophysiological and behavioural level. LFCs are responsible for anxiolysis via inhibition of CeMA cells (Tye et al., 2011) while RFCs are known to promote fear via inhibition of extraamygdala targets (Amano et al., 2011). Our data from the simultaneous recordings of sEPSCs and sIPSCs neurons in GluK4^{Over} mice and wild type mice in CeLA neurons revealed altered balance of excitation and inhibition. On one hand, the RFCs of CeLA in GluK4^{Over} mice had increased proportion of excitatory events in comparison to inhibitory events when compared with wild type mice while the contrary was true for LFCs, which presented larger frequency of IPSCs and lower frequency of EPSCs in comparison to wild type mice.

Consequently, the fear promotion circuit from BLA to CeLA RFC cells showed significant facilitation while the anxiolytic circuit from BLA to CeLA LFC was depressed. This fact was surely exacerbated by the mutual inhibition between both CeLA populations of neurons. These data were further supported by measuring in vivo the neuronal activity through indirect neuronal activity markers (cFos). In the transgenic mouse, the activity of anxiogenic circuit including cells in the BLA and CeMA was selectively enhanced as measured through increased number of cFos positive cells and their mean intensity which also showed a significant increase in case of BLA. We didn´t observed an increase in CeLA neurons labelled by cFos, which could be explained by the presence of mutually inhibiting RFC and LFC populations which could counteract each other.

These evidences make it clear that stable and balanced synaptic transmission is necessary to regulated emotionally relevant behaviours such as fear and anxiety. GluK4^{Over} mice displayed more anxious behaviour in several tests such as EPM and Open field test and also indicated signs of fear (Aller et al., 2015), all compatible with the imbalances in the activity of these intra-amygdala circuits. Accordingly, suppressing the KARs via intra-BLA injections of UBP302 as well as complete knock out of GluK4 causes anxiolysis in mice as measured in the open field test (Aroniadou-Andersjaska et al., 2012). Hence our observations from GluK4^{Over} mice such as increased anxiety and basal activation of BLA in vivo supports these facts.

It is expected that patients suffering from ASD carrying de novo duplications in *GRIK4* gene could have this intrinsic disequilibrium in the intra-amygdala circuits especially in the CeLA neuronal populations leading to symptoms of increased anxiety and depression, anhedonia and social behaviour deficits. This is consistent with previous observations where optogenetic inhibition of PKC δ^+ cells attenuates the inhibitory control of PKC δ^+ over CeMA cells and leads to promotion of fear and anxiety related behaviours (Fadok et al., 2017; Haubensak et al., 2010). In our study *Grik4* overexpression is contributing to a similar effect of inhibition of CeLA late firing cells hence releasing inhibitory control over CeMA cells leading to anxiety related behaviours.

PKC δ+ cells are also able to discriminate between aversive and neutral stimuli (Ciocchi et al., 2010; Botta et al., 2015), hence inhibition of these cells (i.e late firing neurons) through overexpression of *Grik4* in the BLA leads to disruption of this discrimination power, leading to enhanced anxiety behaviour.

4.6 RESCUE OF SYNAPTIC AND BEHAVIOUR ALTERATIONS BY RESTORING GLUK4 PROTEIN LEVEL

To be sure that the behavioural and synaptic abnormalities observed in the transgenic mouse were due exclusively to alterations of GluK4 levels, we tried to normalise the dosage of *Grik4* by crossing GluK4$^{-/-}$ (KO mice) with GluK4^{Over} mice. The difference between these mice and WT mice is that the copy of transgenic *Grik4* remained while one of the alleles of native *Grik4* was absent in GluK4^{Res}. This normalized the amount of GluK4 protein. The pre- and post-synaptic activity in BLA PNs in these mice (GluK4^{Res}) was found to be indistinguishable from the wild type controls. Similarly, increased release probability in the GluK4^{Over} mice measured through paired pulse ratios reverted to the wild type levels in GluK4^{Res} mice. Interestingly, imbalance in the CeLA shown previously through increased frequency of mEPSCs in the RFC and decreased frequency of mEPSCs in the LFC was not persistent anymore in the rescued mice. We also measured synaptic parameters in GluK4$^{-/-}$ mice as negative control and found opposite effects with respect to GluK4^{Over} as in the mEPSCs and eEPSCs amplitudes in the BLA PNs and also in the presynaptic paired pulse ratios that were decreased in the GluK4^{Over} mice. The paired pulse ratios showed increased facilitation in GluK4$^{-/-}$ mice as compared to the GluK4$^{+/+}$ mice. The CeLA regular firing and late firing cells showed similarly opposite effects in GluK4$^{-/-}$ mice contrary to GluK4^{Over} mice and frequencies of mEPSCs was significantly reduced in the regular firing cells while it was increased in the late firing cells when compared with the GluK4$^{+/+}$ mice.

In addition to rescue synaptic alterations in GluK4^{Res} mice, these mice performed normally in behavioural tests with no enhancement of anxiety or depression, and they interacted with novel mice more than familiar mice in the 3-chamber interaction test indicating normalised social interaction as in the GluK4$^{+/+}$ mice.

Anxiolytic and Anti-depressant type behaviour in the GluK4$^{-/-}$ mice (see also Catches et al., 2012) were also normalised in GluK4^{Res} mice giving a strong indication that the dosage of *Grik4* is essential in controlling anxiety and depression related behaviours in animals.

Altogether these data indicate that *Grik4* over-dosage leads to disruption of equilibrium in extrinsic and intrinsic amygdala circuits in terms of excitatory and inhibitory synaptic transmission, underlying aberrant psychiatric behaviours concurrent with diseases such asASDs. Hence GluK4^{Over} mice is a useful model in understanding the aetiology of ASDs in terms of synaptic dysfunctions and aberrant neurotransmission, which additionally may underly abnormal psychiatric behaviours and this understanding will guide the advancement of therapeutic interventions for neuropsychiatric diseases.

4.7 FUTURE PERSPECTIVES

This study is an important contribution to the understanding of the role of the GluK4 KAR subunit. This is an important protein since its mutations have been shown to be associated with neuropsychiatric disorders as discussed above in detail. The evidence for this association from genetic analyses is limited but it is supported by the results presented here, and in the previous paper (Aller et al., 2015) from our lab. The previous paper focussed on changes to the hippocampal circuitry in the *Grik4* overexpressing mice (Aller et al., 2015) whilst this work extends this analysis to the amygdala (Arora et al., 2018). The combination of the two papers therefore present an evolving picture of the circuit effects of GriK4 over expression.

Future experiments can focus on developing transgenic mice specifically overexpressing GluK4 in some neuronal populations of the amygdala like in BLA or CeLA and further study the impact on behaviour, with particular attention to anxiety and depression. Hence it is necessary to identify which parts of the circuit perturbation in the BLA and CeA are causative of the synaptic and behavioural effects in GluK4^{Over} mice. A synapse or cellular specific manipulation to rescue the over expression, behavioural phenotypes and synaptic alterations would be very useful in this regard. Moreover, further experiments are required to look for postsynaptic alterations in the trafficking of glutamate receptors like AMPARs in GluK4^{Over} mice to figure out the possible mechanism of insertion of CP-AMPARs in BLA PNs that increases conductance at the postsynaptic sites and consequently synaptic gain in the BLA.

Also modulatory role of presynaptic KARs in the BLA synapsing with LFCs and RFCs of CeLA can be explored further through application of KA at different concentrations to see if it recapitulates the bimodal actions found here. Whether presynaptic KARs in same or different populations of BLA neurons exert opposing actions on LFCs or RFCs is still is an open question.

Collectively in long term GluK4^{Over} mice can prove to be a powerful tool to understand synaptic dysfunction and aberrant neurotransmission responsible for neuropsychiatric disorders like ASDs and Schizophrenia. This will eventually help to advance preclinical studies aimed at therapeutic development against abnormal GluK4-KARs mediated activity in ASDs.

UNIVERSITAS
Miguel
Hernández

CHAPTER 5. CONCLUSIONS

GENERAL CONCLUSION:

A mild overexpression of GluK4 in the forebrain enhances the efficiency of synaptic transmission in the BLA and specific anxiogenic projections from BLA to CeLA, thus altering the main amygdala outputs and causing a persistant circuit disequilibrium. This drastic circuit imbalance may account for behaviour abnormalities observed in autistic patients, including those having de novo duplications of *GRIK4* gene. The results obtained in our study may represent a step forward towards deciphering the role of the GluK4 KAR subunit in amygdala circuits which are the main processing centers of emotionally relevant behaviours

SPECIFIC CONCLUSIONS:

1. GluK4 is widely expressed in amygdala circuits contrary to previous believe.

2. Overexpressed GluK4 subunits form pre- and postsynaptic high affinity KARs increasing the release probability of glutamate in cortico-amygdala synapses.

3. Overexpressed GluK4 subunits enhance postsynaptic conductance of postsynaptic AMPARs, by changing the number of receptors incorporating GluA2 subunits.

4. Normalizing the *Grik4* dosage rescues the behaviour and synaptic alterations, demonstrating a causality between the excess of GluK4 and aberrant synaptic and animal behaviour

5. Overall, GluK4 overexpression in the mouse forebrain enhances efficiency of excitatory synaptic transmission in the Cortico-BLA and BLA to CeL_A networks and replicates behavioural deficits concurrent with Autistic symptoms in humans.

CONCLUSIÓN GENERAL:

La sobreexpresión leve de GluK4 en el cerebro anterior aumenta la eficiencia de la transmisión sináptica en la amígdala (BLA) y en las proyecciones ansiogénicas específicas desde BLA a CeLA, lo que altera las salidas principales de la amígdala y causa un desequilibrio persistente en el circuito. Este drástico desequilibrio del circuito puede explicar las anomalías de comportamiento observadas en pacientes autistas, incluidos aquellos que tienen duplicaciones de novo del gen *GRIK4*. Los resultados obtenidos en nuestro estudio representan un paso adelante para descifrar el papel de la subunidad GluK4 en los circuitos de la amígdala, que son los principales centros de procesamiento de comportamientos emocionalmente relevantes.

CONCLUSIONES ESPECÍFICAS:

1. GluK4 se expresa ampliamente en la amígdala, contrariamente a lo que se cree anteriormente.

2. Las subunidades GluK4 sobreexpresadas forman KARs de alta afinidad pre y postsinápticas que aumentan la probabilidad de liberación de glutamato en las sinapsis cortico-amígdala.

3. Las subunidades GluK4 sobreexpresadas mejoran la conductancia postsináptica de los AMPAR postsinápticos, al cambiar el número de receptores que incorporan subunidades GluA2.

4. La normalización de la dosis de Grik4 rescata el comportamiento y las alteraciones sinápticas, lo que demuestra una causalidad entre el exceso de GluK4 y el comportamiento sináptico y animal aberrante.

5. En general, la sobreexpresión de GluK4 en el cerebro anterior del ratón aumenta la eficiencia de la transmisión sináptica excitadora en las redes Cortico-BLA y BLA a CeLA y replica los déficits de comportamiento concurrentes con los síntomas autistas en humanos.

UNIVERSITAS
Miguel
Hernández

UNIVERSITAS
Miguel
Hernández

CHAPTER 6. BIBLIOGRAPHY

Acloque, H., D. G. Wilkinson and M. A. Nieto (2008). "In situ hybridization analysis of chick embryos in whole-mount and tissue sections." Methods Cell Biol 87: 169-185.

Ahmad, Y., Bhatia, M. S., Mediratta, P. K., Sharma, K. K., Negi, H., Chosdol, K., et al. (2009). Association between the ionotropic glutamate receptor kainate3 (GRIK3) Ser310Ala polymorphism and schizophrenia in the Indian population. World Journal of Biological Psychiatry, 10, 330–333.

Ali AB, Rossier J, Staiger JF, Audinat E (2001)." Kainate receptors regulate unitary IPSCs elicited in pyramidal cells by fast-spiking interneurons in the neocortex." J Neurosci 21: 2992-2999.

Aller, M. I., V. Pecoraro, A. V. Paternain, S. Canals and J. Lerma (2015). "Increased Dosage of High-Affinity Kainate Receptor Gene grik4 Alters Synaptic Transmission and Reproduces Autism Spectrum Disorders Features." J Neurosci 35(40): 13619-13628.

Allsop, S. A., C. M. Vander Weele, R. Wichmann and K. M. Tye (2014). "Optogenetic insights on the relationship between anxiety-related behaviours and social deficits." Frontiers in behavioural neuroscience 8: 241-241.

Amano, T., S. Duvarci, D. Popa and D. Pare (2011). "The fear circuit revisited: contributions of the basal amygdala nuclei to conditioned fear." J Neurosci 31(43): 15481-15489.

Amorapanth, P., K. Nader and J. E. LeDoux (1999). "Lesions of periaqueductal gray dissociate-conditioned freezing from conditioned suppression behaviour in rats." Learn Mem 6(5): 491-499.

Aroniadou-Anderjaska V, Pidoplichko VI, Figueiredo TH, Almeida-Suhett CP, Prager EM, Braga MF (2012). "Presynaptic facilitation of glutamate release in the basolateral amygdala: a mechanism for the anxiogenic and seizurogenic function of GluK1 receptors." Neuroscience. 2012 Sep 27; 221:157-69.

Arora V., Pecoraro V., Aller M., Román C., Paternain A., Lerma J. (2018). "Increased Grik4 Gene Dosage Causes Imbalanced Circuit Output and Human Disease-Related Behaviours." Cell Reports, Volume 23, Issue 13, 2018, Pages 3827-3838

Ascher, P. and L. Nowak (1988). "The role of divalent cations in the N-methyl-D-aspartate responses of mouse central neurones in culture." J Physiol 399: 247-266.

Ascoli, G. A., L. Alonso-Nanclares, S. A. Anderson, G. Barrionuevo, R. Benavides-Piccione, A. Burkhalter, G. et al. (2008). "Petilla terminology: nomenclature of features of GABAergic interneurons of the cerebral cortex." Nat Rev Neurosci 9(7): 557-568.

Asede, D., D. Bosch, A. Luthi, F. Ferraguti and I. Ehrlich (2015). "Sensory inputs to intercalated cells provide fear-learning modulated inhibition to the basolateral amygdala." Neuron 86(2): 541-554.

Babaev, O., Piletti Chatain, C. & Krueger-Burg, D (2018). "Inhibition in the amygdala anxiety circuitry." Exp. Mol. Med. 50, 18 (2018).

Bahn S, Volk B, Wisden W (1994). "Kainate receptor gene expression in the developing rat brain. Journal of Neuroscience." 14:5525–5547.

Bechara A, Tranel D, Damasio H, Adolphs R, Rockland C, Damasio AR (1995) Double dissociation of conditioning and declarative knowledge relative to the amygdala and hippocampus in humans. Science 269:1115–1118.

Begni S , Popoli M , Moraschi S , Bignotti S , Tura GB , Gennarelli M (2002). " Association between the ionotropic glutamate receptor kainate 3 (GRIK3) ser310ala polymorphism and schizophrenia." Mol Psychiatry 7:416–418.

Bergado, J. A., W. Almaguer, Y. Rojas, V. Capdevila and J. U. Frey (2011). "Spatial and emotional memory in aged rats: a behavioural-statistical analysis." Neuroscience 172: 256-269.

Bettler B., Boulter J., Hermans-Borgmeyer I., et al. (1990). Cloning of a novel glutamate receptor subunit, GluR5: expression in the nervous system during development. Neuron 5, 583–595.

Bettler, B., Egebjerg, J., Sharma, G., Pecht, G., Hermans-Borgmeyer, I., Moll, C., Stevens, C., and Heinemann, S. (1992) Neuron 8,257-265

Beyeler, A., P. Namburi, G. F. Glober, C. Simonnet, G. G. Calhoon, G. F. Conyers, R. Luck, C. P. Wildes and K. M. Tye (2016). "Divergent Routing of Positive and Negative Information from the Amygdala during Memory Retrieval." Neuron 90(2): 348-361.

Bienvenu, T. C., D. Busti, B. R. Micklem, M. Mansouri, P. J. Magill, F. Ferraguti and M. Capogna (2015). "Large intercalated neurons of amygdala relay noxious sensory information." J Neurosci 35(5): 2044-2057.

Bocchio, M., S. B. McHugh, D. M. Bannerman, T. Sharp and M. Capogna (2016). "Serotonin, Amygdala and Fear: Assembling the Puzzle." Front Neural Circuits 10: 24.

Botta, P., L. Demmou, Y. Kasugai, M. Markovic, C. Xu, J. P. Fadok, T. Lu, M. M. Poe, L. Xu, J. M. Cook, U. Rudolph, P. Sah, F. Ferraguti and A. Luthi (2015). "Regulating anxiety with extrasynaptic inhibition." Nat Neurosci 18(10): 1493-1500.

Boulter, J., M. Hollmann, A. O'Shea-Greenfield, M. Hartley, E. Deneris, C. Maron and S. Heinemann (1990). "Molecular cloning and functional expression of glutamate receptor subunit genes." Science 249(4972): 1033-1037.

Bowie D, Mayer ML (1995) Inward rectification of both AMPA and kainate subtype glutamate receptors generated by polyamine-mediated ion channel block. Neuron 15:453–462

Braga MF, Aroniadou-Anderjaska V, Xie J, Li H. (2003) "Bidirectional modulation of GABA release by presynaptic glutamate receptor 5 kainate receptors in the basolateral amygdala". J Neurosci 23:442–452.

Braga, M. F., V. Aroniadou-Anderjaska and H. Li (2004). "The physiological role of kainate receptors in the amygdala." Mol Neurobiol 30(2): 127-141.

Burnashev, N., A. Khodorova, P. Jonas, P. J. Helm, W. Wisden, H. Monyer, P. H. Seeburg and B. Sakmann (1992). "Calcium-permeable AMPA-kainate receptors in fusiform cerebellar glial cells." Science 256(5063): 1566-1570.

Burnashev, N., Villarroel, A. & Sakmann, B. Dimensions and ion selectivity of recombinant AMPA and kainate receptor channels and their dependence on Q/R site residues. J. Physiol. (Lond.) 496, 165–173 (1996).

Butler, R. K., L. C. White, D. Frederick-Duus, K. F. Kaigler, J. R. Fadel and M. A. Wilson (2012). "Comparison of the activation of somatostatin- and neuropeptide Y-containing neuronal populations of the rat amygdala following two different anxiogenic stressors." Exp Neurol 238(1): 52-63.

Capogna, M. (2014). "GABAergic cell type diversity in the basolateral amygdala." Curr Opin Neurobiol 26: 110-116.

Cassell, M. D. and T. S. Gray (1989). "Morphology of peptide-immunoreactive neurons in the rat central nucleus of the amygdala." J Comp Neurol 281(2): 320-333.

Castillo, P. E., R. C. Malenka and R. A. Nicoll (1997). "Kainate receptors mediate a slow postsynaptic current in hippocampal CA3 neurons." Nature 388(6638): 182-186.

Catches, J. S., J. Xu and A. Contractor (2012). "Genetic ablation of the GluK4 kainate receptor subunit causes anxiolytic and antidepressant-like behaviour in mice." Behav Brain Res 228(2): 406-414.

Chattopadhyay B , Baksi K , Mukhopadhyay S , Bhattacharyya NP (2005). "Modulation of age at onset of Huntington disease patients by variations in TP53 and human caspase activated DNase (hCAD) genes. " Neurosci Lett 374: 81–86, 2005.

Christensen JK, Varming T, Ahring PK, Jorgensen TD, Nielsen EO (2004)." In vitro characterization of NS3763, a non-competitive antagonist of GLUK5 receptors." J Pharmacol Exp Ther 309: 1003-1010.

Ciocchi, S., C. Herry, F. Grenier, S. B. Wolff, J. J. Letzkus, I. Vlachos, I. Ehrlich, R. Sprengel, K. Deisseroth, M. B. Stadler, C. Muller and A. Luthi (2010). "Encoding of conditioned fear in central amygdala inhibitory circuits." Nature 468(7321): 277-282.

Clem, R. L. and R. L. Huganir (2010). "Calcium-permeable AMPA receptor dynamics mediate fear memory erasure." Science 330(6007): 1108-1112.

Collingridge, G. L., Isaac, J. T. & Wang, Y. T (2004). " Receptor trafficking and synaptic plasticity." Nature Rev. Neurosci. 5, 952–962 (2004).

Contractor A, Swanson G, and Heinemann SF (2001). "Kainate receptors are involved in short- and long-term plasticity at mossy fiber synapses in the hippocampus." Neuron 29: 209–216.

Cossart, R., Dinocourt, C., Hirsch, J.C., Merchan-Perez, A., De Felipe, J., Ben-Ari, Y., Esclapez, M. & Bernard, C. (2001) Dendritic but not somatic GABAergic inhibition is decreased in experimental epilepsy. Nature Neurosci., 4, 52–62.

Cossart, R., J. Epsztein, R. Tyzio, H. Becq, J. Hirsch, Y. Ben-Ari and V. Crepel (2002). "Quantal release of glutamate generates pure kainate and mixed AMPA/kainate EPSCs in hippocampal neurons." Neuron 35(1): 147-159.

Cull-Candy, S., S. Brickley and M. Farrant (2001). "NMDA receptor subunits: diversity, development and disease." Curr Opin Neurobiol 11(3): 327-335.

Darstein M, Petralia RS, Swanson GT, Wenthold RJ, Heinemann SF (2003) Distribution of kainate receptor subunits at hippocampal mossy fiber synapses. J Neurosci 23: 8013–8019.

Davis, M. (1997). "Neurobiology of fear responses: the role of the amygdala." J Neuropsychiatry Clin Neurosci 9(3): 382-402.

Davis, M., D. S. Gendelman, M. D. Tischler and P. M. Gendelman (1982). "A primary acoustic startle circuit: lesion and stimulation studies." J Neurosci 2(6): 791-805.

Diguet, E., P. O. Fernagut, E. Normand, L. Centelles, C. Mulle and F. Tison (2004). "Experimental basis for the putative role of GluR6/kainate glutamate receptor subunit in Huntington's disease natural history." Neurobiol Dis 15(3): 667-675.

Dingledine, R., K. Borges, D. Bowie and S. F. Traynelis (1999). "The glutamate receptor ion channels." Pharmacol Rev 51(1): 7-61.

Dolman NP, More JC, Alt A, Knauss JL, Pentikainen OT, Glasser CR, Bleakman D, Mayer ML, Collingridge GL, Jane DE. Synthesis and pharmacological characterization of N3-substituted willardiine derivatives: role of the substituent at the 5-position of the uracil ring in the development of highly potent and selective GLUK5 kainate receptor antagonists, J Med Chem , 2007, vol. 50 (pg. 1558-1570)

Dutta, S., S. Das, S. Guhathakurta, B. Sen, S. Sinha, A. Chatterjee, S. Ghosh, S. Ahmed, S. Ghosh and R. Usha (2007). "Glutamate receptor 6 gene (GluR6 or GRIK2) polymorphisms in the Indian population: a genetic association study on autism spectrum disorder." Cell Mol Neurobiol 27(8): 1035-1047.

Duvarci, S. and D. Pare (2014). "Amygdala microcircuits controlling learned fear." Neuron 82(5): 966-980.

Egebjerg, J., Bettler, B., Hermans-Borgmeyer, I., and Heinemann, S. (1991) Nature 351,745-748.

Egebjerg J, Heinemann SF (1993). "Ca2+ permeability of unedited and edited versions of the kainate selective glutamate receptor GluR6." Proc Nat1 Acad Sci USA 90:755-759.

Ehrlich, I., Y. Humeau, F. Grenier, S. Ciocchi, C. Herry and A. Luthi (2009). "Amygdala inhibitory circuits and the control of fear memory." Neuron 62(6): 757-771.

Faber ES, & Sah P (2002). Physiological role of calcium-activated potassium currents in the rat lateral amygdala. J Neurosci 22, 1618–1628.

Fadok, J. P., S. Krabbe, M. Markovic, J. Courtin, C. Xu, L. Massi, P. Botta, K. Bylund, C. Muller, A. Kovacevic, P. Tovote and A. Luthi (2017). "A competitive inhibitory circuit for selection of active and passive fear responses." Nature 542(7639): 96-100.

Fanselow, M. S., J. J. Kim, J. Yipp and B. De Oca (1994). "Differential effects of the N-methyl-D-aspartate antagonist DL-2-amino-5-phosphonovalerate on acquisition of fear of auditory and contextual cues." Behav Neurosci 108(2): 235-240.

Fatt, P. and Katz, B (1952). "Spontaneous subthreshold activity at motor nerve endings." J Physiol 117(1): 109-128.

Felix-Ortiz, A. C., A. Beyeler, C. Seo, C. A. Leppla, C. P. Wildes and K. M. Tye (2013). "BLA to vHPC inputs modulate anxiety-related behaviours." Neuron 79(4): 658-664. Fendt, M. and M. S. Fanselow (1999). "The neuroanatomical and neurochemical basis of conditioned fear." Neurosci Biobehav Rev 23(5): 743-760.

Felix-Ortiz, A. C. (2013). BLA to vHPC inputs modulate anxiety-related behaviors. Neuron 79, 658–664.

Forster GL, Novick AM, Scholl JL, Watt MJ. "The role of the amygdala in anxiety disorders". In: Ferry B, editor. The Amygdala: A Discrete Multitasking Manager. Rijeka: InTech; 2012. pp. 61–102.

Freitag MC. "The genetics of autistic disorders and its clinical relevance: a review of the literature" Mol. Psychiatry, 12 (2007), pp. 2-22

Frerking, M., C. C. Petersen and R. A. Nicoll (1999). "Mechanisms underlying kainate receptor-mediated disinhibition in the hippocampus." Proc Natl Acad Sci U S A 96(22): 12917-12922.

Frerking M, Nicoll RA (2000). "Synaptic kainate receptors." Curr Opin Neurobiol 10:342-351

Frerking, M. & Ohliger-Frerking, P. AMPA receptors and kainate receptors encode different features of afferent activity. J. Neurosci. 22, 7434–7443 (2002).

Fuchs, T., S. J. Jefferson, A. Hooper, P. H. Yee, J. Maguire and B. Luscher (2016). "Disinhibition of somatostatin-positive GABAergic interneurons results in an anxiolytic and antidepressant-like brain state." Molecular Psychiatry 22: 920.

Furukawa, H. and E. Gouaux (2003). "Mechanisms of activation, inhibition and specificity: crystal structures of the NMDA receptor NR1 ligand-binding core." Embo j 22(12): 2873-2885.

Furukawa, H., S. K. Singh, R. Mancusso and E. Gouaux (2005). "Subunit arrangement and function in NMDA receptors." Nature 438(7065): 185-192.

Gabel, L. A. and E. S. Nisenbaum (1998). "Biophysical characterization and functional consequences of a slowly inactivating potassium current in neostriatal neurons." J Neurophysiol 79(4): 1989-2002.

Gafford, G. M. and K. J. Ressler (2016). "Mouse models of fear-related disorders: Cell-type-specific manipulations in amygdala." Neuroscience 321: 108-120.

Geracitano, R., W. A. Kaufmann, G. Szabo, F. Ferraguti and M. Capogna (2007). "Synaptic heterogeneity between mouse paracapsular intercalated neurons of the amygdala." J Physiol 585(Pt 1): 117-134.
Gillot, A., Furniss, F., & Walter, A. (2001). Anxiety in high-functioning children with autism. Autism, 5, 277–286.

Greenwood, TA, Lazzeroni, LC, Calkins, ME, Freedman, R, Green, MF, Gur, RE, Gur, RC, Light, GA, Nuechterlein, KH, Olincy, A, Radant, AD, Seidman, LJ, Siever, LJ, Silverman, JM, Stone, WS, Sugar, CA, Swerdlow, NR, Tsuang, DW, Tsuang, MT, Turetsky, BI, Braff, DL (2016). "Genetic assessment of additional endophenotypes from the Consortium on the Genetics of Schizophrenia Family Study." Schizophrenia Research 170, 30–40

Gregor, P., S. M. Gaston, X. Yang, J. P. O'Regan, D. R. Rosen, R. E. Tanzi, D. Patterson, J. L. Haines, H. R. Horvitz, G. R. Uhl and et al. (1994). "Genetic and physical mapping of the GLUR5 glutamate receptor gene on human chromosome 21." Hum Genet 94(5): 565-570.

Griswold, A. J., D. Ma, H. N. Cukier, L. D. Nations, M. A. Schmidt, R. H. Chung, J. M. Jaworski, D. Salyakina, I. Konidari, P. L. Whitehead, H. H. Wright, R. K. Abramson, S. M. Williams, R. Menon, E. R. Martin, J. L. Haines, J. R. Gilbert, M. L. Cuccaro and M. A. Pericak-Vance (2012). "Evaluation of copy number variations reveals novel candidate genes in autism spectrum disorder-associated pathways." Hum Mol Genet 21(15): 3513-3523.

Gryder, D. S., D. C. Castaneda and M. A. Rogawski (2005). "Evidence for low GluR2 AMPA receptor subunit expression at synapses in the rat basolateral amygdala." J Neurochem 94(6): 1728-1738.

Guzman YF, Ramsey K, Stolz JR, Craig DW, Huentelman MJ, Narayanan V, Swanson GT (2017). "A gain-of-function mutation in the GRIK2 gene causes neurodevelopmental deficits." Neurol Genet 3:e129

Hale, M. W., P. L. Johnson, A. M. Westerman, J. K. Abrams, A. Shekhar and C. A. Lowry (2010). "Multiple anxiogenic drugs recruit a parvalbumin-containing subpopulation of GABAergic interneurons in the basolateral amygdala." Prog Neuropsychopharmacol Biol Psychiatry 34(7): 1285-1293.

Hall, E. (1972). "The amygdala of the cat: a Golgi study." Z Zellforsch Mikrosk Anat 134(4): 439-458.

Haubensak, W., P. S. Kunwar, H. Cai, S. Ciocchi, N. R. Wall, R. Ponnusamy, J. Biag, H. W. Dong, K. Deisseroth, E. M. Callaway, M. S. Fanselow, A. Luthi and D. J. Anderson (2010). "Genetic dissection of an amygdala microcircuit that gates conditioned fear." Nature 468(7321): 270-276.

Herb, A., N. Burnashev, P. Werner, B. Sakmann, W. Wisden and P. H. Seeburg (1992). "The KA-2 subunit of excitatory amino acid receptors shows widespread expression in brain and forms ion channels with distantly related subunits." Neuron 8(4): 775-785.

Hopkins, D. A. and G. Holstege (1978). "Amygdaloid projections to the mesencephalon, pons and medulla oblongata in the cat." Exp Brain Res 32(4): 529-547.

Izzi, A. Barbon, R. Kretz, T. Sander, S. Barlati (2002). "Sequencing of the GRIK1 gene in patients with juvenile absence epilepsy does not reveal mutations affecting receptor structure" Am. J. Med. Genet., 114 (2002), pp. 354-359

Jamain, S., C. Betancur, H. Quach, A. Philippe, M. Fellous, B. Giros, C. Gillberg, M. Leboyer and T. Bourgeron (2002). "Linkage and association of the glutamate receptor 6 gene with autism." Mol Psychiatry 7(3): 302-310.

Janak, P. H. and K. M. Tye (2015). "From circuits to behaviour in the amygdala." Nature 517(7534): 284-292.

Jin XT and Smith Y (2007) Activation of presynaptic kainate receptors suppresses GABAergic synaptic transmission in the rat globus pallidus. Neuroscience 149: 338-349

Jolkkonen, E. and A. Pitkanen (1998). "Intrinsic connections of the rat amygdaloid complex: projections originating in the central nucleus." J Comp Neurol 395(1): 53-72.

Johnston JB (1923). "Further contributions to the study of the evolution of the forebrain." J Comp Neurol, 35 pp. 337-481

Jonas, P. and B. Sakmann (1992). "Glutamate receptor channels in isolated patches from CA1 and CA3 pyramidal cells of rat hippocampal slices." The Journal of physiology 455: 143-171.

Jungling, K., T. Seidenbecher, L. Sosulina, J. Lesting, S. Sangha, S. D. Clark, N. Okamura, D. M. Duangdao, Y. L. Xu, R. K. Reinscheid and H. C. Pape (2008). "Neuropeptide S-mediated control of fear expression and extinction: role of intercalated GABAergic neurons in the amygdala." Neuron 59(2): 298-310.

Kamal, A. M. and T. Tombol (1975). "Golgi studies on the amygdaloid nuclei of the cat." J Hirnforsch 16(3): 175-201.

Kamiya H, Ozawa S (2000)." Kainate receptor–mediated presynaptic inhibition at the mouse hippocampal mossy fibre synapse." J. Physiol. 523: 653-665

Keller, B. U., A. Konnerth and Y. Yaari (1991). "Patch clamp analysis of excitatory synaptic currents in granule cells of rat hippocampus." The Journal of physiology 435: 275-293.

Kilic G, Ismail Kucukali C, Orhan N, Ozkok E, Zengin A, Aydin M, et al (2010). "Are GRIK3 (T928G) gene variants in schizophrenia patients different from those in their first-degree relatives? " Psychiatry Res; 175(1–2):43–6.

Killcross, S., T. W. Robbins and B. J. Everitt (1997). "Different types of fear-conditioned behaviour mediated by separate nuclei within amygdala." Nature 388(6640): 377-380.

Kim, J., Pignatelli, M., Xu S., Itohara,S., Tonegawa,S (2016). "Antagonistic negative and positive neurons of the basolateral amygdala." Nat. Neurosci. 19, 1636–1646.

Kim, J., X. Zhang, S. Muralidhar, S. A. LeBlanc and S. Tonegawa (2017). "Basolateral to Central Amygdala Neural Circuits for Appetitive Behaviours." Neuron 93(6): 1464-1479.e1465.

Kishi, T., T. Tsumori, S. Yokota and Y. Yasui (2006). "Topographical projection from the hippocampal formation to the amygdala: a combined anterograde and retrograde tracing study in the rat." J Comp Neurol 496(3): 349-368.

Klausberger, T. and P. Somogyi (2008). "Neuronal diversity and temporal dynamics: the unity of hippocampal circuit operations." Science 321(5885): 53-57.

Knapska E, Maren S (2009). "Reciprocal patterns of c-Fos expression in the medial prefrontal cortex and amygdala after extinction and renewal of conditioned fear." Learn Mem 16: 486–493

Knight HM, Walker R, James R, Porteous DJ, Muir WJ, Blackwood DHR, Pickard BS. 2012. GRIK4/KA1 protein expression in human brain and correlation with bipolar disorder risk variant status. Am J Med Genet Part B Neuropsychiatric Genet. 159B:21–29.

Kohler, M., N. Burnashev, B. Sakmann and P. H. Seeburg (1993). "Determinants of Ca2+ permeability in both TM1 and TM2 of high affinity kainate receptor channels: diversity by RNA editing." Neuron 10(3): 491-500.

Krettek, J. E. and J. L. Price (1977). "Projections from the amygdaloid complex and adjacent olfactory structures to the entorhinal cortex and to the subiculum in the rat and cat." J Comp Neurol 172(4): 723-752.

Krettek, J. E. and J. L. Price (1978). "Amygdaloid projections to subcortical structures within the basal forebrain and brainstem in the rat and cat." J Comp Neurol 178(2): 225-254.

LaBar, K. S., J. E. LeDoux, D. D. Spencer and E. A. Phelps (1995). "Impaired fear conditioning following unilateral temporal lobectomy in humans." J Neurosci 15(10): 6846-6855.

Lai, I. C., Y. J. Liou, J. Y. Chen and Y. C. Wang (2005). "No association between the ionotropic glutamate receptor kainate 3 gene ser310ala polymorphism and schizophrenia." Neuropsychobiology 51(4): 211-213.

Lauri SE, Bortolotto ZA, Bleakman D, Ornstein PL, Lodge D, Isaac JT, Collingridge GL (2003)." A critical role of a facilitatory presynaptic kainate receptor in mossy fiber LTP." Neuron 32(4):697-709.

Lauri, S. E., M. Segerstrale, A. Vesikansa, F. Maingret, C. Mulle, G. L. Collingridge, J. T. Isaac and T. Taira (2005). "Endogenous activation of kainate receptors regulates glutamate release and network activity in the developing hippocampus." J Neurosci 25(18): 4473-4484.

Lauri SE, Vesikansa A, Segerstrale M, Collingridge GL, Isaac JTR, Taira T (2006) Functional maturation of CA1 synapses involves activity-dependent loss of tonic kainate receptor-mediated inhibition of glutamate release. Neuron 50:415–429.

LeDoux, J. E., C. Farb and D. A. Ruggiero (1990). "Topographic organization of neurons in the acoustic thalamus that project to the amygdala." J Neurosci 10(4): 1043-1054.

LeDoux, J. E., C. R. Farb and T. A. Milner (1991). "Ultrastructure and synaptic associations of auditory thalamo-amygdala projections in the rat." Exp Brain Res 85(3): 577-586.

LeDoux, J. E., J. Iwata, P. Cicchetti and D. J. Reis (1988). "Different projections of the central amygdaloid nucleus mediate autonomic and behavioural correlates of conditioned fear." J Neurosci 8(7): 2517-2529.

Lee, J. H. et al (2012). "TAA repeat variation in the GRIK2 gene does not influence age at onset in Huntington's disease." Biochem. Biophys. Res. Commun. 424, 404–408.

Lee, S., S. J. Kim, O. B. Kwon, J. H. Lee and J. H. Kim (2013). "Inhibitory networks of the amygdala for emotional memory." Front Neural Circuits 7: 129.

Lerma J., Zukin R.S., and Bennett M.V.(1990). Glycine decreases desensitization of N-methyl-d-aspartate (NMDA) receptors expressed in Xenopus oocytes and is required for NMDA responses. Proc. Natl. Acad. Sci. USA. 87:2354–2358.

Lerma J, Paternain AV, Naranjo JR, Mellström B (1993). "Functional kainate-selective glutamate receptors in cultured hippocampal neurons." Proceedings of the National Academy of Sciences of the USA 90:11688–11692.

Lerma J, Morales M, Ibarz JM, Somohano F (1994). "Rectification properties and Ca2+ permeability of glutamate receptor channels in hippocampal cells." Eur J Neurosci. 1994;6:1080–1088.

Lerma J (1997) Kainate reveals its targets. Neuron 19: 1155-1158.

Lerma J, Paternain AV, Rodriguez-Moreno A, Lopez-Garcia JC (2001). "Molecular Physiology of Kainate Receptors." Physiol Rev. 2001;81:971–998.

Lerma, J. (2003). "Roles and rules of kainate receptors in synaptic transmission." Nat Rev Neurosci 4(6): 481-495.

Lerma J., Marques J. M. (2013). Kainate receptors in health and disease. Neuron 80 292–311. 10.1016/j.neuron.2013.09.045

Lesage A. and Steckler T (2010). "Metabotropic glutamate mGlu1 receptor stimulation and blockade: therapeutic opportunities in psychiatric illness." Eur J Pharmacol 639(1-3): 2-16.

Lester, R. A., J. D. Clements, G. L. Westbrook and C. E. Jahr (1990). "Channel kinetics determine the time course of NMDA receptor-mediated synaptic currents." Nature 346(6284): 565-567.

Li, H. and M. A. Rogawski (1998). "GluR5 kainate receptor mediated synaptic transmission in rat basolateral amygdala in vitro." Neuropharmacology 37(10-11): 1279-1286.

Li H, Chen A, Xing G, Wei ML, Rogawski MA (2001) Kainate receptor- mediated heterosynaptic facilitation in the amygdala. Nat Neurosci 4: 612- 620

Li, J. M., Y. J. Zeng, F. Peng, L. Li, T. H. Yang, Z. Hong, D. Lei, Z. Chen and D. Zhou (2010). "Aberrant glutamate receptor 5 expression in temporal lobe epilepsy lesions." Brain Res 1311: 166-174.

Linke, R., G. Braune and H. Schwegler (2000). "Differential projection of the posterior paralaminar thalamic nuclei to the amygdaloid complex in the rat." Exp Brain Res 134(4): 520-532.

Liu S. J., Zukin R. S. (2007). Ca2+-permeable AMPA receptors in synap-tic plasticity and neuronal death. Trends Neurosci. 30 126–134

Lowry, E.R., Kruyer, A., Norris, E.H., Cederroth, C.R. & Strickland, S. (2013) The GluK4 kainate receptor subunit regulates memory, mood and excitotoxic neurodegeneration. Neuroscience, 235, 215–225.

Lucarini, A. Verrotti, V. Napolioni, G. Bosco, P. Curatolo (2007). "Genetic polymorphisms and idiopathic generalized epilepsies" Pediatr. Neurol., 37 (2007), pp. 157-164

Luskin, M. B. and J. L. Price (1983). "The topographic organization of associational fibers of the olfactory system in the rat, including centrifugal fibers to the olfactory bulb." J Comp Neurol 216(3): 264-291.

MacDonald ME, Vonsattel JP, Shrinidhi J et al. (1999). "Evidence for the GluR6 gene associated with younger onset age of Huntington's disease. " Neurology 1999: 53: 1330–1332.

Madden, DR (2002). "The structure and function of glutamate receptor ion channels." Nat Rev Neurosci 3(2): 91-101.

Mahanty, N. K. and P. Sah (1998). "Calcium-permeable AMPA receptors mediate long-term potentiation in interneurons in the amygdala." Nature 394(6694): 683-687. Maren, S. (2013). "Putting the brakes on fear." Neuron 80(4): 837-838.

Marques JM, Rodrigues RJ, Valbuena S, Rozas JL, Selak S, Marin P, Aller MI, Lerma J (2013) CRMP2 tethers kainate receptor activity to cytoskeleton dynamics during neuronal maturation. J Neurosci 33:18298 –18310.

Marowsky, A., Y. Yanagawa, K. Obata and K. E. Vogt (2005). "A specialized subclass of interneurons mediates dopaminergic facilitation of amygdala function." Neuron 48(6): 1025-1037.

Martina, M., S. Royer and D. Pare (1999). "Physiological properties of central medial and central lateral amygdala neurons." J Neurophysiol 82(4): 1843-1854.

Mascagni, F. and A. J. McDonald (2003). "Immunohistochemical characterization of cholecystokinin containing neurons in the rat basolateral amygdala." Brain Res 976(2): 171-184.

Mayford, M., Bach, M. E., Huang, Y. Y., Wang, L., Hawkins, R. D., and Kandel, E. R. (1996). Control of memory formation through regulated expression of a CaMKII transgene. Science 274, 1678–1683.

McCormick, D. A. (1991). "Functional properties of a slowly inactivating potassium current in guinea pig dorsal lateral geniculate relay neurons." J Neurophysiol 66(4): 1176-1189.

McDonald, A. J. (1982). "Cytoarchitecture of the central amygdaloid nucleus of the rat." J Comp Neurol 208(4): 401-418.

McDonald, A. J. (1982). "Neurons of the lateral and basolateral amygdaloid nuclei: a Golgi study in the rat." J Comp Neurol 212(3): 293-312.

McDonald, A. J. (1984). "Neuronal organization of the lateral and basolateral amygdaloid nuclei in the rat." J Comp Neurol 222(4): 589-606.

McDonald, A. J. (1991). "Topographical organization of amygdaloid projections to the caudatoputamen, nucleus accumbens, and related striatal-like areas of the rat brain." Neuroscience 44(1): 15-33.

McDonald, A. J. (1992). "Projection neurons of the basolateral amygdala: a correlative Golgi and retrograde tract tracing study." Brain Res Bull 28(2): 179-185.

McDonald, A. J. (1998). "Cortical pathways to the mammalian amygdala." Prog Neurobiol 55(3): 257-332.

McDonald, A. J. and R. L. Betette (2001). "Parvalbumin-containing neurons in the rat basolateral amygdala: morphology and co-localization of Calbindin-D(28k)." Neuroscience 102(2): 413-425.

McDonald, A. J. and F. Mascagni (1997). "Projections of the lateral entorhinal cortex to the amygdala: a Phaseolus vulgaris leucoagglutinin study in the rat." Neuroscience 77(2): 445-459.

McDonald, A. J. and F. Mascagni (2001). "Colocalization of calcium-binding proteins and GABA in neurons of the rat basolateral amygdala." Neuroscience 105(3): 681-693.

McDonald, A. J. and F. Mascagni (2001). "Localization of the CB1 type cannabinoid receptor in the rat basolateral amygdala: high concentrations in a subpopulation of cholecystokinin-containing interneurons." Neuroscience 107(4): 641-652.

McDonald, A. J. and F. Mascagni (2002). "Immunohistochemical characterization of somatostatin containing interneurons in the rat basolateral amygdala." Brain Res 943(2): 237-244.

McDonald, A. J., F. Mascagni and V. Zaric (2012). "Subpopulations of somatostatin-immunoreactive non-pyramidal neurons in the amygdala and adjacent external capsule project to the basal forebrain: evidence for the existence of GABAergic projection neurons in the cortical nuclei and basolateral nuclear complex." Front Neural Circuits 6: 46.

McIntire SL, Reimer RJ., Schuske K., Edwards RH and Jorgensen EM (1997). "Identification and characterization of the vesicular GABA transporter." Nature 389(6653): 870-876.

Melyan Z., Wheal HV. & Lancaster B. "Metabotropic-mediated kainate receptor regulation of IsAHP and excitability in pyramidal cells." Neuron 34, 107–114 (2002).

Millhouse, O. E. (1986). "The intercalated cells of the amygdala." J Comp Neurol 247(2): 246-271.

Millhouse, O. E. and J. DeOlmos (1983). "Neuronal configurations in lateral and basolateral amygdala." Neuroscience 10(4): 1269-1300.

Minelli, A., C. Scassellati, C. Bonvicini, J. Perez and M. Gennarelli (2009). "An association of GRIK3 Ser310Ala functional polymorphism with personality traits." Neuropsychobiology 59(1): 28-33.

Micheau J, Vimeney A, Normand E, Mulle C, Riedel G (2014). "Impaired hippocampus-dependent spatial flexibility and sociability represent autism-like phenotypes in GluK2 mice." Hippocampus 24:1059–1069.

Monyer, H., R. Sprengel, R. Schoepfer, A. Herb, M. Higuchi, H. Lomeli, N. Burnashev, B. Sakmann and P. H. Seeburg (1992). "Heteromeric NMDA receptors: molecular and functional distinction of subtypes." Science 256(5060): 1217-1221.

Motazacker, M. M., B. R. Rost, T. Hucho, M. Garshasbi, K. Kahrizi, R. Ullmann, S. S. Abedini, S. E. Nieh, S. H. Amini, C. Goswami, A. Tzschach, L. R. Jensen, D. Schmitz, H. H. Ropers, H. Najmabadi and A. W. Kuss (2007). "A defect in the ionotropic glutamate receptor 6 gene (GRIK2) is associated with autosomal recessive mental retardation." Am J Hum Genet 81(4): 792-798.

Muller, J. F., F. Mascagni and A. J. McDonald (2006). "Pyramidal cells of the rat basolateral amygdala: synaptology and innervation by parvalbumin-immunoreactive interneurons." J Comp Neurol 494(4): 635-650.

Muller, J. F., F. Mascagni and A. J. McDonald (2007). "Postsynaptic targets of somatostatin-containing interneurons in the rat basolateral amygdala." J Comp Neurol 500(3): 513-529.

Muller, M., H. Faber-Zuschratter, Y. Yanagawa, O. Stork, H. Schwegler and R. Linke (2012). "Synaptology of ventral CA1 and subiculum projections to the basomedial nucleus of the amygdala in the mouse: relation to GABAergic interneurons." Brain Struct Funct 217(1): 5-17.

Nakanishi S (1992). "Molecular diversity of glutamate receptors and implications for brain function". Science 1992;258:597-603

Niswender CM. and Conn PJ (2010). "Metabotropic glutamate receptors: physiology, pharmacology, and disease." Annu Rev Pharmacol Toxicol 50: 295-322.

Nowak, L., P. Bregestovski, P. Ascher, A. Herbet and A. Prochiantz (1984). "Magnesium gates glutamate-activated channels in mouse central neurones." Nature 307(5950): 462-465.

Nuss, P. (2015). "Anxiety disorders and GABA neurotransmission: a disturbance of modulation." Neuropsychiatric disease and treatment 11: 165-175.

Pabba, M. (2013). "Evolutionary development of the amygdaloid complex." Front Neuroanat 7: 27.

Paddock S, Laje G, Charney D, Rush AJ, Wilson AF, Sorant AJ et al (2007). "Association of GRIK4 with outcome of antidepressant treatment in the STAR*D cohort. " Am J Psychiatry; 164: 1181–1188.

Pare, D. (2003). "Role of the basolateral amygdala in memory consolidation." Prog Neurobiol 70(5): 409-420.

Pare, D., H. C. Pape and J. Dong (1995). "Bursting and oscillating neurons of the cat basolateral amygdaloid complex in vivo: electrophysiological properties and morphological features." J Neurophysiol 74(3): 1179-1191.

Paré D, Smith Y (1993)." Distribution of GABA immunoreactivity in the amygdaloid complex of the cat." Neuroscience 57:1061–1076

Paternain, A. V., Morales, M. & Lerma, J (1995). Selective antagonism of AMPA receptors unmasks kainate receptor-mediated responses in hippocampal neurons. Neuron 14, 185–189.

Paternain, A.V., Vicente, M.A., Nielsen,E and Lerma,J (1996). Comparative antagonism of kainate-activated AMPA and kainate receptors in hippocampal neurons. Eur. J. Neurosci, 8 (1996), pp. 2129-2136

Paternain, A. V., M. T. Herrera, M. A. Nieto and J. Lerma (2000). "GluR5 and GluR6 kainate receptor subunits coexist in hippocampal neurons and coassemble to form functional receptors." J Neurosci 20(1): 196-205.

Penzo, M. A., V. Robert and B. Li (2014). "Fear conditioning potentiates synaptic transmission onto long-range projection neurons in the lateral subdivision of central amygdala." J Neurosci 34(7): 2432-2437.

Perrais D, Pinheiro PS, Jane DE, Mulle C (2009). "Antagonism of recombinant and native GluK3-containing kainate receptors." Neuropharmacology, vol. 56 (pg. 131-140)

Pickard BS, Malloy MP, Christoforou A, Thomson PA, Evans KL, Morris SW, Hampson M, Porteous DJ, Blackwood DH, and Muir WJ (2006) Cytogenetic and genetic evidence supports a role for the kainate-type glutamate receptor gene, GRIK4, in schizophrenia and bipolar disorder. Mol Psychiatry 11:847–857

Pickard BS, Knight HM, Hamilton RS, Soares DC, Walker R, Boyd JK, Machell J, Maclean A, McGhee KA, and Condie A et al. (2008) A common variant in the 3'UTR of the GRIK4 glutamate receptor gene affects transcript abundance and protects against bipolar disorder. Proc Natl Acad Sci USA 105:14940–14945.

Pinheiro P, Mulle C (2006) Kainate receptors. Cell Tissue Res 326:457–482

Pinheiro, P. S., D. Perrais, F. Coussen, J. Barhanin, B. Bettler, J. R. Mann, J. O. Malva, S. F. Heinemann and C. Mulle (2007). "GluR7 is an essential subunit of presynaptic kainate autoreceptors at hippocampal mossy fiber synapses." Proc Natl Acad Sci U S A 104(29): 12181-12186.

Pitkänen, A., Pikkarainen, M., Nurminen, N., Ylinen, A. (2000). "Reciprocal Connections between the Amygdala and the Hippocampal Formation, Perirhinal Cortex, and Postrhinal Cortex in Rat: A Review." 911(1): 369-391.

Prager, E. M., H. C. Bergstrom, G. H. Wynn and M. F. M. Braga (2016). "The basolateral amygdala γ-aminobutyric acidergic system in health and disease." Journal of neuroscience research 94(6): 548-567.

Rainnie, D. G., Mania, I., Mascagni, F. & McDonald, A.J (2006). "Physiological and morphological characterization of parvalbumin-containing interneurons of the rat basolateral amygdala." J. Comp. Neurol. 498, 142–161.

Reiner A, Levitz J (2018) Glutamatergic signaling in the central nervous system: ionotropic and metabotropic receptors in concert. Neuron 98:1080–1098.

Ressler, KJ (2010). "Amygdala activity, fear, and anxiety: modulation by stress." Biol Psychiatry. 2010 Jun 15;67(12):1117-9

Roche KW, Raymond LA, Blackstone C, Huganir RL (1994). "Transmembrane topology of the glutamate receptor subunit GluR6." J Biol Chem 269(16):11679-82.

Rodrigues, R. J. and J. Lerma (2012). "Metabotropic signaling by kainate receptors." 1(4): 399-410.

Rodriguez-Moreno, A. & Lerma, J. (1998) Kainate receptor modulation of GABA release involves a metabotropic function. Neuron 20:1211–1218.

Rodriguez-Moreno, A., O. Herreras and J. Lerma (1997). "Kainate receptors presynaptically downregulate GABAergic inhibition in the rat hippocampus." Neuron 19(4): 893-901.

Rodríguez-Moreno A., López-García J. C. and Lerma J. (2000) Two populations of kainate receptors with separate signalling mechanisms in hippocampal interneurons. Proc. Natl Acad. Sci. USA 97, 1293–1298.

Royer, S., M. Martina and D. Pare (1999). "An inhibitory interface gates impulse traffic between the input and output stations of the amygdala." J Neurosci 19(23): 10575-10583.

Royer, S., M. Martina and D. Pare (2000). "Polarized synaptic interactions between intercalated neurons of the amygdala." J Neurophysiol 83(6): 3509-3518.

Rozas, J. L., A. V. Paternain and J. Lerma (2003). "Noncanonical signaling by ionotropic kainate receptors." Neuron 39(3): 543-553.

Rutkowska-Wlodarczyk. I, Aller MI , Valbuena S, Bologna JC, Prézeau L, Lerma J (2015)." A proteomic analysis reveals the interaction of GluK1 ionotropic kainate receptor subunits with Go proteins." J. Neurosci., 35 (2015), pp. 5171-5179

Sachidhanandam, S., C. Blanchet, Y. Jeantet, Y. H. Cho and C. Mulle (2009). "Kainate receptors act as conditional amplifiers of spike transmission at hippocampal mossy fiber synapses." J Neurosci 29(15): 5000-5008.

Sah, P., E. S. Faber, M. Lopez De Armentia and J. Power (2003). "The amygdaloid complex: anatomy and physiology." Physiol Rev 83(3): 803-834.

Sander.T, Hildmann.T, Kretz.R, Fürst.R, Sailer.U, Bauer.U, Schmitz.U, Beck-Mannagetta.G, Wienker.T.F, Janz.D (1997). "Allelic association of juvenile absence epilepsy with a GluR5 kainate receptor gene (GRIK1) polymorphism" Am. J. Med. Genet., 74, pp. 416-421

Savander, V., C. G. Go, J. E. LeDoux and A. Pitkanen (1995). "Intrinsic connections of the rat amygdaloid complex: projections originating in the basal nucleus." J Comp Neurol 361(2): 345-368.

Scarr, E., M. Beneyto, J. H. Meador-Woodruff and B. Dean (2005). "Cortical glutamatergic markers in schizophrenia." Neuropsychopharmacology 30(8): 1521-1531.

Schiffer HH, Swanson GT, Heinemann S (1997) Rat GluR7 and a carboxy-terminal splice variant, BluR7b, are functional kainate receptor subunits with a low sensitivity to glutamate. Neuron 19:1141–1146

Schiffer HH, Swanson GT, Masliah E, Heinemann SF. 2000. Unequal expression of allelic kainate receptor GluR7 mRNAs in human brains. J Neurosci 20(24): 9025–9033.

Schiffer, H. H. and S. F. Heinemann (2007). "Association of the human kainate receptor GluR7 gene (GRIK3) with recurrent major depressive disorder." Am J Med Genet B Neuropsychiatr Genet 144b(1): 20-26.

Schmitz D, Mellor J, Frerking M, Nicoll RA (2001). "Presynaptic kainate receptors at hippocampal mossy fiber synapses." Proc Natl Acad Sci U S A. 98(20):11003-8.

Segerstrale, M., J. Juuri, F. Lanore, P. Piepponen, S. E. Lauri, C. Mulle and T. Taira (2010). "High firing rate of neonatal hippocampal interneurons is caused by attenuation of afterhyperpolarizing potassium currents by tonically active kainate receptors." J Neurosci 30(19): 6507-6514.

Selak, S., A. V. Paternain, M. J. Fritzler and J. Lerma (2006). "Human autoantibodies against early endosome antigen-1 enhance excitatory synaptic transmission." Neuroscience 143(4): 953-964.

Senn, V., S. B. Wolff, C. Herry, F. Grenier, I. Ehrlich, J. Grundemann, J. P. Fadok, C. Muller, J. J. Letzkus and A. Luthi (2014). "Long-range connectivity defines behavioural specificity of amygdala neurons." Neuron 81(2): 428-437.

Shaltiel, S. Maeng, O. Malkesman, B. Pearson, R.J. Schloesser, T. Tragon, M. Rogawski, M. Gasior, D. Luckenbaugh, G. Chen, H.K. Manji (2008). Evidence for the involvement of the kainate receptor subunit GluR6 (GRIK2) in mediating behavioural displays related to behavioural symptoms of mania. " Mol. Psychiatry, 13 (2008), pp. 858-872

Shi, C. J. and M. D. Cassell (1998). "Cascade projections from somatosensory cortex to the rat basolateral amygdala via the parietal insular cortex." J Comp Neurol 399(4): 469-491.

Shi, C. J. and M. D. Cassell (1999). "Perirhinal cortex projections to the amygdaloid complex and hippocampal formation in the rat." J Comp Neurol 406(3): 299-328.

Shibata, H., T. Aramaki, M. Sakai, H. Ninomiya, N. Tashiro, N. Iwata, N. Ozaki and Y. Fukumaki (2006). "Association study of polymorphisms in the GluR7, KA1 and KA2 kainate receptor genes (GRIK3, GRIK4, GRIK5) with schizophrenia." Psychiatry Res 141(1): 39-51.

Shibata, H., A. Shibata, H. Ninomiya, N. Tashiro and Y. Fukumaki (2002). "Association study of polymorphisms in the GluR6 kainate receptor gene (GRIK2) with schizophrenia." Psychiatry Res 113(1-2): 59-67.

Shuang, M., J. Liu, M. X. Jia, J. Z. Yang, S. P. Wu, X. H. Gong, Y. S. Ling, Y. Ruan, X. L. Yang and D. Zhang (2004). "Family-based association study between autism and glutamate receptor 6 gene in Chinese Han trios." Am J Med Genet B Neuropsychiatr Genet 131b(1): 48-50.

Szatmari, M. Maziade, L. Zwaigenbaum, C. Mérette, M.A. Roy, R. Joober, R. Palmour. "Informative phenotypes for genetic studies of psychiatric disorders" Am. J. Med. Genet. B. Neuropsychiatr. Genet., 144B (2007), pp. 581-588

Smith, Y. and D. Pare (1994). "Intra-amygdaloid projections of the lateral nucleus in the cat: PHA-L anterograde labeling combined with postembedding GABA and glutamate immunocytochemistry." J Comp Neurol 342(2): 232-248.

Soghomonian JJ and Martin DL (1998). "Two isoforms of glutamate decarboxylase: why?" Trends Pharmacol Sci 19(12): 500-505.

Sommer, B., M. Kohler, R. Sprengel and P. H. Seeburg (1991). "RNA editing in brain controls a determinant of ion flow in glutamate-gated channels." Cell 67(1): 11-19.

Sorvari, H., H. Soininen, L. Paljarvi, K. Karkola and A. Pitkanen (1995). "Distribution of parvalbumin-immunoreactive cells and fibers in the human amygdaloid complex." J Comp Neurol 360(2): 185-212.

Sosulina, L., S. Meis, G. Seifert, C. Steinhauser and H. C. Pape (2006). "Classification of projection neurons and interneurons in the rat lateral amygdala based upon cluster analysis." Mol Cell Neurosci 33(1): 57-67.

Spampanato, J., J. Polepalli and P. Sah (2011). "Interneurons in the basolateral amygdala." Neuropharmacology 60(5): 765-773.

Stern-Bach YB, Bettler M, Hartley PO, Sheppard P, Heinemann SF (1994). "Agonist selectivity of glutamate receptors is specified by two domains structurally related to bacterial amino acid-binding proteins." Neuron 13(6): 1345-1357.

Stoop, R., C. Hegoburu and E. van den Burg (2015). "New Opportunities in Vasopressin and Oxytocin Research: A Perspective from the Amygdala." Annual Review of Neuroscience 38(1): 369-388.

Storm, J. F. (1988). "Temporal integration by a slowly inactivating K+ current in hippocampal neurons." Nature 336(6197): 379-381.

Stuber, G. D., D. R. Sparta, A. M. Stamatakis, W. A. van Leeuwen, J. E. Hardjoprajitno, S. Cho, K. M. Tye, K. A. Kempadoo, F. Zhang, K. Deisseroth and A. Bonci (2011). "Excitatory transmission from the amygdala to nucleus accumbens facilitates reward seeking." Nature 475(7356): 377-380.

Swanson CJ, Bures M, Johnson MP, Linden AM, Monn JA, Schoepp DD (2005) Metabotropic glutamate receptors as novel targets for anxiety and stress disorders. Nat Rev Drug Discov 4:131–144

Takenouchi, T., N. Hashida, C. Torii, R. Kosaki, T. Takahashi and K. Kosaki (2014). "1p34.3 deletion involving GRIK3: Further clinical implication of GRIK family glutamate receptors in the pathogenesis of developmental delay." Am J Med Genet A 164a(2): 456-460.

Taverna FA, Wang, LY, MacDonald JF and Hampson DR (1994). "A transmembrane model for an ionotropic glutamate receptor predicted on the basis of the location of asparagine-linked oligosaccharides." J Biol Chem 269(19): 14159-14164.

Tovote, P., J. P. Fadok and A. Luthi (2015). "Neuronal circuits for fear and anxiety." Nat Rev Neurosci 16(6): 317-331.

Tye, K. M., R. Prakash, S. Y. Kim, L. E. Fenno, L. Grosenick, H. Zarabi, K. R. Thompson, V. Gradinaru, C. Ramakrishnan and K. Deisseroth (2011). "Amygdala circuitry mediating reversible and bidirectional control of anxiety." Nature 471(7338): 358-362.

Valbuena, S. and J. Lerma (2016). "Non-canonical Signaling, the Hidden Life of Ligand-Gated Ion Channels." Neuron 92(2): 316-329.

Veening, J. G., L. W. Swanson and P. E. Sawchenko (1984). "The organization of projections from the central nucleus of the amygdala to brainstem sites involved in central autonomic regulation: a combined retrograde transport-immunohistochemical study." Brain Res 303(2): 337-357.

Veres, J. M., G. A. Nagy, V. K. Vereczki, T. Andrasi and N. Hajos (2014). "Strategically positioned inhibitory synapses of axo-axonic cells potently control principal neuron spiking in the basolateral amygdala." J Neurosci 34(49): 16194-16206.

Vignes, M., Clarke, V.R.J., Parry, M. J., Bleakman, D., Lodge, D., Ornstein, P. L. & Collingridge, G. L. (1998) The GluR5 subtype of kainate receptor regulates excitatory synaptic transmission in areas CA1 and CA3 of the rat hippocampus. Neuropharmacology 37:1269–1277.

Viviani, D., A. Charlet, E. van den Burg, C. Robinet, N. Hurni, M. Abatis, F. Magara and R. Stoop (2011). "Oxytocin selectively gates fear responses through distinct outputs from the central amygdala." Science 333(6038): 104-107.

Vouimba, R. M., D. Yaniv and G. Richter-Levin (2007). "Glucocorticoid receptors and beta-adrenoceptors in basolateral amygdala modulate synaptic plasticity in hippocampal dentate gyrus, but not in area CA1." Neuropharmacology 52(1): 244-252.

Walker, D. L., D. J. Toufexis and M. Davis (2003). "Role of the bed nucleus of the stria terminalis versus the amygdala in fear, stress, and anxiety." Eur J Pharmacol 463(1-3): 199-216.

Watanabe, Y., H. Saito and K. Abe (1995). "Nitric oxide is involved in long-term potentiation in the medial but not lateral amygdala neuron synapses in vitro." Brain Res 688(1-2): 233-236.

Werner, P., M. Voigt, K. Keinanen, W. Wisden and P. H. Seeburg (1991). "Cloning of a putative high-affinity kainate receptor expressed predominantly in hippocampal CA3 cells." Nature 351(6329): 742-744.

Whalley HC, Pickard BS, McIntosh AM, Zuliani R, Johnstone EC, Blackwood DH, Lawrie SM, Muir WJ, Hall J (2009). "A GRIK4 variant conferring protection against bipolar disorder modulates hippocampal function." Mol Psychiatry 14:467–468

White, S. W., Oswald, D., Ollendick, T., & Scahill, L. (2009). Anxiety in children and adolescents with autism spectrum disorders. Clinical Psychology Review, 29, 216–229.

Wilding TJ. & Huettner JE. (1995). Differential antagonism of a-amino-3-hydroxy-5-methyl-4-isoxazolepropionic acidpreferring and kainate-preferring receptors by2,3-benzodiazepines. Molecular Pharmacology 47, 582–587

Wilson, G. M., S. Flibotte, V. Chopra, B. L. Melnyk, W. G. Honer and R. A. Holt (2006). "DNA copy-number analysis in bipolar disorder and schizophrenia reveals aberrations in genes involved in glutamate signaling." Hum Mol Genet 15(5): 743-749.

Wisden, W. and P. H. Seeburg (1993). "A complex mosaic of high-affinity kainate receptors in rat brain." J Neurosci 13(8): 3582-3598.

Wo ZG and Oswald ER (1995), Unraveling the modular design of glutamate-gated ion channels, Trends in Neurosciences, Volume 18, Issue 4, , Pages 161-168

Wolff, S. B., J. Grundemann, P. Tovote, S. Krabbe, G. A. Jacobson, C. Muller, C. Herry, I. Ehrlich, R. W. Friedrich, J. J. Letzkus and A. Luthi (2014). "Amygdala interneuron subtypes control fear learning through disinhibition." Nature 509(7501): 453-458.

Yu, K., P. Garcia da Silva, D. F. Albeanu and B. Li (2016). "Central Amygdala Somatostatin Neurons Gate Passive and Active Defensive Behaviours." J Neurosci 36(24): 6488-6496.

Zhou FW, Chen HX, Roper SN (2009). "Balance of inhibitory and excitatory synaptic activity is altered in fast-spiking interneurons in experimental cortical dysplasia" J. Neurophysiol., 102 (2009), pp. 2514-2525

Zhou, Y. and Danbolt, NC (2014). "Glutamate as a neurotransmitter in the healthy brain." J Neural Transm (Vienna) 121(8): 799-817.

Zimmerman, J. M. and S. Maren (2010). "NMDA receptor antagonism in the basolateral but not central amygdala blocks the extinction of Pavlovian fear conditioning in rats." Eur J Neurosci 31(9): 1664-1670.